Colloid Journal (USSR)

Number 6

Volume XVI

(November-December, 1954)

IN ENGLISH TRANSLATION

TABLE OF CONTENTS

Chronicle

IN ENGLISH TRANSLATION

SORPTION OF PARTICLES OF POLYSTYRENE LATEX ON PAPER

E. M. Aleksandrova and P. V. Mochalov

The introduction of some new highly disperse phase into a microheterogeneous system may lead to coagulation. In distinction from the normal volume coagulation of sols, this process is termed heterocoagulation. This term is descriptive of the mechanism of the process: the coagulation of the sol takes place on the surfaces of the particles of the extraneous phase after previous desorption of the stabilizing components. The latter are desorbed and again resorbed on the new surface.

In studying dyeing and tanning processes, Peskov showed the existence of a peculiar type of stability, which he termed sorptional [1]. Particles of such colloidal systems as do not have sorptional stability may become sorbed. The terms "sorptional stability" and "aggregative stability" describe the properties of colloidally dispersed systems and are very valuable in colloid-chemical treatment of a number of processes. The process of impregnation of fibrous materials by various latexes is examined from the same viewpoint. Much work has been carried out in this direction by Sokolov [2], Voyutsky [3], and others.

The present article describes the sorption of particles of polystyrene latex on an ashless filter. The characteristics of the latexes studied, with respect to their aggregative stability, are described in the previous paper [4]. Two latexes were studied — from factory production, and laboratory-made, obtained by the emulsion polymerization method. The stabilizer used in the second case was "Wetting Agent NB", which chemically belongs to the Na salts of sulfonic acids of substituted naphthalenes. The sorption of both latexes was practically the same. The factual data of this paper relate to the laboratory latex. The choice of the adsorbent was based in its purity, standard properties, and high sorptional activity, established for numerous colloidal systems.

The method of sorption determination is based on comparison of optical densities. The accuracy of such a method depends on the initial concentration of the latex, and is found to be satisfactory at concentrations not over 10 g of the dry substance in one liter of latex. The advantage of the method is the possibility of rapid determination and simple calculation of the sorption values [5]. In a number of cases the sorption was determined gravimetrically; agreement was quite good. Sorptional equilibrium is attained after 2-2.5 days, which is explained by the fibrous nature of the paper and the fairly large size of the latex particles (70-80 mμ).

Table 1 shows sorption values after different time intervals.

It was found experimentally that a certain amount of electrolyte must be added for sorption to take place, as without this the latexes were sorptionally stable. This fact, verified repeatedly, confirms the view put forward by Peskov [6] that it is necessary to lower the aggregative stability of a colloidal system somewhat for sorption processes to take place successfully. The addition of weakly acting coagulants, which do not cause volume coagulation of the sol, is quite sufficient to destroy sorptional stability. This confirms the validity of the practical instruction concerning dyeing with colloidally dispersed organic dyes — the dye solution must have decreased aggregative stability with a sufficiently high degree of dispersion. This condition is fulfilled on the addition of electrolytes.

TABLE 1

Kinetics of the Sorption of Latex by Filter Paper in Presence of NaCl

Time in hours	a, mg/g
2	8
30	29.5
54	32.5
74	32.2
77	32.3

Note. Latex concentration — 5.72 g/l; concentration — 2 g/l.

After the time to reach sorptional equilibrium had been determined and the experimental technique checked, a number of sorption isotherms were obtained. The sorption in milligrams of the disperse phase per 1 g adsorbent was calculated from the formula:

$$a = \frac{(c_0 - c)V}{m},$$

where $\underline{a}$ is the number of milligrams of the disperse phase sorbed by 1 g of the adsorbent; $\underline{c_0}$ is the concentration

of the disperse phase before sorption, in g/l; c is the concentration of the disperse phase after sorption; m is the weight of the adsorbent in grams; V is the volume of the latex in milliliters.

As had already been established, the ratio of the concentrations of diluted latexes is practically equal to the ratio of their optical densities, that is

$$\frac{c_0}{c} = \frac{D_0}{D},$$

where D_0 and D are the optical densities of the latex before and after sorption. Sometimes there are deviations from this relationship (for example, when the difference between c_0 and c is large, in the sorption of relatively highly concentrated latexes), and in such cases the values of c_0 and c were determined with the aid of the previously obtained graph for the variation of optical density with concentration [5].

Sorption in presence of NaCl was first studied, latexes with different contents of the dry substance being used; sorption isotherms at 20° were obtained for various concentrations of common salt added to the latex. Figure 1 shows the result of these experiments.

As Figure 1 shows, at relatively low concentrations of NaCl (4-9 mM/l) the isotherms pass through a maximum. This anomalous course of the isotherms may be explained by the simultaneous effect of the concentration and the stability of the latex on the sorption. As was already indicated [4] the stability of these polystyrene latexes decreases with dilution. Thus, by increasing the concentration of the disperse phase of the latex, we favor sorption; but the stability of the latex increases, which decreases sorption. At high concentrations of NaCl the stability of the latex will be decreased sufficiently at all concentrations of the disperse phase, and therefore there will be no decrease of sorption. The isotherms assume the normal appearance with a certain limiting value of a_∞. In the range of medium concentrations of the disperse phase the experimental results may be expressed by the empirical sorption Equation $a = \beta c^a$.

Figure 2 shows the sorption isotherms in logarithmic coordinates, from which it is possible to determine the coefficients a and β and to formulate empirical equations for the sorption. Thus, for $c_{NaCl} = 17.1$ mM/l, $a = 16.2 \cdot c_1^{0.216}$ (c_1 is the concentration of the disperse phase of the latex in g/l); for

$$c_{NaCl} = 34.2 \text{mM/l}, \quad a = 22 \cdot c_1^{0.29}.$$

In addition, sorption in presence of the chlorides of potassium, ammonium, calcium, and aluminum was studied. Curves were plotted for the dependence of the sorption on the concentration c_e of electrolytes added to the latex, with a constant amount of dry residue in the latexes studied. The results of these investigations are shown in Figure 3.

It did not prove possible to show sorption in presence of AlCl$_3$. This may be explained by the excessively strong coagulating power of AlCl$_3$. As we pass from univalent to bivalent cations, on the one hand, the electrolyte concentration required to produce a given degree of sorption decreases, and on the other, the range of electrolyte con-
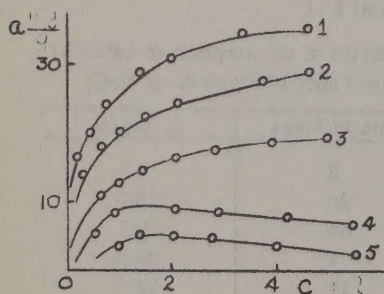

Fig. 1. Sorption isotherms of polystyrene latex with different additions of NaCl: 1 - 68.4; 2 - 34.2; 3 - 17.1; 4 - 8.55; 5 - 4.27 mM/l.
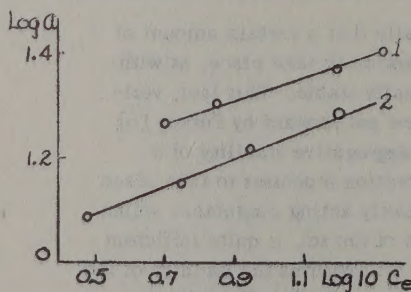
Fig. 2. Sorption isotherms of polystyrene latex on the addition of NaCl electrolyte: 1 - 34.2; 2 - 17.1 mM/l.

centrations in which sorption takes place is shortened. Thus, while with NaCl vigorous sorption occurs at c_e from 9.2-200 mM/l, with CaCl$_2$ vigorous sorption takes place at c_e from 0.45 to 6-8 mM/l. Apparently the concentration range of AlCl$_3$ in which sorption of these latexes occurs is close to zero, and therefore in practice no sorption is observed.

We also studied the sorption of the disperse phase of polystyrene latexes for different values of pH of the latex. In the conditions of our experiments the greatest sorption took place at pH 2-3. Table 2 shows the effect of pH of the latex on the sorption of its particles by ashless filter paper (content of dry residue in the latex was 5.72 g/l). The pH was determined with the glass electrode.

From a comparison of the concentrations of different electrolytes which produce equal sorption it is possible to evaluate the power of different cations to lower the sorptional stability of polystyrene latexes. The investigations show that the cations used may be arranged in a definite series according to their ability to lower the sorptional stability of polystyrene latexes.
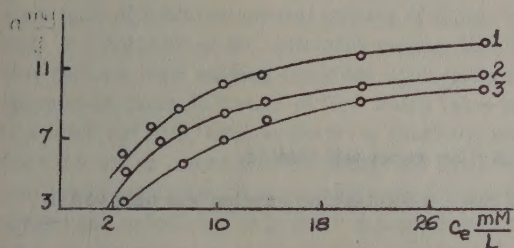

Fig. 3. Effect of electrolyte concentration on the sorption of latex particles of constant concentration by weights (0.68 g/l): 1-NH_4Cl; 2-KCl; 3-NaCl.
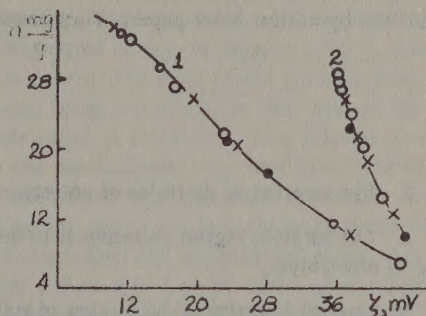

Fig. 4. Relationship between the value of the electrokinetic potential of latex and the sorption of its particles on paper: 1-univalent ions; 2-bivalent ions.

TABLE 2

Effect of pH of the Latex on the Sorption of its Particles by Filter Paper.

pH	a, mg/g
2	33
2.22	30
2.6	23.6
2.84	16
3.18	8.4

The analogy between the power of different cations to lower the sorptional stability, their coagulating power, and their ability to lower the value of the ξ-potential, is very striking. The existence of this analogy leads to the need for a more detailed study of the relationship between the value of the ξ-potential, aggregative stability, and sorptional stability. It may be concluded from a comparison of the values of sorption of latexes on ashless filters, determined for the most diverse cases, with the data of earlier electrophoretic measurements [4], that the region of the most intensive sorption coincides with the lowest values of ξ-potential. The value of the ξ-potential may be assumed to vary steadily with the value of the sorption. This assumption is confirmed for sodium and potassium ions, as these ions decrease both the ξ-potential and the sorptional stability to practically the same extent. To verify this view for as many cations as possible, supplementary experiments were carried out on measurements of electrokinetic potentials and sorption values in the presence of rubidium, magnesium, and barium chlorides.

Seven different cations were used for the verification: Na^+, K^+, NH_4^+, Rb^+, Mg^{2+}, Ca^{2+}, Ba^{2+}. It was found that, if the sorption values in milligrams per 1 g were plotted along the ordinate axis, and the ξ-potential in mV along the abscissa axis, all the univalent cations studied — Na^+, K^+, NH_4^+, Rb^+ — give practically the same curve (Fig. 4).

In the case of bivalent cations (Mg^{2+}, Ca^{2+}, Ba^{2+}) larger sorption values correspond to given values of the ξ-potential than in the case of univalent cations. Bivalent cations, as already stated, form less soluble compounds with the stabilizer used in our experiments. This not only leads to a decrease in the thickness of the ionic solvation layers, but to further destabilization of the latex as the result of hydrophobization of the phase separation surface. This apparently explains the high sorption of the disperse phase of latexes in presence of bivalent cations. Further destabilization by the action of polyvalent cations also leads to destruction of the aggregative stability of the latexes. As a result there is a decrease in the difference between the concentration of the electrolyte which causes sorption and the concentration of electrolyte which causes coagulation (threshold of coagulation), that is, the concentration range in which sorption is observed becomes shorter (for Al^{3+} ions this range is close to zero). For this reason, to obtain sorptionally unstable polystyrene latexes, it is recommended in practice to use salts of univalent metals, because this permits a decrease of the sorptional stability of latexes without causing coagulation.

It may be noted from a comparison of the results obtained in the study of the sorption of polystyrene latexes

with earlier studies on latex coagulation [4] that the presence of the adsorbent (ashless filter paper) lowers the coagulation threshold of latexes. On the addition of chlorides of univalent metals, perceptible coagulation occurs in absence of the adsorbent at electrolyte concentrations of 250-300 mM/l, and in presence of 0.5 g of the adsorbent (per 15 ml latex), at 190-220 mM/l. On the addition of chlorides of bivalent metals in absence of adsorbent, coagulation occurs at electrolyte concentrations of 15-27 mM/l, and in presence of 0.5 g adsorbent, at 6-8 mM/l. Thus, the adsorbent introduced into the latex has a destabilizing effect. The destabilizing action of the adsorbent on polystyrene latex may be explained on the basis of Peskov's views, quoted earlier, on the adsorption of stabilizers by an adsorbent introduced into the latex. To confirm this, experiments were carried out on adsorption of the stabilizer by ashless filter paper. Very considerable sorption was found.

SUMMARY

1. The sorption of particles of polystyrene latex on ashless filter paper was studied.

2. The sorption region corresponds to decreased values of the ξ-potential; no sorption was observed in absence of electrolyte.

3. Parallel lowering of both types of stability — aggregative and sorptional — takes place by the action of electrolytes.

4. Desorption of the stabilizer and its transfer from the latex particles to the paper was noted; this explains the decrease of stability of latexes in presence of adsorbents.

LITERATURE CITED

[1] N. P. Peskov, Bull. Textile Ind., No. 5, 25 (1926); Course of Colloid Chemistry, Chemical Press, Moscow (1940).

[2] S. I. Sokolov, Physical Chemistry of Collagen and its Derivatives, State Light Ind. Press (1937).

[3] S. S. Voyutsky, Collected Papers on the Theory and Practice of Impregnation of Shoe Soles, State Light Ind. Press (1952).

[4] E. M. Aleksandrova and P. V. Mochalov, Colloid J., 14, No. 3, 161 (1954).

[5] E. M. Aleksandrova and P. V. Mochalov, Trans. Mendeleev Chem. Tech. Inst., Moscow, 18 (1953).

FLUIDITY OF LUBRICANT GREASES

D. S. Velikovsky

Structural-mechanical properties constitute the main factor which determines the behavior during use of many dispersions and colloidal solutions; these include lubricant greases, a widespread class of lubricants [1]. The main mass of lubricant greases consists of thixotropic structurized dispersions of salts of organic acids in mineral oils. In conditions of use, lubricant greases, like all lubricants, may undergo the most varied deformations; they may perform their working functions under insignificantly small loads, being practically at rest, and, in the great majority of cases, in a state of flow which takes place in a very wide range of velocities. The velocity gradients in a lubricant film, even at the same frictional points of machines and mechanisms, may vary from insignificantly small to tens or hundreds of thousands and even millions of $\sec^{-1}$. Because of this wide range of possible deformation conditions in use, it is not sufficient to study the flow of lubricant greases in a relatively small range of shear stresses and velocities, as is usual in measurements of "viscosity" of dispersions and colloidal solutions. For a complete characterization of the fluidity of greases it is necessary to plot a rheological graph which covers shear stresses from the smallest to millions of $\text{dynes}/\text{c.m}^2$, and velocity gradients from zero to hundreds of thousands, and sometimes even to millions of $\sec^{-1}$. Investigations over such a wide range of shear stresses and velocities cannot be made in the same apparatus and by the same method. However, by a comparison of the results obtained in different limits of shear stresses and velocities by different methods [4, 9, 10, 12, 14] it is possible to plot practically universal rheological flow diagrams for lubricant greases. The laws established for lubricant greases may apparently be extended also to other dispersions close to them in structure.

The structural-mechanical properties of dispersions should be examined in relation to the mechanical properties of the dispersion medium and the disperse phase. The solid-like properties of lubricant greases (as of other structurized dispersions) which appear at low shear stresses, are determined by the mechanical properties of the structural skeleton of the dispersion. The flow of dispersions at very high shear stresses in conditions when the structure in flow has been disrupted to the maximum extent, is mainly determined by the viscosity of the dispersion medium. The nature of the deformations of structurized dispersions at all intermediate shear stresses is determined on the one hand by the part played in these deformations by the structural skeleton and its constituent disperse particles, by the dispersion medium on the other, and also by their mutual influence on the deformability of each other.

The structural skeleton of "soap" lubricant greases is formed from soap crystallites (the crystal lattice of which contains, according to all available data, a certain amount of the dispersion medium, oil [2, 15, 16]), which are threadlike or ribbonlike in form; their width, and especially their thickness are of ultramicroscopic dimensions, while their length may attain hundreds of microns. Under the polarization microscope, even with the strongest magnification, only accumulations (bundles) of such threads and ribbons may be seen [1, 3, 4]. The electron microscope shows the structural skeleton of the grease as touching and partially interwoven or tangled fiber-like and ribbonlike particles, sometimes twisted like cords. Many of the ribbons and threads only touch each other at isolated points, while others, especially those lying parallel to each other, touch at many points [4, 5]. Thus, the separate disperse particles are held together by different forces. However, the structural skeleton of greases as a whole is a solid.*

---

* When I state that the structural skeleton of lubricant greases is a solid, I examine the solid state from the viewpoint of generally accepted concepts. The constantly discussed question whether all solids exhibit relaxation over very prolonged periods of time "to zero" at stresses which are less than the experimentally established limits of elasticity (flow), is essentially meaningless in relation to lubricant greases (and for many other structurized dispersions). As the result of aging processes, inevitable in colloidal dispersions, which are the consequence of progressive coagulation of the dispersed particles (first, cohesion of particles situated close and parallel to each other in the skeleton), and also as the result of the growth of crystals from the molecularly dissolved and very finely dispersed particles of soap in the dispersion medium, the strength of the structural skelton varies with time, often increasing gradually to an appreciable extent. This excludes the possibility of a prolonged development of the "experimentally unmeasurable relaxation" process, even if it took place. On the other hand, the experimentally observable decrease of strength of chemically unstable lubricants with time, in which free acids favor peptization of the dispersed particles, may be taken to be "relaxation".

Like all solids, the structural skeleton of greases clearly differs from the included liquid phase by elasticity of form, which is manifested by a capacity for reversible deformation (accompanied by fully reversible residual after-effects), and by the capacity for brittle deformation with loss of structural unity at stresses above the strength limit.*　At shear stresses above the elastic limit, the structural skeleton of greases, as of all solids in the generally accepted sense, undergoes a very slow but quite measurable irreversible flow deformation (creep). The creep of solids is not associated with any loss of structural unity, and according to accepted views is due to slippage along crystal planes.

In distinction from true solids, the structural skeleton of dispersions may become deformed (creep or flow) very slowly, continuously and irreversibly, without loss of structural unity not only as the result of intra-crystallite displacements, but, as was indicated by P. A. Rebinder, as the result of displacement of the points of contact between contacting crystallites. In both cases the broken bonds between the displacing elements are restored practically instantaneously at new points, as in the flow of true solids.
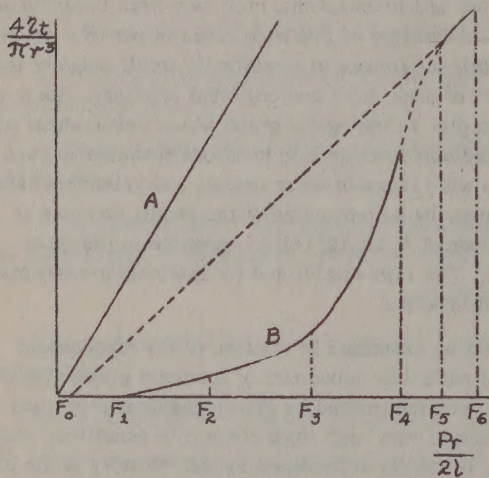

Fig. 1. Flow of lubricant greases at shear stresses above the strength limit of the structural skeleton: a - the liquid component of the grease (spindle oil); b - grease.

Elastic deformations and irreversible flow of the structural skeleton are manifested by elastic deformations and "flow" of the grease as a whole, although the liquid phase plays a purely passive role in these deformations. Thus, the elastic limit (limit of flow or creep) of the structural skeleton of the grease is at the same time the elastic limit (limit of creep, minimum limit of flow) of the lubricant grease.

The rheological curve in Figure 1 shows the flow of lubricant greases at shear stresses above the strength limit of the structural skeleton of the greases, based on experimental data obtained by the author of the present communication and experimental data published by other authors. A proportional scale could not be used in this figure; it merely illustrates the principle of the behavior. Curve A represents the flow of the liquid component of the grease (mineral oil); curve B, the flow of the grease as a whole; the shear stress F_1 is the elastic limit of the structural skeleton of the grease (minimum limit of flow of the grease). In the range of shear stresses from F_1 to F_2 flow of the grease takes place, due to "creep" of the structural skeleton, which occurs without loss of structural unity. As all the destroyed bonds are restored practically instantaneously, the rate of flow of the grease in this range is proportional to the effective shear stress $F - F_1$ and the flow obeys "Shvedov's law":

$$\frac{F - F_1}{dv/dx} = \text{const.}$$

This flow takes place at velocity gradients from 10^{-8} to 10^{-9} $\sec^{-1}$, and therefore it cannot be shown on the usual scale in linear rheological graphs.

This nature of the creep of lubricant greases is confirmed by the experimental data of Rebinder and Segalova [6, 7] obtained in studies of "models" of lubricant greases, and results obtained by the present author, obtained in studies of commercial lubricant greases, Solidols.

At the shear stress F_2 the strength limit of the structural skeleton of the grease is reached, and, as in case of true solids, brittle deformation begins. This may be accompanied both by the detachment of separate dispersed particles at single contact points and separation of particles joined at many contact points, and also by rupture of particles (especially interwoven and tangled particles). Being in a liquid medium, the separate detached particles and aggregates and conglomerates of them approach, as the result of thermal motion, to distances at which molecular forces can act at isolated points; new bonds are formed at these points. As the

* Elastic deformation of oleogels of soaps and lubricant greases was first studied by Vinogradov and Klimov [13], Rebinder and Segalova [6, 7], and Trapeznikov and Shlosberg [11].

particles approach and collide, purely mechanical cohesion, interweaving, and twisting of the threadlike and ribbon-like particles can also occur. However, in contrast to what occurs during the "flow" of the skeleton which has not lost its structural unity, the new "thixotropic" bonds are formed not instantaneously, but after a certain time interval which is necessary for the detached particles to approach to a distance at which molecular forces can act.

As the result of the rupture of bonds between the particles, the oil immobilized in the skeleton becomes able to flow under the action of shear stresses, and in its flow it picks up separate particles and fragments of the skeleton which, by colliding and forming new bonds, hinder the flow of the oil.

In a field of nonhomogeneous stress (as, for example, in flow through capillaries or between coaxial cylinders), the destruction of the structural skeleton begins in the zones of greatest shear stress, and spreads gradually to other zones as the total shear stress increases. However, this regular effect, which is the basis of the development of flow of all "Shvedov" bodies, is accompanied by the destruction of stronger bonds in zones where the skeleton has already lost its structural unity and displacement of separate agglomerates of particles takes place. As a result, in nonhomogenized greases (with undestroyed original "condensation" bonds formed on cooling from the melt), at shear stresses which exceed the strength limit of the weakest bonds, displacement of separate "grains" or "nuclei" of irregular shape takes place, as was observed and recorded by Vinogradov by microcinematography in polarized light. The general picture is superficially analogous to the flow of continuous ice at the start of break-up. As the shear stress increases, the separate nuclei and grains slowly break up and disperse. This grain formation is not observed in well-homogenized greases [8].
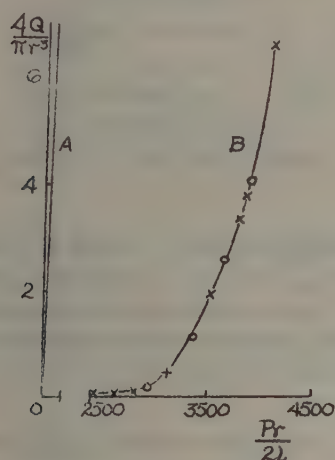
Fig. 2. Flow curve for Solidol at shear stresses above the upper flow limit; A - liquid component of the grease (spindle oil); B - grease.

Thus, the flow of greases at stresses above the strength limit of the structural skeleton of the grease differs in principle from the creep of greases with undestroyed structural skeleton by the fact that the former takes place in the liquid phase, while the solid phase, fragments of the structure, and dispersed particles hinder its normal development; decreasingly so as the shear stress and therefore the rate of flow increases (as in unit time or distance the number of broken bonds increases, while the number of bonds which have time to be restored decreases). Thus, the strength limit of the structural skeleton F_2 coincides with the upper flow limit of the grease. At stresses greater than F_2 the law which governed the flow at lower shear stresses can no longer apply, and the flow no longer obeys the Shvedov equation.

Figure 2 shows, in linear coordinates and with correct scales, an experimental curve, obtained by the author jointly with G. F. Shuleiko, for the flow of Solidol (in absence of slippage) at shear stresses above the upper flow limit, and also the flow curve for the liquid phase of this Solidol (spindle oil). As Figure 2 shows, in this region the work of destruction of the structural skeleton rises sharply with increase of shear stress, which is due to the gradual destruction of increasing numbers of primary bonds as the shear stress increases. When all the primary bonds are completely destroyed and the flow is opposed only by secondary bonds, formed as the result of thixotropic structure formation in the stream, the rate of increase of the work of destruction of the structural skeleton begins to fall (in Figure 1 at shear stresses above F_3). On further increase of the shear stress and rate of flow, the nature of the rheological curve is determined only by the number of destroyed secondary bonds which have time to be restored in unit time or distance. As the rate of flow increases, the number of bonds restored will be less, and the specific value of the viscous resistance of the liquid phase in the total resistance to flow of the grease will increase; this is clearly seen in Figure 3, which shows, in logarithmic coordinates, the curve for the flow of Solidol in the limits of six logarithmic orders of velocity gradients, experimentally determined by the author jointly with G. F. Shuleiko. This curve, of a form similar to the experimental curves published by Vinogradov and co-workers [9], corresponds to the region between the shear stresses F_3 and F_4 on the graph of Figure 1.

At greater shear stresses and correspondingly greater velocity gradients, viscosimetric measurements no longer give sufficiently reliable results. For investigations in this region, the author used the method of mechanical equivalents [10], and obtained values which correspond to the portion of the curve between shear

stresses F_5 and F_6 of Figure 1. As the Figure shows, in this region the curve passes into a straight line, the continuation of which crosses the stress axis at the point F_0. At shear stresses greater than F_5 the velocity increases so much that restoration of structure has no time to occur, and the separate dispersed particles, overcoming thermal motion, are completely oriented in the direction of the stream.

In this region the flow of the grease with a completely destroyed structure again obeys the Shvedov equation:

$$\frac{F-F_0}{dv/dx} = \text{const.}$$

In this equation F_0 is the quantitative measure, not of the resistance of the structural skeleton to destruction, but of the resistance of the oriented dispersed particles to thermal motion.*

SUMMARY

The flow of structurized dispersions of anisodiametric particles in a liquid medium, which include lubricant greases, obeys different laws in different regions of stresses and rates of shear, depending on the elementary deformation of the disperse phase and the dispersion medium. Three zones of flow are clearly distinguished:

a) Zone of creep. The flow obeys the Shvedov equation:

$$\frac{F-F_1}{dv/dx} = \text{const.}$$

where F_1 is the elastic limit of the structural skeleton.

Fig. 3. Flow curve for Solidol:
A - liquid component of the grease (spindle oil); B - grease.

b) Zone of flow with continuing destruction and restoration of the structural skeleton. The rate of flow in this zone depends on changes of the equilibrium strength of the structural skeleton, which is a function of the strength limit of the structural skeleton and the rate of thixotropic restoration. Only if these elemental factors are taken into account is it possible to derive an equation for the flow of lubricant greases and similar structurized dispersions in this zone; however, the possibility is not excluded of the selection of an empirical equation which would more or less satisfactorily describe the flow of individual types of greases in this zone.

c) Zone of flow with completely destroyed structure. The flow obeys the Shvedov Equation $\frac{F-F_0}{dv/dx} = \text{const.}$, where F_0 is the orientation stress of the dispersed particles.

LITERATURE CITED

[1] D. S. Velikovsky, Lubricant Greases, State Fuel Technology Press (1945).

[2] A. A. Trapeznikov, Collected papers "Low Temperature Properties of Petroleum Products", State Fuel Technology Press, 98 (1949); A. A. Trapeznikov and E. M. Shlosberg, Colloid J., 8, 421 (1946).

[3] D. S. Velikovsky, Collected papers, "Theory and Practice of the Production and Application of Lubricant Greases," State Fuel Technology Press, 5 (1939).

[4] G. V. Vinogradov, Prog. Chem., 21, No. 6, 758 (1952).

[5] L. W. Sproule, W. C. Pattenden, Canad. J. of Res., 26, 465, 1948; B. B. Farrington, D. H. Birdsdall, The Inst. Spokesman, 11, 4, 1947; D. H. Birdsdall, B. B. Farrington, J. Phys. Coll. Chem., 12, No. 9, 1415, 1948; E. Ammot, L. W. McLennan, The Inst Spokesman, 14, No. 12, 7, 1951; J. A. Brown, C. N. Hudson, L. D. Loring, The Inst. Spokesman, 15, No. 10, 8, 1952.

[6] E. E. Segalova and P. A. Rebinder, Colloid J., 10, No. 3, 223 (1948).

---

* In addition to brittle deformations of the structural skeleton, the flow of lubricant greases is also affected by elastic deformations of the structural skeleton and of the separate dispersed particles. For the sake of simplification these were not examined separately, and the energy consumed in maintaining them was considered to be part of the energy consumed in the destruction of the structural skeleton and the orientation of the dispersed particles, respectively.
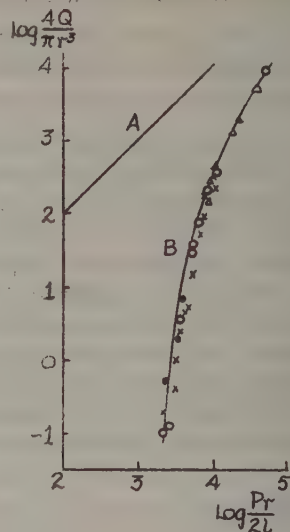
[7] P. A. Rebinder and E. E. Segalova, Proc. Acad. Sci. U.S.S.R., 71, 85 (1950).

[8] G. V. Vinogradov, Proc. Acad. Sci. U.S.S.R., 71, No. 3, 505 (1950).

[9] G. V. Vinogradov, V. P. Pavlov, and K. I. Klimov, Petroleum Economy, No. 1 (1948). G. V. Vinogradov and V. P. Pavlov, Trans. 2nd Conf. on Friction and Wear in Machines, 3, 311 (1949); Proc. Acad. Sci. U.S.S.R., 58, No. 7, 1391 (1947); Proc. Acad. Sci. U.S.S.R., 61, No. 6, 1049 (1948); G. V. Vinogradov and V. V. Sinitsin, Petroleum Economy, No. 12 (1950); No. 1 (1951).

[10] D. S. Velikovsky, Trans. Conf. on Viscosity of Liquids and Colloids, 1, 215 (1941).

[11] A. A. Trapeznikov and E. M Shlosberg, Proc. Acad. Sci. U.S.S.R., 62, No. 6, 791 (1948); collected papers, "New Methods of Investigation of Surface Phenomena", 1, 39 (1950).

[12] M. P. Volarovich, Colloid J., 9, No. 5, 325 (1947); M. P. Volarovich, D. M. Tolstoy, and E. P. Loshakova, Trans. 2nd Conf. on Friction and Wear in Machines, 1, 119 (1947).

[13] G. V. Vinogradov and K. I. Klimov, Trans. 2nd Conf. on Friction and Wear in Machines, 3, 300 (1949); J. Tech. Phys. 18, 355 (1948).

[14] V. P. Varentsov, Collected Papers, "Theory and Practice of the Production and Application of Lubricant Greases," State Fuel Technology Press, 93 (1939); Trans. Conf., Viscosity of Liquids and Colloids, 1, 197 (1941).

[15] P. A. Demchenko, A. V. Dumansky, and L. G. Demchenko, Colloid J., 14, 164 (1952).*

[16] R. D. Vold and M. L. Vold, J. Phys. and Coll. Chem., 52, 1424, 1948.

* See Consultants Bureau Translation, p. 183.

INFLUENCE OF OXIDATION OF RUBBERS ON THE KINETICS OF THEIR SWELLING

V. E. Gul, I. V. Khodzhaeva, and B. A. Dogadkin

The penetration of a solvent into the volume of a high polymer is caused jointly by the appearance of molecular interaction forces and change in the entropy of the system. The equilibrium state of a swollen high polymer placed in a solvent has been examined from this standpoint by numerous authors [1, 2]. Although the effect of the nature of the molecular interaction on the kinetics of swelling was recognized in several studies, this side of the question was developed little. Study of the rate of swelling of different rubbers in different solvents first required the development of a technique with the aid of which it is possible to measure the change of weight or volume of the swollen specimen without taking into account the effect of interaction with oxygen.
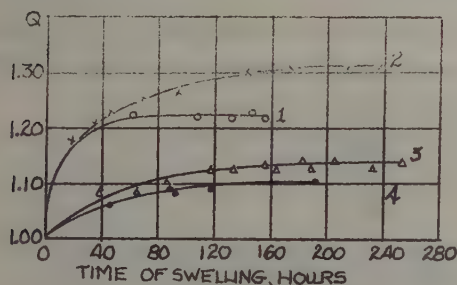
Fig. 1. Kinetics of swelling of SKS-30 rubber of various degrees of thermal aging in ethyl alcohol; 1 - before aging; 2 - aged 8 days; 3 - aged 15 days; 4 - aged 23 days.

As the observed picture may be distorted by structure formation and degradation processes in the polymer, caused by the action of atmospheric oxygen, developing simultaneously with swelling, appropriate experiments were carried out in order to take into account the effect of the action of oxygen. To elucidate the effect of oxidation of the rubber hydrocarbon on its swelling kinetics, the swelling kinetics of rubbers aged for different times was observed, and swelling rates of rubbers with and without added antioxidant were also determined.

Figures 1 and 2 show kinetic swelling curves for butadiene-styrene rubber thermally aged for different times in an air thermostat at 80°. In this experiment the solvent was so chosen that the absolute values of swelling were not too low, and in which the oxidized product swells more than the unaged. For this reason, the swelling kinetics of SKS-30 rubber of different aging times in ethyl methyl ketone, and in ethyl and methyl alcohols, was studied. As the aged specimens showed unlimited swelling in ethyl methyl ketone, the use of this solvent was abandoned. The degree of swelling of SKS-30 rubber of different aging times in ethyl alcohol was considerably less than in methyl alcohol, but the nature and the configuration of the swelling curves were much the same as in methyl alcohol. The testing technique consisted of cutting out eight specimens 3.5 x 3.5 mm from different places in the sheet of rubber and placing them in tall vessels with well-fitting ground glass covers, containing 5 ml of the solvent.

The degree of swelling Q was determined from the Equation :

$$Q = \frac{P_s}{P_e} \, ,$$

where P_s was the weight of the swollen specimen and P_e the weight of the specimen after evaporation of the solvent.

Examination of the swelling kinetics of SKS-30 rubbers of different degrees of aging in methyl alcohol shows that unaged rubber reaches the maximum degree of swelling in methyl alcohol in 30 hours, after which there is no significant change of Q during 110 hours of swelling.

All the rubbers subjected to aging show continuously increasing swelling in methyl alcohol. The kinetic swelling curves for these specimens are more smooth, and pass into straight lines after about 200 hours swelling.

Fig. 2. Kinetics of swelling of SKS-30 rubber of various degrees of thermal aging in methyl alcohol: 1 - before aging; 2 - aged 8 days; 3 - aged 15 days; 4 - aged 23 days.

There is a sharp increase of the degree of swelling in methyl alcohol for rubber aged for 8 days, followed by a greater degree for rubber aged 15 days. Further increase of the aging time to 23 days does not significantly alter the degree of swelling.

Similar behavior is observed for rubbers swollen in ethyl alcohol.

This variation of the swelling kinetics and of the absolute swelling values apparently indicates processes of degradation, structure formation, and accumulation of polar groups, taking place in divinyl-styrene rubber during aging. During the first 8 days of aging the predominant process is the breakdown of the molecular chains accompanied by accumulation of polar groups. Subsequently, the degradation process begins to be suppressed by joining of the rubber molecules with the formation of a spatial network. The formation of cross-links decreases the mobility of the chain molecules of rubber, and consequently some configurations become inaccessible. These latter changes in the rubber structure lead to a decrease of the entropy of swelling.

Further increase of the aging time of butadiene-styrene rubber apparently does not lead to any significant changes in its structure, and as a result the degree of swelling of the specimen after the 3rd aging period (Curve 4) is only slightly less than that of rubber after the 2nd aging period (Curve 3).

It should be noted that these results are in good agreement with the plasticity data (Defo) for these rubbers.

We give below the plasticity values (Defo) for butadiene-styrene rubbers of different aging times:

Before aging 350
Aged 8 days 1850
  " 15 "   2000
  " 23 "   2200

The sharp decrease of the plasticity (Defo) after 8 days aging indicates deep degradative processes which are subsequently increasingly masked by processes of cross-linking of the degraded molecules.

This peculiar type of structure formation does not greatly affect the plasticity (Defo) since it leads to the formation of branched molecules.

Thus, oxidative degradation and accumulation of polar oxidation products in butadiene-styrene rubber is accompanied by increased swelling in methyl and ethyl alcohols, while the process of structurization is accompanied by decrease of maximum swelling. The effect of oxidation of rubber on the kinetics of swelling is seen even more clearly in tests of butadiene-styrene rubber after previous removal of antioxidant and soluble oxidation products. Specimens of butadiene-styrene rubber were extracted with methyl alcohol, dried in a vacuum, and again subjected to swelling in methyl alcohol. The Graph (Figure 3) shows kinetic swelling curves for butadiene-styrene rubber containing Neozone D (nonextracted) and without antioxidant (extracted). These results show quite clearly the change in the

Fig. 3. Kinetics of swelling of SKS-30 rubber in methyl alcohol before (Curve 1) and after (Curve 2) preliminary extraction with methyl alcohol for 10 days.

nature of swelling of rubber after removal of substances which protect it from the oxidizing action of oxygen. Rubber which was not subjected to preliminary extraction reaches its maximum swelling in the first 20 hours, after which the degree of swelling does not change. If the antioxidant is removed from the rubber, the degree of swelling increases continuously and maximum swelling is only reached after 320 hours.

By a comparison of molecular weight values it is possible to follow the effect of structural changes which take place in butadiene-styrene rubber during its thermal aging, and the influence of these changes on the swelling of this rubber in methyl alcohol. As was shown by Dogadkin [3], the value of the molecular weight determined by any one method is not sufficient for drawing definite conclusions concerning the changes taking place in the rubber. It, therefore, became necessary to obtain molecular weight values determined by the viscosimetric method or by light scattering. The viscosity and light scattering methods for solutions were used for the determination of the molecular weights of butadiene-styrene rubbers of different degrees of aging. The viscosimetric molecular weight values were calculated from the formula:

$$[\eta] = kM^{\alpha},$$

where $[\eta]$ is the intrinsic viscosity, $\underline{M}$ is the molecular weight, $\underline{k}$ is a constant for butadiene-styrene copolymer solutions, equal to 5.4×10^{-4}; α is a constant equal to 0.66.

Figure 4 shows the variation of the molecular weight determined by viscosity and light scattering, with the time of aging of butadiene-styrene rubber in an air thermostat at 80°.

It follows from the results shown in Figure 4 that aging in these conditions is accompanied by increase of the weight-average molecular weight and decrease of viscosity due to the joining of chain fragments into branched formations.

The molecular weight, determined viscosimetrical-ly, decreased due to the fact that the branched molecules formed have a smaller effective volume and therefore result in a decreased solution viscosity. The viscosimetric molecular weights of rubbers aged for 0, 8, and 15 days were 217,000, 103,000, and 64,000 respectively.

Thus, it is confirmed that aging of butadiene-styrene rubber is accompanied by formation of spatial structures, which, at a certain stage of the oxidation, leads to an increase of the gel fraction content and to a decrease of the degree of swelling.

Fig. 4. Variation of molecular weight determined by the light scattering and relative viscosity methods for solutions of SKS-30 rubber, with aging time: 1) Molecular weight; 2) relative viscosity.

Figure 5 shows graphically the relationship between the gel fraction content and the aging time. Examination of this relationship shows that after 15 days of thermal aging appreciable cross-linking of the chain molecules occurs, which apparently produces a sharp decrease in the degree of swelling.

Fig. 5. Variation of the gel fraction content of SKS-30 rubber with aging time.

As the oxidation of butadiene-styrene rubber is accompanied by a change of structure which does not follow the oxidation in a regular manner (from the viewpoint of its effect on swelling), the effect of the oxidation process on swelling was also examined with natural rubber.

Figure 6 and 7 show the swelling kinetics of different specimens of natural rubber in methyl alcohol, and also the swelling kinetics of smoked sheet rubber, aged for 9 and 20 days at 80°.

The kinetic swelling curve for the 3rd specimen of rubber, which rises steadily, is worthy of attention. This type of curve is evidence of continuous oxidation of the polymer during swelling, as a result of which the degree of swelling increases continuously. It will later be shown that specimen 3 has, in fact, poor resistance to the action of oxygen, and, therefore, it readily reacts with the oxygen dissolved in methyl alcohol during the swelling process. This leads, on the one hand, to an accumulation of polar oxidized groups, and on the other, to formation of branched molecules of rubber, which increases the degree of swelling of the rubber. To confirm these views concerning the oxidative processes which take place during the swelling of rubber, a special experiment was performed on the swelling of natural rubber with and without antioxidant.

The rubber was dissolved in benzene and reprecipitated, and the pure rubber hydrocarbon so obtained, containing no antioxidants, was subjected to swelling in methyl alcohol. All the operations in the preparation of pure hydrocarbon of natural rubber were carried out in an atmosphere of purified nitrogen. Figure 8 shows data on the swelling kinetics of the pure hydrocarbon and of rubber containing natural protective substances. These data confirm the views put forward above. The swelling curve for the pure hydrocarbon is smooth and gradually passes into a straight line, and it proved impossible to reach the maximum swelling, while the original rubber reaches its limit of swelling after about 70 hours.

Similar behavior is shown, as can be seen from Figure 7, also by rubber subjected to thermooxidative action for a definite period. Figure 7 shows kinetic swelling curves for natural rubber, not aged and aged at 80°

Fig. 6. Kinetics of swelling of different specimens of smoked sheet rubber in methyl alcohol.
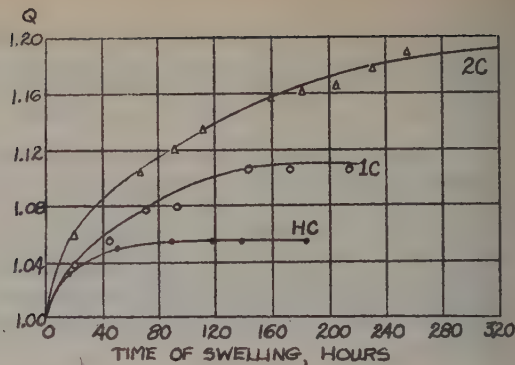

Fig. 7. Kinetics of swelling of smoked sheet rubber after different times of thermal aging: <u>HC</u> - nonaged rubber; <u>1C</u> - aged 9 days; <u>2C</u> - aged 20 days.

for 9 and 20 days. The rubber, the molecules of which did not undergo the degradative action of oxygen, has a lower degree of swelling than the aged rubber of lower molecular weight. In addition, the swelling curve for the specimen aged for 20 days rises steadily, which is evidence that the swelling process is accompanied by the addition of oxygen to the rubber. This is a consequence of the fact that preliminary aging led to impoverishment of the rubber in its natural antioxidants. It will be shown later that this rubber has practically no induction period in oxidation at 143°, while the specimen not subjected to preliminary aging has an 11-hour induction period at the same temperature.

The increase of the degree of swelling of natural rubber with aging must be attributed to the effect of accumulating polar groups of atoms. Accumulation of polar groups of atoms increases both the equilibrium degree of swelling (due to the energy factor) and also the rate of penetration of the solvent into the volume of the polymer.

To confirm our views concerning the influence of oxidative processes on the swelling kinetics of rubber, we determined the oxidation kinetics of the natural rubber studied, and also determined its molecular weight. The oxidation kinetics was studied by the barometric method at 143° in the Dufraisse apparatus. The results of the experiments are shown in Figure 9 and 10.

It is seen from Figure 9 that the rubber specimens studied have different induction periods. The greatest induction period is shown by

Fig. 8. Kinetics of swelling of natural rubber in methyl alcohol: 1) Smoked sheet containing natural substances; 2) pure hydrocarbon of smoked sheet rubber.

specimen <u>1</u> - about 12 hours, which is followed by specimen <u>4</u>, about 8 hours, then specimens <u>5</u> and <u>2</u>, about 4-6 hours, and finally, the smallest induction period is shown by specimen <u>3</u>, which is apparently not so well protected by natural antioxidants as the other specimens.

As regards rubber subjected to preliminary aging, it can be seen from Figure 10, that the induction period is less as the preliminary aging time of the rubber is greater. Rubber aged for 20 days has practically no induction period. Rubber aged for 9 days has an induction period of about 4 hours, and unaged rubber, 10 hours.

We now turn to an examination of the molecular weights of the natural rubbers studied. It can be seen from the data of Table 1 that the rubbers lie in the following order by their molecular weight values: specimen <u>5</u> has the greatest average molecular weight. Specimen <u>4</u> has, like specimen <u>5</u>, a high molecular weight, determined by the osmotic method. Specimen <u>2</u> is a little below specimen <u>5</u>; specimen <u>1</u> has the same value of molecular weight, determined by the osmotic method. The lowest values of molecular weight determined by the osmotic and viscosimetric methods are shown by Specimen 3.

We are of the opinion that the conditions of formation of rubber in the plant ensure in all cases an approximately equal degree of branching of the macromolecules, if it occurs at all. Therefore, the difference between the
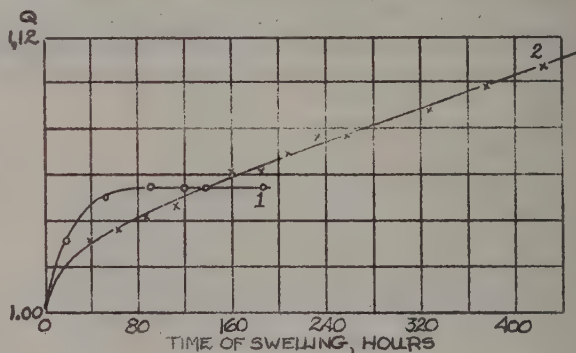
Fig. 9. Kinetics of oxidation of different specimens of smoked sheet rubber by molecular oxygen at 143°.

molecular weights determined by the osmotic and viscosimetric methods is mainly due to the polydispersity of the product. Accordingly, the least polydisperse specimen must be considered specimen 5, for which the viscosimetric and osmometric molecular weights are practically equal. The most polydisperse are specimens 1 and 4, the osmotic and viscosimetric molecular weights of which differ considerably. All the above considerations are only valid if the ratio of sol to gel fractions is approximately the same for all the rubbers. As can be seen from the data of Table 2, the gel fraction content in the smoked sheet specimens varies from 3 to 6% which, in our view, could not significantly affect either the molecular weights of the soluble fraction, or the other physico-chemical properties of the rubber.

Investigations showed (see Figures 6 and 7) that the natural rubbers studied, having greater molecular weights, have lower maxima of swelling in methyl alcohol.

TABLE 1
Molecular weights of specimens 1, 2, 3, 4 and 5 of smoked sheet rubber, and of smoked sheet rubber not subjected to aging and aged for 9 and 20 days at 80°, determined by the visocity, osmometric, and light scattering methods.

Rubber specimen	Viscosity method	Osmometric method	Light scattering method
1	330 000	270 000	—
2	240 000	270 000	—
3	160 000	180 000	—
4	270 000	310 000	—
5	310 000	290 000	—
HC	380 000		380 000
1C	310 000		280 000
2C	210 000		100 000

Note. HC - rubber not subjected to aging; 1C - rubber aged for 9 days; 2C - rubber aged for 20 days.

Fig. 10. Kinetics of oxidation of smoked sheet rubber after different periods of thermal aging at 143°; 1) aged 9 days; 2) aged 20 days; 3) nonaged rubber.

The greatest differences between the molecular weights of the rubbers were most probably the result of the action of oxygen. In this connection, specimen 3, with a high content of polar oxidized groups, has the lowest molecular weight. Specimens 4 and 5, with the highest molecular weights, which is evidence of their low degree of oxidation, show the least swelling in methyl alcohol – their swelling curves lie below all the others. Specimen 1 occupies an intermediate position.

TABLE 2
Gel fraction content of the smoked sheet specimens studied.

Specimen	1	2	3	4	5
Gel fraction, %	5.9	4.3	2.5	3.7	5.3

Thus, the experimental material presented here supports the supposition that there is a definite relationship between the degree of oxidation of natural rubber and the value of the maximum swelling in polar solvents. The greater the degree of oxidation of the rubber, the greater is the value of the maximum swelling in methyl alcohol.

It must be noted that swelling in a polar solvent excludes partial solubility of the polymer, and consequently the changes in the rubber as the result of the action of oxygen and of differences in the molecular characteristics are not masked by superimposition of swelling and solution processes. In addition, in these experimental conditions, the non-rubber, oxygen-containing impurities, which have considerably lower molecular weights, are taken up by the methyl alcohol, and therefore, the swelling value found is characteristic of the rubber hydrocarbon itself. Numerous experiments on the swelling of natural rubber showed that on the average, methyl alcohol takes up about 3% of the weight of the specimen taken, so that most of the low-molecular non-rubber impurities are washed out.

The swelling of rubber in a polar solvent can be used to obtain information on the stability of rubber to the action of oxygen. In this case the swelling process may be considered as an accelerated test method for the resistance of rubber to aging. This method has the advantage over those previously known (aging in a thermostat, aging in an oxygen bomb) of being sufficiently rapid at room temperature, and to obtain information on the behavior of rubber in storage it is not necessary to determine the temperature coefficients of the reactions which occur during aging.

In the swelling process the solvent molecules penetrate among the polymer molecules, and so facilitate the access of oxygen dissolved in the solvent to the most reactive regions of the rubber molecules — the double bonds.

Since the addition of oxygen is not instantaneous, but takes time, the degree of swelling also increases continuously during the whole time the rubber is in contact with the swelling agent. In consequence, the kinetic swelling curve for rubber, when the interaction with oxygen takes place beyond the region characteristic of rapid diffusion, has a practically linear region, which reflects a slow change of the degree of swelling as the result of oxidative processes.

If the rubber is effectively protected by natural antioxidants, the addition of oxygen at normal temperature is very slow, and the above effect is not observed. The swelling maximum is attained in a relatively short time, and the degree of swelling subsequently does not alter.

Thus, with the kinetic swelling curves shown in Figures 1 - 8 it is possible to evaluate both the degree of oxidation of the rubbers studied, or the functionally related length of the molecular chain, and also their capacity to withstand the oxidative action of oxygen.

The absolute values of the maximum swelling (in consequence of the absence of oxidative processes) depend on the molecular characteristics of the high polymer, such as the molecular weight, polydispersity, and the ratio of gel and sol fractions. In addition, the degree of swelling is also determined by the molecular interaction between the solvent and the polymer. From this point of view the composition of the impurities which pass into solution during swelling, and also the degree of oxidation of the rubber, are by no means insignificant.

SUMMARY

1. The swelling of rubber in conditions of interaction with oxygen is represented by a kinetic curve which has a sharply rising region, which corresponds to diffusional penetration of the solvent, followed by a practically straight region, which reflects a slow change of the degree of swelling as the result of oxidative processes accompanying swelling.

2. The swelling maximum of rubber in a polar solvent, if the effect of oxidation is excluded, characterizes the molecular weight, the polydispersity, and other structural characteristics of the rubber. The inclination of the straight portion of the kinetic swelling curve may serve as a measure of the stability of the rubber to oxidation.

LITERATURE CITED

[1] S. Papkov, V. A. Kargin, and Z. Rogovin, J. Phys. Chem., 10, 607 (1937); 13, 206, (1939); A. A. Tager and V. A. Kargin, Acta phys. chim. 14, 6, 703, 1941; Trans. Faraday Soc. 38, 1947, 1942; A. A. Tager and V. A. Kargin, Colloid J., 10, No. 6, 455 (1948).

[2] S. M. Lipatov, Colloid J., 8, 1-2, 73, 1946.

[3] B. A. Dogadkin, M. I. Arkangelskaya, and I. G. Soboleva, Investigations in the Field of High Polymers, 253 (1949).

THE THIOXOTROPY OF SOILS AND THE VIBRATIONAL METHOD

B. M. Gumensky

During the last 3-4 years vibrators have been extensively used in building construction for pile driving; they are also being used for drilling loose and clay soils. Thus, a new type of operation has appeared — vibrational pile driving and vibrational drilling of soils, which is being used increasingly each year, as even during the development period these processes enabled their operating time and cost to be shortened several times. It may confidently be said that when these methods have been fully adopted and developed, their value will increase still further. At the same time, the literature on these methods [1-4], contains no definite data on the nature of the processes which take place during the operation in clay soils. There are only very broad generalizations that in such cases there is a great decrease of the shear resistance of the soils, so that the pile or the vibrator cylinder can sink into the soil by the action of its own weight and the weight of the vibrator, easily, "like a knife through butter". In this connection the view of one of the specialists in the field of application of vibrators for driving piles and vibrational drilling, D. D. Barkan, is of interest. In his book on the vibration of building foundations [5] Barkan writes: "The physical processes which cause changes in the properties of soil during vibration, and in particular, the decrease of resistance to external loads, are still not definitely clarified. Apparently, under the action of vibration, the physical effects which occur in the soil produce a decrease in the forces of friction and cohesion in the soil."

It is natural that in the absence of clear concepts of the nature of the processes which take place in these cases it is not possible to control them deliberately, to develop the appropriate construction of vibrators, and to establish a rational technology of the operations in relation to the conditions in which they are carried out.

In our studies of clay soils in vibrational drilling, we set ourselves the problem of clarifying the nature of the processes which take place. With this aim vibrational drilling was carried out in clay soils of different granulometric compositions and physical states, and also of different origins and ages.

Observations show that in vibrational drilling, and also in vibrational pile driving, etc., the clay soils during vibration, that is, temporarily, change their physical state and pass in some cases from a solid, in others, from a semisolid, and in yet others, from a plastic state, into a viscofluid state (to different extents), depending on the granulometric composition, the strength of the structural bonds, consistency, etc., and also the power and special properties of the vibrator and its operating conditions.

We put forward the view that the thixotropic effects which occur in the vibration of clay soils are due to the transition of physically bound water into free water [2]. The appearance of the latter produces the above-mentioned decrease in the resistance to shear of clay soils, as a result of which the vibrator cylinder sinks into them. The time for the vibrator cylinder to sink in to a depth of 2 meters is measured in minutes, and sometimes even less, depending on a number of conditions, while in drilling by hand this requires several hours.

Fig. 1. Diagram of a divided vibrator cylinder.

The thixotropic effect, as is known, consists of two reversible processes: transition of a gel to a sol, and of a sol to a gel. The state of affairs described above represents the transition of a gel to a sol. Transition from a sol to a gel is observed after the cessation of vibration of clay soils, as can be seen from the following observations and investigations. During vibration, in the vibrator cylinder extracted from the borehole, containing lower Cambrian semihard clay which, as was established by special investigations, contained only physically bound water, a film of free water appeared on the clay serface and conferred a luster to it. As soon as the vibration ceased, however, the film disappeared at once, the free water passed into physically bound water, and the soil changed its physical state and became dull
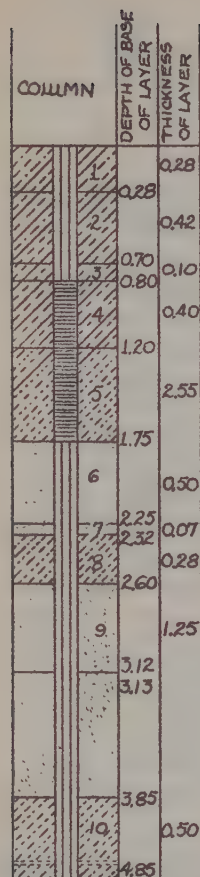
Fig. 2. Structure of the soil in a river valley (scale 1:25): 1) Brown loam; 2) light brown loam; 3) loam and gravel; 4) brown loam; 5) sandy loam, reddish-brown in color, with layers of greyish loam in slanting beds; 6) fine-grained micaceous moist reddish brown sand; 7) medium-grained brown sand; 8) slightly moist reddish brown sandy loam; 9) fine-grained, pale yellow sand with layers of dark sand; 3.12 - 3.13 m — sooty layer; 10 — sandy loam, light brown, slightly moist; a layer of medium-grained sand at a depth of 4.25 - 4.27 m.

in appearance. In this case 1-2 minutes or less were necessary before the soil, which previously was so viscous that it flowed freely but slowly from the cylinder, like pitch, became dense and lost all power of flow. Furthermore, it became so compact that a great effort was needed to extract it from the cylinder. A similar state of affairs was found in vibratory drilling of toughly plastic moraine soils and other types of deposits.

In our view the sol—gel transition described above also depends on a process of transformation of water, but one which occurs in the reverse direction: free water passes into physically bound water.

Confirmation of this view, which arose as the reult of observations of vibratory drilling of clay soils in 1952, is given by the results of 1953 observations, when about a dozen boreholes were made on an experimental site by the vibratory method. In a number of cases the holes were made with the aid of a divided cylinder 1 m in length (Figure 1). It is seen from the figure that the divided cylinder consists of two halves making a hollow cylinder with an inner diameter of 102 mm. During the boring these halves are joined at the top by a head and at the base by a shoe. The vibratory drilling was carried out through an alluvial layer making up a terrace above the river in a valley. The structure of this layer is shown diagrammatically in Figure 2, prepared by N. M. Markova.

It is seen from Figure 2 and the appended descriptions of the soils that a peculiarity of the layers of alluvial loams is the presence of thin layers of sand.

When the divided cylinder described above was raised, in a number of instances a thin stream of water was observed, flowing from a number of points of the gap separating the cylinder into two halves, onto their outer surface. This gave observers the impression that water-bearing layers, the soils in which were saturated with water, had been passed in the drilling process. However, no free water was found in the borehole. In addition, when the soil samples extracted by the divided cylinder were examined, they were found to be so "dry" that there could be no question of their being water-bearing. It is important to note that the flow of water was correlated with the sites of the clay layers.

The question arises: what is the source of the free-flowing water at a number of points in the gap ? If we accept the above view concerning the transition of physically bound water into free water during the vibration of clay soils, and conversion of the free water into physically bound water when vibration ceases, then it appears that this view is once again confirmed by these data on the flow of free water from the gap. Confirmation of this viewpoint is seen in the data given in the Table, obtained from one of the experimental sites at the place indicated above — where the flow of free water was observed through the gap in the divided cylinder.

TABLE

Data on Natural Moisture of Soils in   Borehole No. 3.

Sampling depth, in m	Natural moisture content, %		Loss %	Sampling depth, in m	Natural moisture content, %		Loss %
	Drilled hole	Borehole by vibratory drilling			Drilled hole	Borehole by vibratory drilling	
1.05 - 1.10	25.1	23.5	1.6	1.35 - 1.40	19.65	15.20	4.45
1.15 - 1.20	19.6	17.9	1.7	1.45 - 1.47	20.3	16.00	4.3
1.25 - 1.30	18.65	17.75	0.90	1.55 - 1.60	21.3	20.8	0.5
				1.65 - 1.69	17.4	16.7	0.7

It is likely that if there was not transition of physically bound water to free water during the vibration of clay soils, then the same natural moisture content would

be expected both in the drilled hole and in the borehole made by vibratory drilling, in samples from the same depths, at which the flow of free water was observed. However, the table shows that the natural moisture content of the same soils is considerably higher in the drilled than in the vibrodrilled hole.

After this, the question may arise, why no flow of water takes place in drilling with an undivided cylinder (Figure 3), as was shown by special experiments on vibratory drilling with such a cylinder in the same soils as were bored with the divided cylinder. The above effect of flow of free water was not observed with the undivided cylinder; because the free water which was released as the result of the transformation of the physically bound water, was able to become, and in fact immediately did become, bound by the soil which was on the surface at the opening. In the divided cylinder, on the other hand, this free water had an outlet to the outside through the gap, and it passed through this, covering the outer surface of the halves which constitute the cylinder. By passing to the outside, the water decreased the natural moisture content of the soil in the vibratory-drilled hole, as was shown by the investigations (see Table).

Fig. 3. Diagram of undivided cylinder.

SUMMARY

In the vibration of clay soils, thixotropic changes occur, caused by the transition of bound water into free water. The presence of the latter sharply lowers the shear resistance forces of the soils, which is the reason why various bodies such as piles, etc., can be sunk into them.

LITERATURE CITED

[1] D. D. Barkan, Hydrotech. Construction, No. 5, 7 (1951).

[2] B. M. Gumensky and N. S. Komarov, Vibratory Boring of Soils in Railroad Prospecting, Rail Transport Press (1953).

[3] O. A. Savinov, A. Ya. Luskin, V. M. Pazhi, M. G. Tseitlin and M. L. Sheikov, Bldg. Industry, No. 10, 8 (1953).

[4] P. S. Yatsenko, Use of Vibratory Equipment for Hole Boring, Collected Papers "River Transport," River Press (1951).

[5] D. D. Barkan, Dynamics of Foundations, Machinery Construction Press (1948).

The V. N. Obraztsov Institute for
Railroad Transport Engineers
Leningrad

THEORY OF HETEROCOAGULATION, INTERACTION, AND COHESION OF UNLIKE PARTICLES IN SOLUTIONS OF ELECTROLYTES*

B. V. Deryagin

1. In previous papers we developed a theory of the interaction of particles [1] and the coagulation of hydrophobic colloids, which led to the establishment of criteria for the cohesion of particles and for the coagulation of hydrophobic sols and suspensions, both weakly charged [2] and strongly charged [3]; the criteria found provided a theoretical basis for the further developed rules of Hardy and Schulze [3] and Wo. Ostwald [3], and also of Eilers and Korff** [5, 7].

The basis of this theory was the calculation for the symmetrical case of interaction in a solution of electrolyte (with van der Waals forces taken into account) between particles of the same kind, charged at the same potential.

However, the development of the theory of heterocoagulation — the coagulation of heterogeneous mixtures of particles, and also of the theory of adhesion of particles to surfaces of different nature — adagulation***, according to Smoluchowsky [8] demands the examination of a general "nonsymmetrical" case. In this case, the sign (direction) can change, not only of the electrostatic interaction force, but also of the resultant van der Waals interaction.

Let us first examine a plane-parallel layer, of thickness h, of a solution of a binary electrolyte between the surfaces of plates 1 and 2, charged to the potentials ψ_1 and $\psi_2 > \psi_1$. We assume that the potential in the electrolyte solution obeys the equation:

$$\frac{d^2\psi}{dx^2} = \frac{a}{2}(e^{z_1 b\psi} - e^{-z_2 b\psi}), \qquad (1)$$

where $b = \frac{e}{kT} = \frac{F}{RT}$; e is the electronic charge; F is the Faraday number; k is the Boltzmann constant; R is the gas constant; T is the absolute temperature; z_1 and z_2 are the electrovalencies of the anion and the cation.

$$a = \frac{8\pi}{D} eNc = \frac{8\pi}{D} ez_1 n_1 N\gamma = \frac{8\pi}{D} ez_2 n_2 N\gamma,$$

where D is the dielectric constant; N is the Avogadro number; c is the concentration in g-equiv. per 1 cm^3; γ is the concentration in mole per 1 cm^3; n_1 and n_2 are the dissociation numbers.

Equation (1) is transformed into the form:

$$\frac{d^2\varphi}{d\chi^2} = \frac{1}{2}(e^\varphi - e^{-\beta\varphi}), \qquad (2)$$

by the introduction of the parameter $\beta = \frac{z_2}{z_1}$ and the dimensionless variables:

---

* The contents of Part 1 are based on work carried out jointly with V. G. Levich [15].

** The derivation of these rules by Verwey and Overbeek (the second of these rules without an indication of its kinship with the Eilers and Korff rule) was published considerably later [4] without citation of our work and communications, and with erroneous stressing of the authors' priority (pages VI and 188).

*** By heterocoagulation we understand the cohesion, as the result of Brownian movement, of particles heterogeneous in nature, as happens, for example, in mixtures of two sols; by adagulation it is appropriate to understand the adhesion of Brownian particles to macrosurfaces or fibers and other macrosurfaces, the Brownian movement of which may be neglected because of their large mass. In cases when it is important to stress that the nature of the surfaces of the Brownian particles and the "macroparticles" differs (it may also be the same in some instances) it is logical to use the term "heteroadagulation". It is then important to stress that the terms "heterocoagulation" and "adagulation" are by no means equivalent — the first stresses the different nature of the particle surfaces, and the second, the difference in their dimensions and masses, and consequently in their Brownian mobility.

$$\varphi = z_1 b\psi, \qquad \chi = \frac{x}{d} = \kappa x, \tag{2'}$$

where

$$\kappa = \frac{1}{d} = \sqrt{abz_1}. \tag{2''}$$

From Equation (2), by integration, we have:

$$\left(\frac{d\varphi}{d\chi}\right)^2 = e^\varphi + \frac{1}{\beta}e^{-\beta\varphi} \tag{3}$$

where the value of $\underline{C}$ must be so chosen that the difference $\chi_1 - \chi_2$ of the values of $\chi = \chi_1$ and $\chi = \chi_2$, for which $\varphi = \varphi_1 = z_1 b\psi_1$ and $\varphi = \varphi_2 = z_1 b\psi_2$ should be equal to $H = h/d$. As was shown previously [1], the repulsion between the plates per unit area, $\underline{P}$, is:

$$P = \frac{kTNc}{z_1}\,\omega, \tag{4}$$

where

$$\omega = C - 1 - \frac{1}{\beta} \tag{5}$$

Fig. 1. Schematic representation of a group of isodynamic curves for the case of the interaction, in a solution of electrolyte, of surfaces the potentials of which have given unequal values.
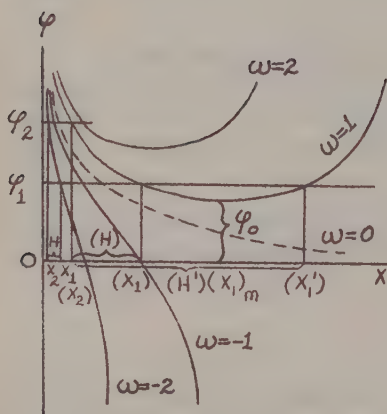
Instead of establishing the relationship between $\underline{H}$ and ω by determination of values of ω corresponding to various values of $\underline{H}$, it is much simpler, although less natural in the physical sense, to determine $\underline{H}$ as a function of ω (for any given values of φ_1, φ_2 and of the parameter β). For this purpose let us examine in Figure 1 a group of integral curves $\varphi = \varphi(\chi, C)$ for Equation (3), passing through a point with the coordinates $\chi = 0$, $\varphi = \infty$, that is, asymptotic to the χ-axis and corresponding to different values of $\underline{C}$ and therefore to different values of ω.

For the case $\omega < 0$, $d\varphi/d\chi$ is not equal to zero for any values of φ, and therefore the integral form of Equation (3) may be written in the form:

$$\chi = \int_\varphi^\infty \frac{d\varphi}{\sqrt{e^\varphi + \frac{1}{\beta}e^{-\beta\varphi} - 1 - \frac{1}{\beta} - \omega}} \tag{6}$$

When $\omega = 0$, the integral curve (shown by a dotted line in Figure 1) also has the abscissa axis as an asymptote.

When $\omega > 0$, each integral curve has a minimum of height $\varphi = \varphi_0$, determined from the equation:

$$e^{\varphi_0} + \frac{1}{\beta}e^{-\beta\varphi_0} = C = 1 + \frac{1}{\beta} + \omega, \tag{7}$$

which in this case always has one positive root.

The abscissa of the minimum is equal to:

$$\chi_m = \int_{\varphi_0}^\infty \frac{d\varphi}{\sqrt{e^\varphi + \frac{1}{\beta}e^{-\beta\varphi} - e^{\varphi_0} - \frac{1}{\beta}e^{-\beta\varphi_0}}} \tag{8}$$

For $\chi \leqslant \chi_m$ the integral of Equation (3) is also given by Equation (6).

For $\chi > \chi_m$

$$\chi' = \chi_m + \int_{\varphi_0}^\varphi \frac{d\varphi}{\sqrt{e^\varphi + \frac{1}{\beta}e^{-\beta\varphi} - 1 - \frac{1}{\beta} - \omega}}. \tag{9}$$

404

$$\chi' = 2\chi_m - \int_{\varphi}^{\infty} \frac{d\varphi}{\sqrt{e^{\varphi} + \frac{1}{\beta} e^{-\beta\varphi} - 1 - \frac{1}{\beta} - \omega}} \qquad (9')$$

$$\chi' = \chi + 2 \int_{\varphi_0}^{\varphi} \frac{d\varphi}{\sqrt{e^{\varphi} + \frac{1}{\beta} e^{-\beta\varphi} - 1 - \frac{1}{\beta} - \omega}} \qquad (9'')$$

By intersection of one of these "isodynamic" curves, corresponding to a definite value of ω = const., with straight lines parallel to the abscissa axis, drawn at the levels $\varphi = \varphi_1$ and $\varphi = \varphi_2$, we obtain the possible abscissas of the corresponding surfaces χ_1 and χ_2, the difference of which gives $\underline{H}$.

For the case $\omega \leqslant 0$ each such straight line intersects the isodynamic curve at one point, and from Equation (6) we have:

$$H = \chi_1 - \chi_2 = \int_{\varphi_1}^{\varphi_2} \frac{d\varphi}{\sqrt{e^{\varphi} + \frac{1}{\beta} e^{-\beta\varphi} - 1 - \frac{1}{\beta} - \omega}} \qquad (10)$$

Evidently, when $\omega \longrightarrow \infty$, $H \longrightarrow 0$, in accordance with the asymptote law:

$$\omega \approx -\frac{(\varphi_2 - \varphi_1)^2}{H^2} \qquad (11)$$

When $\omega = 0$ (absence of interaction):

$$H = H_0 = \int_{\varphi_1}^{\varphi_2} \frac{d\varphi}{\sqrt{e^{\varphi} + \frac{1}{\beta} e^{-\beta\varphi} - 1 - \frac{1}{\beta}}} \qquad (12)$$

When $\omega > 0$, attraction passes into repulsion. In that case each straight line φ = const. $> \varphi_0$ will cut the isodynamic curve twice.

The intersections lying to one side (for example, the left) of the minimum on the isodynamic curve will give the values of $\underline{H}$, which can also be found from Equation (10).

The intersections lying on different sides of the minimum will give a greater value of $\underline{H} = \underline{H}''$, which, from (6) and (9), is equal to:

$$H' = \chi_1' - \chi_2' = 2\chi_m \int_{\varphi_1}^{\infty} \frac{d\varphi}{\sqrt{e^{\varphi} + \frac{1}{\beta} e^{-\beta\varphi} - 1 - \frac{1}{\beta} - \omega}} -$$

$$- \int_{\varphi_2}^{\infty} \frac{d\varphi}{\sqrt{e^{\varphi} + \frac{1}{\beta} e^{-\beta\varphi} - 1 - \frac{1}{\beta} - \omega}} \; . \qquad (13)$$

It is easily seen that at the value of $\varphi_0 = \varphi_1$, and therefore when

$$\omega = \omega_m = e^{\varphi_1} + \frac{1}{\beta} e^{-\beta\varphi_1} - 1 - \frac{1}{\beta} \; , \qquad (14)$$

the straight line $\varphi = \varphi_1$ will touch the isodynamic curve and $\underline{H}'$ will be equal to $\underline{H}$. When $\omega > \omega_m$, the straight line $\varphi = \varphi_1$ will not cut the isodynamic curve, and therefore the corresponding values cannot be obtained for any value of $\underline{H}$.

Thus, for any values of φ_1 and φ_2 of the same sign, the force of repulsion reaches a maximum at a certain value of $\underline{H}$:

$$H = H_m = \int_{\varphi_1}^{\varphi_2} \frac{d\varphi}{\sqrt{e^{\varphi} + \frac{1}{\beta} e^{-\beta\varphi} - e^{\varphi_1} - \frac{1}{\beta} e^{-\beta\varphi_1}}} \qquad (15)$$

Figure 2 is a schematic representation of the dependence of ω on H, which follows from the above analysis.

The case when $\varphi_2 > 0 > \varphi_1$, is more trivial, when ω is negative for all values of H, and steadily increases in absolute magnitude with decrease of H.

For the case ($\beta = 1$) the relationship between H and ω is expressed by elliptic integrals, and we have $\omega \leq 0$ when from Formula (10):

$$H = k \int_{\frac{1}{\mathrm{ch}\frac{\varphi_2}{2}}}^{1/\mathrm{ch}\left(\frac{\varphi_1}{2}\right)} \frac{du}{\sqrt{1-u^2}\sqrt{1-k_1^2 u^2}} , \qquad (16)$$

where $k_1^2 = 1 + \dfrac{\omega}{4} < 1$.

For H' we have from Equation (13):

$$H' = k \int_{u_1}^{1} \frac{du}{\sqrt{1-u^2}\sqrt{1-k^2 u^2}} + \int_{u_2}^{1} \frac{du}{\sqrt{1-u^2}\sqrt{1-k^2 u^2}} \qquad (17)$$

where

$$k = \frac{1}{\mathrm{ch}\frac{\varphi_0}{2}} , \qquad u_1 = \frac{\mathrm{ch}\frac{\varphi_2}{2}}{\mathrm{ch}\frac{\varphi_1}{2}} , \qquad u_2 = \frac{\mathrm{ch}\frac{\varphi_0}{2}}{\mathrm{ch}\frac{\varphi_2}{2}} .$$

Figures 3 and 3a show the exact form of the family of curves for $\omega = \omega(H, \varphi_1)$ for the case $\beta = 1$ and for the particular values $\varphi_2 = 10$ (which is close to ∞) and $\varphi_2 = 1$ (Figure 3a *). The thickness H_0 at which ω changes sign, is equal to:

$$H_0 = \int_{\varphi_1}^{\varphi_2} \frac{d\varphi}{\sqrt{e^{\varphi} + e^{-\varphi} - 2}} = \frac{1}{2} \ln \left\{ \frac{\left(e^{\frac{\varphi_2}{2}} - 1\right)\left(e^{\frac{\varphi_1}{2}} + 1\right)}{\left(e^{\frac{\varphi_2}{2}} + 1\right)\left(e^{\frac{\varphi_1}{2}} - 1\right)} \right\} \qquad (18)$$

For ω_m we have

$$\omega_m = e^{\varphi_1} + e^{-\varphi_1} - 2 = 4\mathrm{sh}^2 \frac{\varphi_1}{2} , \qquad (19)$$

and for H_m:

$$H_m = k \int_{u_0}^{1} \frac{du}{\sqrt{(1-u^2)(1-k^2 u^2)}} \qquad (20)$$

where

$$k = \frac{1}{\mathrm{ch}\frac{\varphi_1}{2}} , \qquad u_0 = \frac{\mathrm{ch}\frac{\varphi_1}{2}}{\mathrm{ch}\frac{\varphi_2}{2}} \qquad (21)$$

For the case $\varphi_1 < \varphi_2 \ll 1$ and any value of β instead of (7), (16), (17), (18), (19) and (20), we have:

$$\omega = \left(\frac{1+\beta}{2}\right) \varphi_0^2 \qquad (22)$$

Fig. 2. Forces of repulsion between unequally charged surfaces in a solution of electrolyte as a function of the distance between them (schematic).

---

* Figure 3a also shows curves for which $\varphi_1 > \varphi_2$.
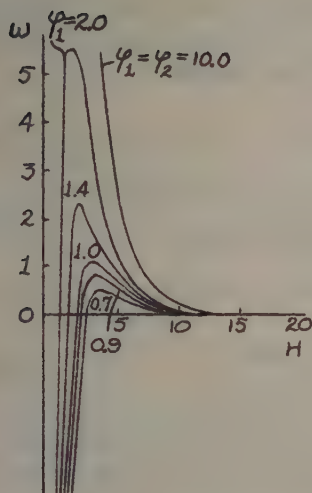
Fig. 3   Fig. 3a

Fig. 3. Specific repulsion as a function of distance (isotherms of the electrical component of the wedging pressure) for a highly charged plane and different values of the potential of the other plane in a solution of a symmetrical electrolyte (exact graph).
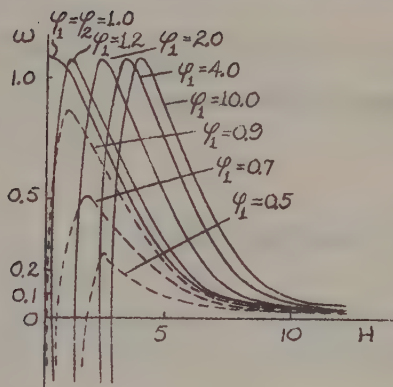
Fig. 3a. Specific repulsion as a function of distance for a weakly charged plane and different values of the potential φ_1 of the other plane in a solution of a symmetrical electrolyte (exact graph).

$$H = \ln \frac{\left(\varphi_2 + \sqrt{\varphi_2^2 - \omega \dfrac{2}{1+\beta}}\right)}{\left(\varphi_1 + \sqrt{\varphi_1^2 - \omega \dfrac{2}{1+\beta}}\right)}, \tag{23}$$

$$H' = \ln\left(\frac{\varphi_1}{\sqrt{\omega}} + \sqrt{\frac{\varphi_1^2}{\omega} - \frac{2}{1+\beta}}\right)\left(\frac{\varphi_2}{\sqrt{\omega}} + \sqrt{\frac{\varphi_2^2}{\omega} - \frac{2}{1+\beta}}\right) \tag{23'}$$

$$H_0 = \frac{1}{2}\ln\frac{\varphi_2}{\varphi_1}, \tag{24}$$

$$\omega_m = \left(\frac{1+\beta}{2}\right)\varphi_1^2 \tag{25}$$

$$H_m = \ln\left(\frac{\varphi_2}{\varphi_1} + \sqrt{\left(\frac{\varphi_2}{\varphi_1}\right)^2 - 1}\right). \tag{26}$$

2. The force of interaction N of any convex charged surfaces can be found from the general formula derived previously [5]:

$$N = G \int_y^\infty P(h)\,dh = Gd\,\frac{kTNc}{z}\int_Y^\infty \omega(H)\,dH, \tag{27}$$

where y is the width of the gap at its narrowest point, $Y = y/d$; G is a form factor which depends on the radius of curvature of both surfaces near the region of proximity and on the mutual orientation of their principal normal sections; for the case of two spheres of radius r, $G = \pi r$. Formula (27) is valid when the radii of curvature are much greater than the radius of the force of interaction between the surfaces:

$$(r \gg d). \tag{28}$$

Without giving all the calculations, we will restrict ourselves to reporting the following results.

With values of φ_1, and φ_2 of the same sign, the value of $\underline{N}$ increases with decrease of $\underline{y}$ and $\underline{Y}$, and reaches a maximum value of $N = N_m$, the abscissa $\underline{Y_m}$ of which is evidently equal to $\underline{H_0}$ in Equations (12), (18), and (24), and then decreases, changing sign and tending at $h \longrightarrow 0$ to $(-\infty)$ according to the formula:

$$N = -Gd^2 \frac{kTNc}{z} \frac{(\varphi_2 - \varphi_1)^2}{y} \tag{29}$$

The height of the maximum is

$$N_m = Gd \frac{kTNc}{z} \int_{Y_m = H_0}^{\infty} \omega(H)\, dH = Gd \frac{kTNc}{z} \int (H' - H)\, d\omega, \tag{30}$$

but, according to (10), (13), and (9"):

$$H' - H = \chi_1^i - \chi_1 = 2 \int_{\varphi_2}^{\varphi_1} \frac{d\varphi}{\sqrt{e^{\varphi} + \frac{1}{\beta} e^{-\beta\varphi} - 1 - \frac{1}{\beta} - \omega}} \tag{31}$$

consequently:

$$N_m = 2Gd \frac{kTNc}{z} \int_0^{\omega_m} d\omega \int_{\varphi_0}^{\varphi_1} \frac{d\varphi}{\sqrt{e^{\varphi} + \frac{1}{\beta} e^{-\beta\varphi} - 1 - \frac{1}{\beta} - \omega}}, \tag{32}$$

where φ_2 is determined as a function of ω from Formula (7), and ω_m as a function of φ_1 from Equation (14), identical in form with Equation (7).

Thus, from Formula (32) we have the remarkable result: the force barrier N_m, like ω_m, depends only on the potential of the surface with the lower charge.

By changing the order of integration in Equation (32); it may be transformed into:

$$N_m = 4Gd \frac{kTNc}{z} \int_0^{\varphi_1} \sqrt{e^{\varphi} + \frac{1}{\beta} e^{-\beta\varphi} - 1 - \frac{1}{\beta}} \cdot d\varphi \tag{33}$$

In particular, for $\varphi_1 \gg 1$

$$N_m \approx 8Gd \frac{kTNc}{z} e^{\frac{\varphi_1}{2}} \tag{34}$$

and for $\varphi_1 \ll 1$

$$N_m \approx 2Gd \frac{kTNc}{z} \sqrt{\frac{1 + \beta}{2}}\, \varphi_1^2 \tag{35}$$

when $\beta = 1$, Equation (33) gives on integration:

$$N_m = 8Gd \frac{kTNc}{z} \left(e^{\frac{\varphi_1}{2}} + e^{-\frac{\varphi_1}{2}} - 2 \right) = 32Gd \frac{kTNc}{z} \operatorname{sh}^2 \frac{\varphi_1}{2}. \tag{36}$$

We note that

$$\frac{N_m}{G} = 32\, d \frac{kTNc}{z} \operatorname{sh}^2 \frac{\varphi_1}{4}$$

is the height of the energy barrier in relation to thinning of a flat layer.

3. Let us now examine the resultant energy of dispersional interaction of two unlike particles in a liquid medium. If we assume additivity of interaction of different elements in the volume * and applicability of London's formula to the latter, then for the case of plates separated by a plane parallel gap of width $\underline{h}$ the force of attraction $\underline{Q}$ per unit area in a vacuum will be [9]:

$$Q = \frac{A_{12}}{6\pi h^3}, \tag{37}$$

---

* This assumption is evidently invalid for condensed bodies, but the relationship which follows from it between the particle interaction and distance (37) is apparently valid for small distances.

where A_{12} is the constant for dispersional interaction of elements of the volume of the first and second particles. For the case when the particles are in a medium which corresponds to the index (3), we have, instead of Equation (37):

$$Q = \frac{A_{12} + A_{33} - A_{13} - A_{23}}{6\pi h^3} = \frac{A}{6\pi h^3} \qquad (38)$$

When the particles 1 and 2 are of the same kind, there are reasons for believing [7] that in all cases $Q > 0$.

In the present instance, with unlike particles, these reasons do not apply, and cases are undoubtedly possible when

$$A = A_{12} + A_{33} - A_{13} - A_{23} < 0. \qquad (39)$$

For the force of dispersional interaction S for convex particles we have:

$$S = G \int_{y}^{\infty} Q(h)\,dh = GU(y) = \frac{GA}{12\pi y^2} \qquad (40)$$

It should be noted that for distances greater than the dispersional wavelengths, according to Casimir and Polder [10], and Abrikosova and Deryagin [11], electromagnetic retardation should be taken into account, and Equations (38) and (40) are then replaced by the following:

$$Q = \frac{B}{h^4}, \qquad (41)$$

$$S = \frac{GB}{3y^3} \qquad (42)$$

4. Let us examine the application of the theory developed above to the cases when $A > 0$ and $A < 0$.

The case $A > 0$.

In this case a force (or energy) barrier is possible only when the particles have similar charges. In the theory of coagulation and cohesion of hydrophobic sols and suspensions [3] it was shown that there are two characteristic types of coagulation:

1. Coagulation as the result of the fall of potential of the surface below a certain critical value ψ_C, which satisfies the Equation [2]:

$$\frac{dD\psi_C^2}{A} = \text{const.} \qquad (43)$$

2. Coagulation as the result of compression of the ionic double layer on increase of the electrolyte concentration above the critical value satisfying the Equation [3]:

$$\gamma \cdot c\,\frac{D^3(kT)^5}{f(\beta)A^2 e^6 z_1^6 n_1 N}, \qquad (44)$$

R=P-Q
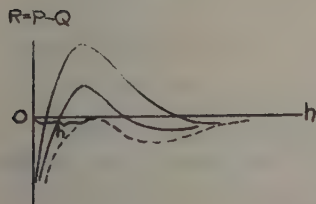
Fig. 4. Interaction of two plates as a function of distance in a solution of electrolyte for different values of the potential of one of them, close to the disappearance of the force barrier (schematic diagram).

Accordingly, in the present case of $\varphi_2 \neq \varphi_1$ the main interest is presented by cases of adhesion, either as the result of compression of the double layer when $\varphi_2 > \varphi_1 \gg 1$, or as the result of fall of the potential φ_1 *; as, for the case $\varphi_2 > \varphi_1 \gg 1$, the interaction of the particles will differ appreciably from the symmetrical case, according to Formulas (12) and (15) only for very small values of H, which will affect the strength of adhesion but not the condition of its occurrence, we will, therefore, confine ourselves to the case of adhesion as the result of fall of φ_1, assuming further for the sake of simplicity and definiteness, that:

$$\varphi_2 \gg 1 \gg \varphi_1. \qquad (45)$$

As a condition of the adhesion of flat surfaces, according to [3], we require the disappearance of the force barrier (which includes both electrostatic and

* Cases of simultaneous fall of φ_1 and φ_2 are rarer and less characteristic, and therefore are not examined here, particularly as these cases may be easily analyzed with the aid of the approximate Formulas (22 - 26).

molecular interaction), when the force diagram P–Q,h has the form shown in Figure 4 by a dotted line. Evidently, the values of ω and P which lie to the right of the maxima (that is $H > H_m$) must be examined, and therefore φ_0 will have real values satisfying the inequality:

$$\varphi_0 < \varphi_1 \ll 1. \tag{46}$$

In this case we must use Equation (13) and, taking into account (8) and (45), we have:

$$H' = \int_{\varphi_0}^{\infty} \frac{d\varphi}{\sqrt{e^\varphi + \frac{1}{\beta}e^{-\beta\varphi} - 1 - \frac{1}{\beta} - \omega}} +$$

$$+ \int_{\varphi_0}^{\varphi_A} \frac{d\varphi}{\sqrt{e^\varphi + \frac{1}{\beta}e^{-\beta\varphi} - 1 - \frac{1}{\beta} - \omega}} = I_\infty + I_1. \tag{47}$$

An approximate value of I_∞ for small values of φ_0 may be found using the fact that the relationship between I_∞ and φ_0 is identical to the relationship between $\kappa'h/2$ and η_1 in equation (14) of paper [3] when $z_1 = 1$. As follows from equation (21) of the same paper [3], for small values of φ_0, I_∞ is great, and is asymptotically expressed as:

$$I_\infty \approx \sqrt{\frac{2}{1+\beta}} \ln\left(\frac{K}{\varphi_0}\right), \tag{48}$$

where K is a function only of β; for $\beta = 1$, $K = 8$. Further simplification of I_1, with (22) and (46) taken into account, gives

$$H' \approx \sqrt{\frac{2}{1+\beta}} \left\{ \ln\frac{K}{\varphi_0} + \ln\left(\frac{\varphi_1}{\varphi_0} + \sqrt{\left(\frac{\varphi_1}{\varphi_0}\right)^2 - 1}\right)\right\} \tag{49}$$

Conditions for the disappearance of the force barrier are given by the equations:

$$\frac{dP}{dh} = \frac{dQ}{dh}, \tag{50}$$

$$P = Q = \frac{A}{6\pi h^3}, \tag{51}$$

and therefore

$$\frac{d\ln P}{d\ln h} = -3. \tag{52}$$

Determination from this of the abscissa h_0 of the force barrier (see Figure 4) and substitution into (51) gives the adhesion criterion.

Passing to the dimensionless magnitudes ω and H', instead of (52) and (51) we have, taking (4) into account:

Fig. 5.

$$\frac{dH'}{d\ln\varphi_0} = -\frac{2}{3}H', \tag{53}$$

$$\frac{Az_1}{6\pi d^3 kTNc} = \omega H'^3. \tag{54}$$

From Equations (49) and (53) we have:

$$\frac{3}{2}\sqrt{\frac{1+\beta}{2}}\left[1 + \frac{\frac{\varphi_1}{\varphi_0}}{\sqrt{\left(\frac{\varphi_1}{\varphi_0}\right)^2 - 1}}\right] - \ln\frac{\varphi_1}{\varphi_0} -$$

$$- \ln\left(\frac{\varphi_1}{\varphi_0} + \sqrt{\left(\frac{\varphi_1}{\varphi_0}\right)^2 - 1}\right) = \ln\frac{K}{\varphi_1}. \tag{55}$$

410
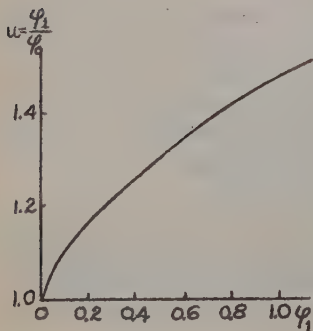
With the aid of this Equation it is possible, knowing φ_1, to find $\underline{u} = \dfrac{\varphi_1}{\varphi_0}$, and conversely. Fig. 5 shows a graph for the relationship between $\underline{u} = \dfrac{\varphi_1}{\varphi_0}$ and φ_1 which shows that when $\varphi < 0.3$, $\dfrac{\varphi_1}{\varphi_0}$ is close to unity. By determining $\underline{u}$ as a function of φ_1, we can find $\varphi_0 = \varphi_1/\underline{u}$ and by substitution in (54), we obtain the required criterion.

Assuming, as a simplification, that $\underline{u} \approx 1$ and $\varphi_0 \approx \varphi_1$, we obtain the criterion for adhesion in the form

$$\frac{Az_1}{6\pi d^3 kTNc} \approx \sqrt{\frac{2}{1+\beta}}\; \varphi_1^2 \ln^3\left(\frac{K}{\varphi_1}\right), \tag{56}$$

or, replacing φ_1 and $\underline{d}^2$ according to (2') and (2"), and denoting the concentration in mole./cm^3 by γ, and the dissociation numbers by $\underline{n_1}$ and $\underline{n_2}$, we have, instead of Formula (56),:

Fig. 6. Force diagram for two parallel plates in a solution of electrolyte, for the case $A < 0$ (repulsion resulting from the balance of van der Waals' interaction).

$$\frac{A}{Dd\psi_1^2} = \frac{3}{4}\sqrt{\frac{2}{1+\beta}}\; \ln^3\left(\frac{KkT}{z_1 e\psi_1}\right). \tag{57}$$

The condition obtained resembles the condition for adhesion of two plates, charged to an equal, small potential (corrected rule of Eilers and Korff):

$$\frac{A}{Dd\,\psi_1^2} = \text{const.} \tag{58}$$

However, in the given case of small values of ψ_1, the right hand side of the Equation (57) is greater than that of Equation (58) (where it is usually of the order of 1) [2]. Therefore, the critical potential of the start of adhesion will be lower than in the symmetrical case.

The case $A < 0$.

In this case, at small and great distances, repulsion always predominates — the two force barriers never vanish, but when $\psi_2 \neq \psi_1$ *, the force diagram may be of a form (see Figure 6) characterized by the presence of a force pit of depth R_{min}.

If the right-hand force barrier of height R_{max} is overcome by the action of an external force, and the system enters the pit, then R_{min} will evidently represent the force of adhesion.

With change of the electrolyte composition and of the potentials ψ_1 and ψ_2 simultaneous changes will also take place in R_{min} and R_{max}.

At low concentrations and values of ψ_1 and ψ_2 which are not too close and have the same sign R_{max} may be calculated, neglecting van der Waals' forces, with the aid of Formulas (2'), (4), and (14):

$$R_{max} \approx P_{max} = \frac{kTNc}{z_1}\left(e^{\frac{z_1 e\psi_1}{kT}} + \frac{1}{\beta}e^{-\beta\,\frac{z_1 e\psi_1}{kT}} - 1 - \frac{1}{\beta}\right) \tag{59}$$

for small values of $\underline{c}$ and ψ_1, this "activational" force barrier is not high, and adhesion is easily effected.

With increase of $\underline{c}$ and ψ_1, P_{max} increases, and P_{min} decreases, and for a certain value $\underline{c} = \underline{c_c}$, $P_{min} = 0$.

The condition for the complete disappearance of adhesion for the case $\psi_2 \gg 1$, as before, may be found from the same Equations (50), (51), (52), and (54), as before. However, in this case instead of $\underline{H'}$ we must take the value $\underline{H}$ from Formula (10), and as a result, instead of Equation (53) we have:

$$\frac{dH}{d\ln\omega} = -\frac{1}{3}H, \tag{60}$$

where, assuming that

$$\varphi_1 \ll 1,\; \omega < 0, \tag{60'}$$

$$H \approx \sqrt{\frac{2}{1+\beta}}\left\{\ln K - \ln\left(\varphi_1 + \sqrt{\varphi_1^2 - \frac{2}{1+\beta}\omega}\right)\right\} \tag{61}$$

* ψ_2 is taken as positive, while ψ_1 may have either sign.

From Equation (60) we have instead of Equation (55):

$$\frac{3}{2}\sqrt{\frac{1+\beta}{2}}\left[1-\frac{\varphi_1}{\sqrt{\varphi_1^2-\frac{2}{1+\beta}\,\omega}}\right]+\ln\left(\varphi_1+\sqrt{\varphi_1^2-\frac{2}{1+\beta}\,\omega}\right)\diagup\ln K. \qquad (62)$$

Hence, assuming $K \gg 1$, and taking into account $(60')$, we have, approximately:

$$\omega_c' = -\,\omega_c \approx \left(\frac{1+\beta}{2}\right)K_e^2{}^{-3\frac{\sqrt{1+\beta}}{2}}, \qquad (63)$$

(when $\beta = 1$, since $K = 8$, $\omega' \approx 3$);

$$H_c \approx \frac{3}{2} \qquad (64)$$

Substitution of H_c and ω_c into Equation (54) gives the condition for the disappearance of adhesion:

$$\frac{A'z_1}{6\pi kT'Ncd^3} = \left(\frac{3}{2}\right)^3 \omega_c', \qquad (65)$$

where $\underline{A}'$ denotes $(-A)$, $\omega' = (-\omega)$; hence follows the condition for total impossibility of adhesion, and simultaneously the condition for "peptization" for $1 \gg \varphi_1 > 0$:

$$\gamma > \frac{3^5 D^3 (kT)^5}{\pi\,4^5 e^6 z_1^6 n_1 A'^2 N}. \qquad (66)$$

For the case $\varphi_2 > 0 > \varphi_1$, ω is always positive, and for small values of $\underline{c}$ there is also a pit of force. Let us examine the simplest limiting case, when

$$\varphi_2 \gg 1 \ll -\varphi_1. \qquad (67)$$

Analogously, with the foregoing, we write the conditions:

$$\frac{dH}{d\ln\omega'} = -\frac{1}{3}H, \qquad (68)$$

$$\frac{A'z_1}{6\pi d^3 kTNc} = \omega'H^3, \qquad (69)$$

$$H = \int_{-\infty}^{+\infty} \frac{d\varphi}{\sqrt{e^\varphi + \frac{1}{\beta}e^{-\beta\varphi} - 1 - \frac{1}{\beta} + \omega'}}. \qquad (70)$$

Substituting this value of $\underline{H}$ in Equation (68), we determine the values of H_c and ω_c', which evidently depend only on β. Then, with the aid of Formula (69), we find the stability criterion in the form:

$$\gamma = \frac{c'}{\underline{f}'(\beta)}\frac{D^3(kT)^5}{A^2 e^6 z_1^6 n_1 N}. \qquad (71)$$

Adhesion will occur when the following condition is fulfilled:

$$\gamma < \frac{c'}{\underline{f}'(\beta)}\frac{D^3(kT)^5}{A^2 e^6 z_1^6 n_1 N} \qquad (72)$$

For similar and strongly charged surfaces, the stability criterion had [3] the same form [71] [although with a different numerical coefficient: $c/f(\beta)$]. However, the condition for cohesion was expressed by an inequality opposite in kind to Formula (72). In other words, in the case of unlike particles cohesion and coagulating action may be produced not by the addition of electrolyte, but by its dilution as the result of thickening of the double layer.*

* Another distinction is the fact that for obvious reasons the stability criterion must be symmetrically expressed in terms of the charges $\underline{z}_1$ and $\underline{z}_2$ on both ions, and it is therefore necessary that the function $\underline{f}'(\beta)$ in Formula (71) should satisfy the condition:

$$z_1^6\underline{f}'(\beta) = z_2^6\underline{f}'\left(\frac{1}{\beta}\right), \quad \text{or the condition } \underline{f}'(\beta)\beta^{-3} = \underline{f}'\left(\frac{1}{\beta}\right)\left(\frac{1}{\beta}\right)^{-3}$$

An example of this type of "coagulation" is given by the adhesion of mercury to glass in weak solutions of electrolytes, observed and investigated by Frumkin, Gorodetskaya, and Titievskaya [12].

To determine the force of adhesion for a given concentration, it is first necessary to find the abscissa of the force pit h_{min} from Equation (50) written in the form:

$$\frac{1}{H'^4} \frac{dH'}{d\omega'} = \frac{2\pi ckTNd^3}{z_1 A'} \tag{73}$$

Obtaining from this ω'_i, H_{min} and then h_{min}, we have

$$R_{min} = Q_{min} - P_{min} = \frac{ckTN}{z_1} \omega'_{min} - \frac{A'}{6\pi d^3 H'^3_{min}} \tag{74}$$

For small values of c the right hand side of Equation (73) is large ($\sim c^{-\frac{1}{2}}$), and it follows that $H' \ll 1$, while $\omega' \gg 1$. In this case a formula equivalent to Formula (11) is applicable:

$$H' = \frac{\varphi_2 - \varphi_1}{\sqrt{\omega'}}. \tag{75}$$

From Equations (73), (74), and (75) we have, after simple transformations:

$$R_{min} = \frac{2D}{3\pi} \frac{(\psi_2 - \psi_1)^6}{A'^2}. \tag{76}$$

This simple result may also be obtained by shorter reasoning.

5. The results obtained may easily be generalized for the case of adhesion of convex surfaces. However, because of the cumbersome calculations we will restrict ourselves to giving only some conclusions.

The case $A > 0$; $\varphi_2 \gg 1 \gg \varphi_1$.

In this case instead of the criterion (56), we obtain a criterion of similar type, but more complex in the form of its right-hand side. Its resemblance to Equation (58) remains.

The case $A < 0$; $\varphi_2 \gg 1$; $(-\varphi_1) \gg 1$.

In this case the criterion of stability will differ from Equation (71) and (72) only by the value of the coefficient $\frac{c}{f(\beta)}$. As in the "plane" case, adhesion and coagulation should take place on dilution of the electrolyte.

6. The theory which has been developed may be applied to explain the adhesion of mineral particles to bubbles of air in flotation, and coagulation effects in mixtures of two sols. It is clear from the above, especially if it is considered that for particles of different types A may not only have abnormally low values but may even become negative, that the theory explains the effect of group coagulation [13], in which the aggregates formed contain only particles of either one kind or another, but mixtures are absent.

It is clear that in this case three thresholds of concentrational coagulation are possible, the third of which, which indicates the start of formation of heterogeneous particles, for the case $A < 0$, may not only be lower in the value of the concentration, but may correspond to a reversal of the Hardy-Schulze rule, and denote the lower limit of concentrations which confer stability (in relation to the aggregation of heterogeneous particles).

Analogous considerations may be applied to the coagulation of a sol the surfaces of the particles of which are nonuniform in the value of the potential, and in particular may explain the interesting investigations of Brom-berg, Chmutov, Lukyanovich, Radushkevich, and Nemtsova [14].

The theory may also be successfully applied to other phenomena of particle adhesion, for example, of dyes to fibers and other surfaces, and explains why, on addition of electrolytes, adagulation commences before coagulation, and results in stronger bonds than does homogeneous adhesion. Of course, in the rarer cases when $A < 0$, effects of an opposite nature may occur.

SUMMARY

1. Up to the present time, the theory developed by the author, dealing with the interaction of surfaces divided by thin layers of electrolyte, with consideration of molecular forces and the energy of overlapping of ionic envelopes, was applied only to the symmetrical case of particles of like kind with similar charges, or to the case

of wetting films, with zero charge on the outer surface, which can be reduced to the symmetrical case.

2. Extension of the theory to the most general asymmetric case may be achieved by examination of iso-dynamic curves, that is, of curves which correspond to equal values of electrostatic repulsion forces.

3. Detailed examination of ionic-electrostatic interaction between plane, parallel-situated surfaces with given potentials of the same sign shows that as the surfaces approach each other, forces of repulsion first appear and increase, reach a maximum, then decrease and turn into forces of attraction; on further decrease of the distance to zero, the forces of attraction increase without limit.

4. The maximum value of the repulsion forces — the height of the force barrier — depends only on the potential of the surface with the weaker charge. This rule is strictly valid also for surfaces of any form.

5. With potentials of different sign the surfaces are attracted at any distance.

6. Formulas are derived for individual limiting special cases, and in particular (derived jointly with V. G. Levich), for low potentials.

7. With consideration of van der Waals' forces of attraction it is possible, with the aid of the Deryagin-Landau method, to find the criterion for adhesion of surfaces and particles of different kinds. Examination of the limiting case, when one surface remains strongly charged, and the potential of the second is low, leads to a generalization of the previously derived criterion for the adhesion and coagulation of weakly charged particles.

8. In the presence of particles of unlike nature in a liquid dispersion medium, the case is possible when the total balance of intermolecular action in the system leads to a resultant repulsion; in this case adhesion is possible only if the two surfaces have unequal potentials, while spontaneous flocculation of fairly large particles (in absence of external action) is possible only for potentials of different sign and in sufficiently diluted solutions (with ionic atmospheres which are not too thick).

9. For the case of very high potentials of different sign, the condition for adhesion and flocculation has been derived, analogous to the Hardy-Schulze-Ostwald rule in the Deryagin-Landau form, but of opposite sign; in other words, flocculation in this case (on the assumption that van der Waals' forces of repulsion are present) should take place not on the addition of electrolyte, but on dilution.

10. With the method of isodynamic curves it is also possible to calculate the interaction of surfaces with given charges.

11. The theory is also in agreement with the experiments of Frumkin, Gorodetskaya, and Titievskaya on the adhesion of mercury to glass in solutions of electrolytes, and it may also find application in the theory of bipolar coacervation.

12. The theory explains why, in the suspension method of dyeing, the fixation of dye particles may take place at an electrolyte concentration which is lower than the coagulation threshold of the dye suspension. The theory is also applicable to the problem of the fundamental effect in flotation — cohesion between bubbles and mineral particles.

LITERATURE CITED

[1] B. V. Deryagin, Bull. Acad Sci. U.S.S.R., chem. ser., 1937, No. 5, 1153; Acta, Phys. Chim, 10, 333, 1939; Trans. Faraday Soc., 36, 1, 203 ,1940; 36, II, 730, 1940; Colloid J., 6, 291 (1940); 7, 285 (1941).

[2] B. V. Deryagin, Colloid J., 7, 285 (1941); Trans. Faraday Soc. 36, II, 730, 1940.

[3] B. V. Deryagin, and L. D. Landau, J. Exp. Theoret. Phys., 2, 802 (1941); reprinted, J. Exp. Theoret. Phys., 15, 662, 1945; Acta phys. chim. 14, 633, 1941.

[4] E. Verwey and J. Overbeek, see, e.g. Theory of the Stability of Lyophobic Colloids, New York — Amsterdam, 1948.

[5] B. V. Deryagin, Colloid J., 7, 285 (1941). Trans. Faraday Soc. 36, II, 730, 1940.

[6] E. Verwey, Trans. Faraday Soc. 36, II, 723, 1940.

[7] H. Eilers and T. Korff, Trans. Faraday Soc. 36, I, 229, 1940.

[8] M. Smoluchowsky, Z. phys. Chem. 22, 129, 1918.

[9] H. Hamaker , Physica 4, 1058, 1937.

[10] H. Casimir and D. Polder., Phys. Rev. 73, 360, 1948.

[11] I. I. Abrikosova and B. V. Deryagin, Proc. Acad. Sci. U.S.S R., 90, 1055 (1953).

[12] A. V. Gorodetskaya, A, N. F rumkin. and A. S. Titievskaya, J. Phys. Chem., 21, 675 (1947).

[13] Tuoku Matuhasi and Kunio Acto, J. Coll.Science 3, 63, 1948.

[14] A. V. Bromberg, K. V. Chmutov, V. M. Lukyanovich, L. A. Radushkevich, and R. V. Nemtsova, J. Phys. Chem., 27, 379 (1953).

[15] B. V. Deryagin and V. G. Levich, Proc. Acad. Sci. U.S.S.R., 98, No. 6 (1954).

Institute of Physical Chemistry
Academy of Sciences U.S.S.R.
Laboratory of Surface Phenomena
Moscow

EFFECT OF INORGANIC SALTS ON THE SURFACE TENSION

AT THE WATER-MERCURY BOUNDARY

D. O. Zeiliger

The surface tension of aqueous solutions of inorganic salts at the boundary with mercury has been studied systematically in conditions of polarization of this boundary in relation to the magnitude of the increase of potential [1-3].

Literature data on the dependence of the surface tension of salt solutions on concentration at the so-called natural potential over a wide range of concentrations are almost completely lacking. Such data as have been published [4, 5] relate to a very limited number of substances, cover a narrow range of concentrations, and were usually obtained by very imperfect experimental methods. For this reason, we have carried out measurements of surface tension of solutions of a number of salts at the boundary with mercury over the whole concentration range permitted by the solubility of the salts.
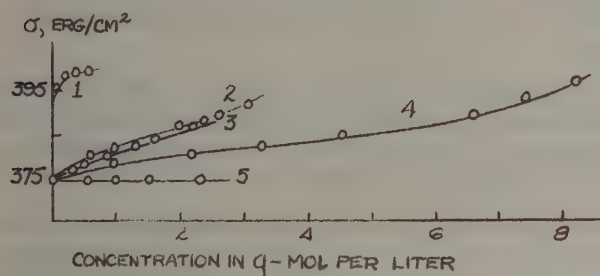
Fig. 1. Isotherms for the dependence of surface tension of salt solutions on their concentration: 1) Na_3PO_4; 2) K_2CO_3; 3) K_2HPO_4; 4) KNO_2; 5) $KHCO_3$.

For the investigations, the method of maximum pressure of drop formation was used, which gives reliable and sufficiently accurate results for the separation boundary between liquid 1 and liquid 2.

A somewhat modified scheme of the apparatus of P. A. Rebinder was used [6].

The temperature of the measurements (20°) was kept constant to an accuracy of $\pm$ 0.05° with the aid of a specially equipped water thermostat. The standard liquid used was twice-distilled water; the surface tension of mercury at its boundary with it was taken as equal to 375 erg/cm^2.

Both the mercury and the salts used were subjected to thorough purification.

The determinations showed that carbonates, neutral orthophosphates, acid phosphates, and nitrites increase the surface tension of water at the boundary with mercury; bicarbonates have no appreciable effect; chlorides, nitrates, bromides, and iodides lower the surface tension, being surface-active.

Isotherms for the dependence of the surface tension of solutions on concentration, for some of the salts studied, are shown in Figs. 1 and 2.

From an examination of the experimental results obtained it is possible to establish the following lyotropic series of anions in order of increasing activity at the boundary with mercury:

$$OH' < PO_4''' < CO_3'' < HPO_4'' < NO_2' < HCO_3' < Cl' < NO_3' < Br' < I' *,$$

This series, determined at the natural potential at the mercury/solution boundary, for solutions of inorganic salts, covers the whole concentration range accessible to measurement. It is entirely similar to the lyotropic series obtained by Gouy in his study of electrocapillary effects [2], and somewhat extends it.

From the experimental data it was also possible to calculate the work of adhesion to mercury of unimolar solutions of a number of potassium salts. Such calculations are not given in the literature, although they present an undoubted interest, since the work of adhesion is a measure of the activity of a substance at a given interphase surface.

The work of adhesion was determined from the formula:

$$W_a = (\sigma_{10} - \sigma_{12}) + \sigma_{20},$$

* The position of the hydroxyl group in the series is based on the data of Lenkewitz [4].

417

TABLE

Work of Adhesion of Potassium Salts to Mercury

1 M salt solution	σ_{10} erg/cm^2	σ_{12} erg/cm^2	W_a
K$_2$CO$_3$	76.10	381.6	170.5
KNO$_2$	74.00	379.0	171.0
KCl	74.15	357.5	192.7
KNO$_3$	73.76	338.5	211.3
KBr	74.07	318.5	231.4
KI	73.60	305.0	244.6

Fig. 2. Isotherms for the dependence of surface tension of salt solutions on their concentration: 1) KCl; 2) KNO$_3$; 3) KBr; 4) KI.

where σ_{10} and σ_{20} are the respective surface tensions at the solution/air boundary, from literature data [4], and at the mercury/air boundary ($\sigma_{20} = 476$ erg/cm^2); σ_{12} is the surface tension at the salt solution/mercury boundary from our determinations.

The results of the calculations are shown in the Table.

It follows from the results in the table that the work of adhesion is determined by the nature of the anion, and increases with its activity. The greatest values of work of adhesion are shown by salts with halogen ions, as is also found for halogen-containing organic compounds [3].

From an analysis of the values of the work of adhesion it is possible to draw conclusions concerning the definite orientation of the salt molecules in the surface layer, with the anions toward the mercury. This conclusion is in full agreement with the known results of electrocapillary measurements by Gouy and by Frumkin and coworkers.

The dependence of the surface tension on the salt concentration in the solution at the natural potential, shown in Figs. 1 and 2, agrees basically with certain data known from the work of Gouy and Frumkin [1]. There are only some differences in the shape of the curves; for the hydrolyzing salts, carbonate, acid phosphate, and nitrite of potassium, in conditions of the natural potentials they are characterized by points of inflexion, which are absent from the isotherms for the concentration dependence of the maxima of the electrocapillary curves according to Gouy.

Thus, the measurement of surface tension at the mercury/aqueous salt solution boundary in given polarization conditions near the maximum of the electrocapillary curve does not significantly change the dependence of the surface tension of solutions of inorganic salts on their concentration, and does not alter the order in which the ions are placed according to their surface activity, corresponding to the lyotropic series.

It may be assumed that the natural potentials at the mercury/solution boundary lie in the region of the electrocapillary curve close to the maximum, and, therefore, the dependence of the natural potential on the electrolyte concentration does not greatly affect the value of the surface activity of the cations.

It is clear that a considerable charge on the surface, especially in presence of anodic polarization, would lead, in agreement with Frumkin's work, to complete prevention of adsorption of organic molecules, and even more so of anions.

SUMMARY

1. The surface tension of aqueous solutions of a number of inorganic salts at the boundary with mercury has been studied. It is shown that carbonates, neutral orthophosphates, acid phosphates, and nitrites increase the surface tension of water at the mercury boundary; bicarbonates have no appreciable effect; chlorides, nitrates, bromides, and iodides lower the surface tension, being surface-active.

2. The lyotropic series of anions at the water/mercury boundary at the natural potential has been established.

3. The work of adhesion between mercury and unimolar solutions of a number of potassium salts has been calculated.

It is shown that the work of adhesion is determined by the nature of the anion and increases with increased activity of the latter.
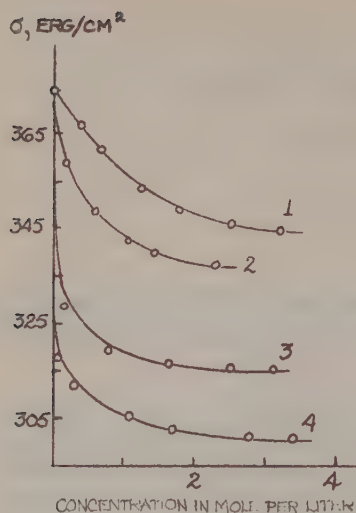
4. The experimental data obtained were compared with the results of electrocapillary measurements made by Gouy and Frumkin. From the analogy which was established it may be considered that the natural potentials at the mercury/aqueous solution boundary for inorganic salt solutions lie in the region of the electrocapillary curve close to the maximum.

LITERATURE CITED

[1] A. N. Frumkin, Electrocapillary Phenomena and Electrode Potentials (1919); A. N. Frumkin, et. al., Trans. Karpov Chem. Inst., No. 2, 106 (1924); No. 5, 17 (1926).

[2] M. G. Gouy, Ann. chim. phys., 29, 145 (1903).

[3] N. K. Adam, Physics and Chemistry of Surfaces, United State Press (1947).

[4] Handbook   of Physical and Chemical Values, Vol. 10, United State Press (1932).

[5] Chemist's   Handbook   Vol. 1, State Chemical Press (1951).

[6] P. A. Rebinder, J. Exp. Biol. Med., 4, 939 (1927); see also Ostwald and Luther, Ed. by Drucker, Physico-Chemical Measurements, Vol. 1 (translation), State   Sci.-Tech. Press (1935).

THE ACTION OF SODIUM CARBONATE AND PYROPHOSPHATE ON CLAY SUSPENSIONS

V. L. Kvirikashvili

Investigations of structure formation in clay suspension in the light of their aggregative instability have a great scientific and practical importance. Investigations in this field are firmly associated with the use of clay suspensions for drilling deep wells [1], for building construction, ceramic technology, and also with numerous problems of soil science and engineering geology.

For the study of the influence of alkaline electrolytes on structure formation in clay suspensions, two clays of Georgian origin were chosen, greatly different in their colloidal properties: 1) bentonite clay (Askangel) and 2) non-bentonite Kavtiskhev clay. Preliminary experiments established that a clay suspension prepared from Kavtiskhev calcium clay is aggregatively unstable, while a suspension of bentonite clay —mainly sodium-based— has greater aggregative stability.

The basic characteristics of the clay suspensions studied were the structural viscosity η, the dynamic shear stress θ_D, the static shear stress θ_{st}, and the rate of water evolution (in 30 minutes) by V. S. Bartenev's method, W_{30}.

The following fact was taken into account in the experiments. The strength of the structure of a clay suspension, as is known, becomes appreciable above a certain concentration of the solid phase. The formation of structure, and the associated immobilization of the dispersion medium (water), obscures the coagulating (dehydrating) effect of certain electrolytes. Therefore, in filtration from concentrated clay suspensions, the rate of water evolution on addition of electrolyte coagulants is not only not increased, but is even diminished. On the other hand, at low concentrations of clay, when a cellular structure is practically absent, and therefore, water is not immobilized, the coagulating action of electrolytes is always manifested by an increase in the rate of water evolution. For these reasons the action of additions of alkaline electrolytes on structure formation in clay suspensions was studied both at low and at high concentrations of clay.

The structural-mechanical properties of the suspensions of Askangel and Kavtiskhev clay, were studied with the aid of a capillary viscosimeter of the Ubbelohde type [2] and, parallel to this, with the Veiler-Rebinder apparatus [3], based on the tangential displacement of a plate within the structurized system. The addition of soda (Na_2CO_3) to aggregatively unstable suspensions of Kavtiskhev clay, by hydrating both the external and the developing internal surface of the primary particles, favors their dispersion. In a suspension of Kavtiskhev clay, which in itself is aggregatively unstable, increase of the number of particles in unit volume, according to Serb-Serbina and Rebinder [4, 5], leads to an intensive development of the coagulational structure, whish is shown by an increase both of the initial (residual) strength of the structure (dynamic yield stress) θ_D, and of the strength of the structure formed at rest —the static yield stress θ_{st} (Fig. 1). Here the surface of the particles may be found to be on the average even more hydrated: the number of coagulation centers per unit area will become less under the action of electrolyte additions. The coagulational structure, however, will develop as the result of the sharp increase of the number of particles per unit volume, and of the consequent increase in the number of effective collisions.

The addition of soda to aggregatively stable suspensions of bentonite clay (Askangel), as in the case of Kavtiskhev clay suspensions, outwardly leads to an increase of the structure strength (Fig. 2). However, the increase of strength in the case of Askangel is caused by an opposite effect of the electrolyte, namely, by its coagulating action, which results in dehydration of the particle surfaces,and in consequence increases the initial strength of the structure (Table 1, Fig. 2). Here the number of free particles in unit volume of the suspension is decreased. The strength of the coagulational structure is still sharply increased as the result of increased strength of bonding between the separate particles.

In aggregatively unstable suspensions additions of soda increase the initial strength of the structure (Table 2, Fig. 1) due to the hydration of the particle surfaces by the action of exchange adsorption of cations (more complete conversion into Na-clay), and consequently, to the dispersion of the particles. In aggregative stable suspensions of Askangel, which are fairly well dispersed in water alone, the same additions of soda increase the initial strength of the structure as the result of dehydration of the particle surfaces (local decrease of hydration), i.e., as the result of their coagulation (Table 1, Fig. 2). Thus, the sharp increase of the strength of the structure in suspensions of bentonite clay (Askangel) is the result of a coagulating and not of a dispersing action of the soda.

TABLE 1

Action of Soda (Na_2CO_3) on the Mechanical Properties of Suspensions Made from Bentonite Clay

Dispersion medium	Concentration of suspension (%)	Soda added (%)	Mechanical properties		
			η centipoises	θ_D mg/cm^2	W_{30} (ml)
Water....................................	1	0	1.12	1.51	18.5
0.02% solution of soda	1	0.02	1.15	1.51	18.5
0.02% solution of soda followed by addition of remaining amount....................................	1	0.25	1.25	1.51	21.5
The same	1	0.5	1.28	1.51	22.0
"	1	0.75	1.46	1.51	25.0
"	1	1.0	1.25	3.01	27.0
Water....................................	5	0	1.8	3.02	9
0.02% solution of soda....................................	5	0.02	1.82	3.02	9
0.02% solution of soda followed by addition of remaining amount....................................	5	0.25	3.2	3.02	9.5
The same	5	0.5	3.02	6.8	12.5
"	5	0.75	2.76	9.05	14.0
Water....................................	10	0	5.3	12.1	8.5
0.02% solution of soda	10	0.02	5.5	12.1	9
0.02% solution of soda followed by addition of remaining amount....................................	10	0.1	8.5	57.4	8
The same	10	0.25	9.5	130.0	7
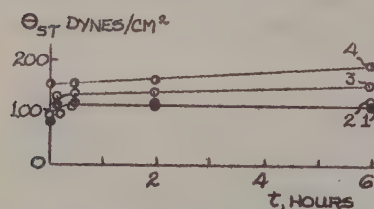
Fig. 1. Strengthening of the structure of 14% suspensions of Kavtiskhev clay by the dispersing action of soda: 1) without soda; 2) 0.02%; 3) 0.25%; 4) 0.5% soda.

Fig. 3. Action of soda: 1) hydrating, in suspensions of Kavtiskhev clay, and 2) dehydrating, in suspensions of bentonite clay (Askangel).

Fig. 2. Strengthening of the structure of 10% bentonite suspensions by the coagulating action of soda: 1) without soda; 2) 0.02%; 3) 0.25%; 4) 0.5% soda.
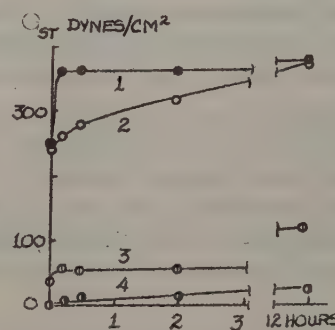
Fig. 4. Stabilizing effect of sodium pyrophosphate on 20% suspensions of Kavtiskhev clay: 1) without sodium pyrophosphate; 2) 0.02%; 3) 0.1%; 4) 0.25% sodium pyrophosphate.

The dual (opposing) action of soda —hydrating in suspensions of non-bentonite and dehydrating in the case of bentonite— finally leads to the same coagulational structure formation effect, i.e., to the strengthening of the continuous network structure. However, supplementary investigations of the kinetics of water evolution show a distinction between these opposite effects in dilute suspensions (Fig. 3, Tables 1, 2).

When soda is added to the aggregatively unstable suspensions of Kavtiskhev clay and the strength of the structure measured, it is seen that at low concentrations of soda (Fig. 1, Table 2) additions of soda have little effect. As the concentration of soda increases, its effect is greater, and at 0.25% concentration of electrolyte the strength of the structure reaches a maximum.

The hydration of the particle surfaces, which in these conditions is the most important factor of aggregative stability, does not confer complete stability to the particles of Kavtiskhev clay. This can be understood if it is taken into account that increase of the bond strength between the dispersion medium (water) and the surfaces of the clay particles in presence of soda relates only to certain regions of the surfaces, where exchange adsorption of cations takes place. The presence of unprotected regions will always cause aggregation of particles, and the suspension retains aggregative instability even after treatment with soda.

TABLE 2.

Action of Soda (Na_2CO_3) and Sodium Pyrophosphate ($Na_4P_2O_7$) on the Mechanical Properties of Aggregatively Unstable 10% Suspensions of Kavtiskhev Clay

Dispersion medium	Sodium pyrophosphate on the volume of clay suspension (%)	Soda on the volume of clay suspension (%)	Mechanical properties		
			η centipoises	θ_D mg/cm^2	W_{30} (ml)
Water.................	0	0	1.39	9.06	30
Sodium pyrophosphate solution..	0.025	0	1.39	6.05	—
The same	0.03	0	1.46	4.53	6.5
"	0.10	0	1.71	1.51	5.5
Soda solution	0	0.05	1.55	12.1	21
The same	0	0.25	2.17	22.6	14
"	0	1.0	1.81	11.5	14.5

To bring the suspension of Kavtiskhev clay into an aggregatively stable state, sodium pyrophosphate ($Na_4P_2O_7$) was added to it [6, 7]; with a suitable addition the bonds between the clay particles are removed and fairly complete stabilization occurs. This is shown by the sharp decrease of the initial strength of the structure almost to zero (Fig. 4, Table 2). Measurements of the kinetics of water evolution in these suspensions show a sharp decrease of the filtration rate (Fig. 3, Table 2).

In presence of additions of sodium pyrophosphate the decrease in the water evolution of the clay suspensions and at the same time the decrease of the structure strength are caused by the presence of stabilized clay particles which are not bound to each other, forming closely packed precipitates (filtering skin). The most probable explanation of the mechanism of the action of sodium pyrophosphate in this case is apparently that both the cation and the anion of this salt favor the hydration of the particle surfaces. In fact, the interaction of the pyrophosphate ion with the calcium cation on the clay surface leads to the formation of insoluble calcium phosphate in the colloidal state, which is fixed on the particle surface in the form of a hydrophilic coating, which leads to stabilization of the particles. The sodium cation, in its turn, enters the exchange complex of the clay particle, and increases the hydrophilic nature of the surface. The concentration of free electrolyte in the surrounding medium is always very small, which leads to a fairly high aggregative stability of the suspension. Thus we consider on the basis of the experimental data that additions of soda result in a higher degree of dispersion of the primary particles in suspensions of Kavtiskhev clay, which leads to increased effectiveness of coagulational structure formation and greater strength of the structure, while additions of sodium pyrophosphate produce stabilization by producing aggregative stability, and, as a consequence, a sharp decrease in the strength of the structure.

SUMMARY

1. Addition of soda to aggregatively unstable suspensions of Kavtiskhev clay has mainly a dispersing effect; similar additions of soda to aggregatively stable suspensions of Askangel (sodium bentonite) have mainly coagulant effects.

2. The dual action of additions of soda —hydration in suspensions of Kavtiskhev clay and dehydration in suspensions of sodium bentonite— results in outwardly identical structure formation. This property of soda permits its use on a large industrial scale for improving the properties of clay suspensions.

3. A distinction should be made between: a) stabilization of particles in a clay suspension which ensures aggregative stability in the system and as a result lowers the initial strength of the structure, and b) dispersion, which decreases the size of the primary particles in the system and as a result, raises the initial strength of the structure. Soda, which causes a change in the exchange complex and increases the degree of hydration of the particle surfaces, is a dispersing agent. Sodium pyrophosphate acts as a stabilizer.

I offer my sincere thanks to P. A. Rebinder and N. N. Serb-Serbina for valuable advice in the present work.

LITERATURE CITED

[1] V. L. Kvirikashvili and A. I. Tsurinov, chapter in book: "New Knowledge on Clay Suspensions", Tsurinov, et. al., pp. 1, 90, 160 (1940); V. L. Kvirikashvili and N. I. Shatsov, ibid., p. 61.

[2] N. N. Serb-Serbina, Collected Papers: "Conference on Viscosity of Liquids and Colloidal Solutions", 1, 381 (1941).

[3] S. Ya. Veiler and P. A. Rebinder, Proc. Acad. Sci. USSR, 49, No. 5, 354 (1945).

[4] N. N. Serb-Serbina and P. A. Rebinder, Colloid J., 9, No. 5, 381 (1947).

[5] P. A. Rebinder, Collected Papers: "Conference on Viscosity of Liquids and Colloidal Solutions", 1, 361 (1941).

[6] P. A. Rebinder, K. F. Zhigach, and L. A. Shreiner, J. Petroleum Ind., No. 5, 54 (1940).

[7] L. V. Lyutin, Stabilization of Mineral Suspensions, Moscow-Leningrad (1947).

GELATINIZED EMULSIONS

XII. EFFECT OF THE LENGTH OF THE HYDROCARBON CHAIN IN THE MOLECULE OF THE STABILIZER ON EMULSIFICATION

L. Ya. Kremnev and N. I. Kuibina

Research workers have long been interested in the question of the length of the hydrocarbon chain in the molecule of alkali salts of monobasic fatty acids which first begins to exert an emulsifying action. Donnan established as early as 1910 that the alkali salts of myristic and lauric acids are good stabilizers for concentrated direct emulsions, while salts of acids of lower molecular weight do not favor the formation of stable emulsions [1]. This was later confirmed [2], and is usually explained by the fairly clearly defined colloidal properties of alkaline soaps beginning with the laurate.

TABLE

Maximum Concentration Emulsions with Salts of Triethanolamine and Fatty Acids

Salts of triethanolamine and fatty acids	Stabilizer concentration (mol/1)	S_{∞}, m^2	δ_{crit}, $\mu \cdot 10^{-3}$	S_0, m^2	$\overline{d}$, μ
Stearic (C_{18})	0.20	83	12	69	1.1
	0.22	91	11	69	1.1
	0.33	91	11	46	1.1
Palmitic (C_{16})	0.25	100	10	66	1.1
	0.30	125	8	69	1.2
	0.40	125	8	52	1.1
Myristic (C_{14})	0.39	200	5	85	1.1
	0.50	200	5	66	1.1
Lauric (C_{12})	0.49	333	3	112	1.1
	0.57	333	3	97	1.1
	0.72	333	3	76	1.1
Capric (C_{10})	0.81	333	3	69	1.4
	0.93	333	3	60	1.3
	1.12	333	3	49	1.3
Pelargonic (C_9)	0.98	333	3	46	1.5
	1.20	333	3	46	1.5

In this connection we studied direct emulsions of maximum concentration made with alkali salts of the homologous series of fatty acids. As a direct measure of emulsifying power, a special interest was presented by determination of the maximum surface of the protective layers formed from unit volume of the stabilizer solution, S_{∞} [3], and also by a study of the structural peculiarities and properties of these layers on the droplets. In view of the insufficient solubility in water of the potassium and sodium salts of some of the intermediate and especially of the higher fatty acids, so that emulsification isotherms over a wide range of stabilizer concentrations cannot be obtained, the emulsions were prepared with salts of triethanolamine and fatty acids, which have good solubility in water. A complete dispersion analysis of the emulsions was carried out by the microscopic method, and the results were used, as before [4], to characterize the adsorption-solvation layers surrounding the droplets.

The table presents the collective results of investigations of emulsions stabilized by relatively concentrated solutions of soaps, at which constant values are reached by the maximum area of the protective layers S_{∞}, formed from 1 ml of the stabilizer solution in emulsions of maximum concentration, and the minimum thickness of the layer δ_{crit} [4]. The packing density of the molecules in the adsorptional layers is characterized by values of the

area S_0 per molecule of the stabilizer in the interphase surface. The degree of dispersion of the emulsions is represented by values of the mean droplet diameter $\bar{d}$ and also by the differential curves for the droplet size distribution in certain emulsions, shown in Figs. 3, 4 and 5.
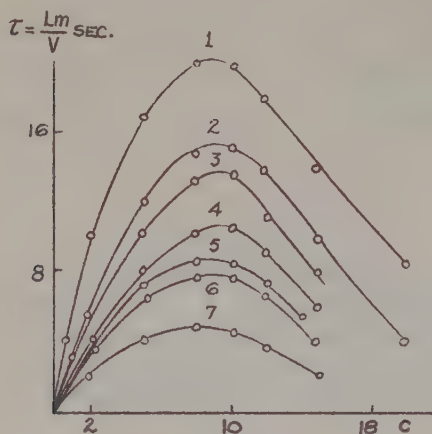
Fig. 1. Stability of two-sided films: 1) laurate; 2) myristate; 3) caprate; 4) palmitate; 5) pelargonate; 6) stearate; 7) caprylate.
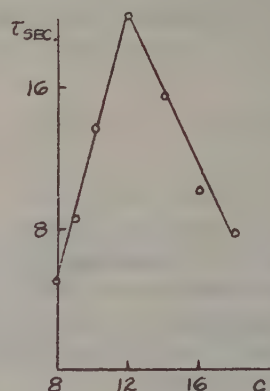
Fig. 2. Maximum stability of two-sided films as a function of the length of the fatty acid chain.

Emulsifying power first appears in the caprylate (C_8), but maximum concentration emulsions with it are completely unstable and break immediately after preparation. A certain measure of stability appears in emulsions with pelargonate, and the life of these is about 1 hour. Emulsions stabilized by caprate last about twenty-four hours, and emulsions with the other stabilizers are stable for months without apparent breaking. In emulsions with caprate and perlargonate, coalescence of the droplets undoubtedly took place during preparation for dispersion analysis. Therefore, the data on these emulsions in the table cannot be considered quite reliable.

As before [3, 4], S_∞ and δ_{crit} reach constant values at high concentrations of stabilizer. But as the length of the hydrocarbon chain decreases, the stabilizer concentration at which the value of S_∞ and δ_{crit} becomes constant is appreciably higher.

By their emulsifying power, expressed solely by the objective values of S_∞ [3], the homologs lie in the natural series:

stearate < palmitate < myristate < laurate (caprate, pelargonate).

The reverse series shows the variation of the thickness of the adsorption-solvation layers δ_{crit}:

stearate > palmitate > myristate > laurate > (caprate, pelargonate).
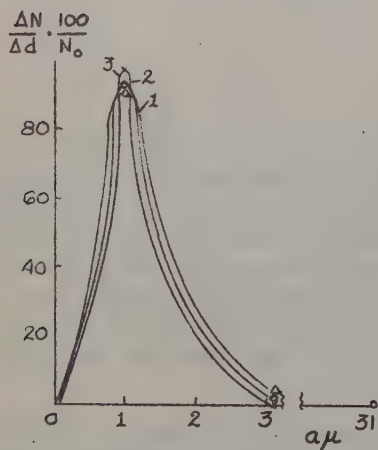
Fig. 3. Size distribution curves of the droplets in emulsions with triethanolamine palmitate with concentrations: 1) 0.10; 2) 0.22; 3) 0.40 mole/l.
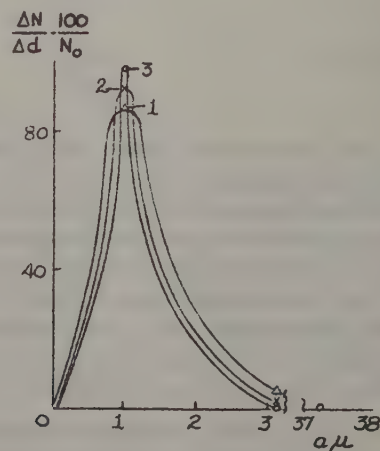
Fig. 4. Size distribution curves of the droplets in emulsions with triethanolamine myristate with concentrations: 1) 0.10; 2) 0.30; 3) 0.50 mole/l.

The highest emulsifying power is shown by triethanolamine laurate. Apparently in laurate, we find a complete balance between the independent surface action of the polar groups and of the hydrocarbon radicals of the surface- active molecules. In this case at the separation boundary of the liquids there is an equilibrium between the tendency of the polar groups to "immerse" the molecules in water and the attraction of the hydrocarbon chains into the benzene phase. The adsorption-solvation layers then have the greatest stability with least thickness. With a chain with less than 12 carbon atoms, the action of the polar groups prevails, resulting in frequent interruptions of the continuity of the protective layers and appreciable coalescence of the droplets, which is the cause of the poor stability of emulsions with caprate and pelargonate, and also ot the complete instability of the emulsions with the shorter caprylate molecules. When the chain length exceeds 12 carbon atoms, the action of the nonpolar chains predominates, and the droplets are protected against coalescence by the thicker adsorption-solvation layers.
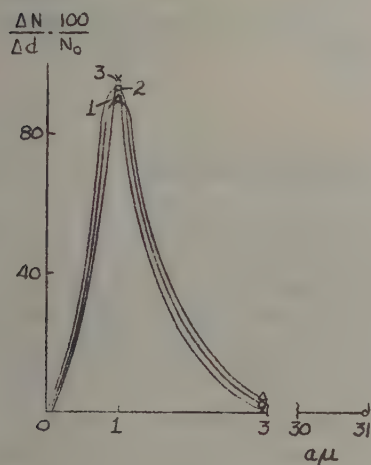
Fig. 5. Size distribution curves of the droplets in emulsions with triethanolamine laurate with concentrations: 1) 0.22; 2) 0.46; 3) 0.72 mole/l.

The validity of the above views is supported by measurements of the stability of macrofilms in the Rebinder and Smirnova apparatus [5]. The rate of drawing of the films was 1.6 cm/sec, the concentration of the solutions of the homologs studied was in the range $1 \cdot 10^{-4} - 2 \cdot 10^{-3}$ mole/l. The results of the measurements are shown in Fig. 1.

As was to be expected, the maximum stability is shown by films made from aqueous solutions of triethanolamine laurate at all salt concentrations, which corresponds to the maximum emulsifying power of this stabilizer. The stability isotherms of aqueous films of all the other salts lie lower; very low stability is shown by films of caprylate solutions, which give quite unstable emulsions. The dependence of the film stability on the length of the molecular chain is shown still more clearly in Fig. 2, for salt concentrations of $1 \cdot 10^{-3}$ mole/l, when all the stability isotherms pass through a maximum.

The stability maximum of the films corresponds to concentrations of the stabilizer solutions at which the adsorptional layers, although close to saturation, are apparently not yet saturated. If we denote by S_0 the surface area which corresponds to one molecule of the stabilizer, and by N, the number of molecules in a gram molecule, we have the maximum adsorption Γ_∞ of triethanolamine stearate

$$\Gamma_\infty = \frac{1}{S_0 \cdot N} = 2.6 \cdot 10^{-10} \text{ mole/cm}^2.$$

In the region of maximum stability, calculation from Gibbs' equation, based on data for the interphase tension on the benzene-solution separation boundary [6], gives considerably lower values. At a stearate concentration of $9 \cdot 10^{-4}$ mole/l, the surface activity is

$$\left(-\frac{d\sigma}{dc} \right) = 4000$$

and

$$\Gamma = -\frac{c}{RT} \left(-\frac{d\sigma}{dc} \right) = 1.5 \cdot 10^{-10} \text{ mole/cm}^2$$

The degree of dispersion of the emulsions studied is very high, as is seen from the values of the mean diameter $\bar{d}$ of the droplets and the distribution curves in Figs. 3, 4 and 5 for a number of systems. As previously, the maximum on the distribution curves corresponds to a droplet diameter of the order of 1 μ, which is in full agreement with the conclusions drawn from our analysis of the mechanism of dispersion and stabilization of emulsions [7].

SUMMARY

1. Emulsions of maximum concentration, stabilized with salts of triethanolamine and the homologous series of fatty acids from caprylic to stearic, were prepared and studied.

2. Concentrated emulsions with triethanolamine caprylate are unstable. The stability of emulsions with triethanolamine pelargonate and caprate is low; stabilizers with greater molecular length give high stability to concentrated emulsions.

427

3. The greatest emulsifying power is shown by triethanolamine laurate, which is in agreement with the durability of macrofilms drawn from aqueous solutions of the stabilizers studied.

4. The emulsions are stabilized by adsorptional monolayers.

5. The degree of dispersion of the emulsions is very high, and the maximum on the distribution curves corresponds to a droplet size of the order of 1μ.

LITERATURE CITED

[1] F. G. Donnan, Koll.-Z., 4, 208 (1910).

[2] Clayton, Theory of Emulsions and Their Technical Treatment, translated from English (1950).

[3] L. Ya. Kremnev and S. A. Soskin, Colloid J., 9, 269 (1947).

[4] L. Ya. Kremnev and R. N. Kagan, Colloid J., 10, 436 (1948).

[5] P. A. Rebinder and A. M. Smirnova, Proc. Acad. Sci. USSR, new series, 52, 319 (1946).

[6] Yu. K. Novodranov, Colloid J., 8, 415 (1946).

[7] L. Ya. Kremnev and A. A. Ravdel, Colloid J., 16, No. 1, 17 (1954). *

---

* See Consultants Bureau Translation, page 19.

DIFFUSION OF PHENOL IN POLYAMIDE FILMS AND FIBERS*

E. K. Mankash and A. B. Pakshver

As was shown earlier [1], when polyamide fibers and films are treated with aqueous solutions of phenols, the latter are combined with the amide groups of the polyamide molecules, so weakening the intermolecular bonds. The rate of sorption of phenols by polyamides is determined by their rate of diffusion into the substance, and the diffusion coefficient D may be calculated from the equation:

$$x = \frac{4}{r} \sqrt{\frac{D}{\pi}} \sqrt{t} \quad \text{or} \quad x = \frac{2}{a} \sqrt{\frac{D}{\pi}} \sqrt{t} \qquad \text{(1 and 2)}$$

where r is the fiber radius; a is the half-thickness of the film; t is the sorption time in seconds; x is the amount of absorbed phenol as a fraction of the equilibrium amount during the time from the start to a given instant.

The same authors showed that the diffusion coefficient depends on the structure of the fiber, and decreases with increasing degree of orientation of the fiber and with strengthening of the structure by heating the fiber.

The present paper gives supplementary data on the rate of sorption of phenol by drawn and undrawn polyamide fibers after various pretreatments. Data are also presented on the rate of sorption of phenol by polyamide films, also previously subjected to various treatments. Isotherms for the sorption of phenols by films and fibers, for different treatments of the polyamides, are also given.

The diffusion coefficients were calculated by means of the equations (1 and 2). These equations characterize nonsteady diffusion into the fiber or film from the start of the sorption process till equilibrium is reached between the phenol in the aqueous solution and the polyamide fiber or film. To characterize steady state diffusion of the same phenol from aqueous solution into the film, experiments were carried out analogous to those described in the previous communication [2] with hydrate cellulose films. In this case the diffusion coefficient D was calculated from the equation:

$$D = \frac{sQ}{F(c_0 - c)} \qquad (3)$$

where s is the film thickness in cm; Q is the amount of substance diffusing through the film in g/sec; F is the area of the film in cm^2; c_0 and c are the concentrations of phenol in the aqueous solution on the two sides of the film, in g/ml.

TABLE 1

Diffusion of Phenol into Undrawn Capron Fiber, $t = 20°$

Initial concentration in bath (g/l)	Equilibrium concentration in bath		Equilibrium sorption of fiber		$D \cdot 10^{10}$	Treatment of the fiber
	in g/l	in mole/1·10³	in g/g·10³	mole/res·10³		
0.09	0.08	0.85	4.79	5.75	0.02	Extraction with toluene
0.2	0.13	1.4	7.75	9.32	1.21	and water in the cold
0.3	0.17	1.8	5.48	6.60	7.9	The same
0.4	0.28	3.0	6.0	7.2	17.3	''
0.5	0.34	3.65	8.0	9.6	16.0	''
1.0	0.65	7.0	17.3	20.8	27.2	''
5.0	3.74	40.5	63.0	76.6	7.85	24 hours in autoclave at 2 atm
5.0	3.82	40.6	58.8	67.7	1.65	Same, drawn fiber

---

* 10th communication in the series on studies of the molecular structure of high polymers.

As was shown by Barrer [3], experimental data obtained in studying the diffusion process in steady state conditions through a film may also be used to determine the rate of diffusion in the initial nonsteady period, into the depth of the film. Diffusion in the initial nonsteady period, according to Barrer, is determined by the equation

$$L = \frac{s^2}{6D} \tag{4}$$

where L is the time interval from the start of diffusion till equilibrium is reached, in seconds. This equation is approximate, and the experimental results given in Table 3 are exploratory in character. The results of the measurements are shown in Tables 1-3.

TABLE 2

Diffusion of Phenol into Capron Films, $\underline{t}$ = 20°

Treatment of the film	Concentration in bath (g/l)		Equilibrium concentration in bath, mole/l · 10^3	Equilibrium sorption of phenol		$D \cdot 10^3$
	initial	equilibrium		$g/g \cdot 10^3$	mole/res · 10^3	
Washed with hot water	2.5	2.0	21.5	25.5	30.6	—
The same	5	3.62	38.7	68.6	83.3	2.25
"	5	4.07	43.7	46.6	56	3.52
"	10	7.7	82.5	115	138	3.10
"	15	11.25	120	175	210	—
"	20	15.3	164	237	285	16.7
"	25	—	Dissolves	—	—	—
Previously treated with phenol, 15 g/l	5	3.46	37.1	76.6	93.0	7.1
Previously treated with vaseline at 150°.	5	3.70	39.4	64.5	78.3	2.9

TABLE 3

Diffusion of Phenol Through Capron Film, $\underline{t}$ = 25°, area $\underline{s}$ = 9.1 cm^2

Treatment of the film	Thickness of the film in cm · 10^3	Concentration of phenol (g/l)		Permeability P in g/sec · · 10^6	$D \cdot 10^6$	Attainment of equilibrium, approximate	
		in bath	in solution flowing through			L	$D_{nonsteady}$
Film first treated with 7 g/l phenol and washed after 4 days	5.0	6.95	0.34	7.5	0.61	48 hours	$0.26 \cdot 10^{-10}$
The same, after 6 days		6.95	0.31	10.0	0.80	—	—
				Mean	0.70		
Film first treated with hot water, after 1 day	5.0	13.2	0.28	9.5	0.40	24 hours	$0.52 \cdot 10^{-10}$
The same, after 3 days		13.2	0.66	10.3	0.42	—	—
				Mean	0.41		
Film first treated with 15 g/l phenol and washed, after 4 days	5.3	12.3	0.57	15.0	0.73	—	—
The same, after 5 days		17.3	0.63	14.0	0.72	—	—
				Mean	0.72		
Film first treated with vaseline at 150°.	5.3	12.3	0.17	19.9	0.91	—	—
		12.9	0.36	18.7	0.88	—	—
				Mean	0.90		

From the experimental data in the Tables it is possible to evaluate the general laws of the mechanism and the nature of the sorption of phenol by polyamide fibers and films.

As is seen from Tables 1 and 2, the isotherms for the sorption of phenol by polyamide fibers and films are different for polyamides of different molecular structure. This fact, which was also previously noted by various authors in the sorption of water vapor by hydrate cellulose fibers, and also the sorption of the vapors of various organic solvents by polyethylene and other polymer films, may be explained by the view that the sorption of an active substance from solution (in the present case, phenol) is achieved by addition of it to the polar groups of the polymer with the formation of hydrogen bonds or other intermolecular bonds [2]. In polymers with different molecular structure (for example, with different degrees of orientation) the number of free active groups differs, and decreases with increased order in the structure. In polyamide fibers previously drawn under tension or heated to a high temperature, the number of free amide bonds capable of combining with phenol decreases. Polyamide film occupies an intermediate position, as it is made under a certain amount of tension, but without subsequent drawing. Preliminary treatment of the films with phenols increases the sorption of phenol, while heating to 150° in vaseline decreases the sorption of phenol. In the first case, the number of free amide groups, not occupied by intermolecular bonds, increases as the result of weakening of the structure in the aqueous phenol medium, while in the second case it decreases, as is shown by the value of the equilibrium sorption.

The rate of diffusion into fibers or films (nonsteady state diffusion) sharply decreases when the molecular structure of the polyamide is made more compact, when the fiber is drawn, heated, etc.. In this case, also, polyamide film occupies an intermediate position between drawn and undrawn fiber, but the differences between the different structures are seen much more prominently. Preliminary treatment of films or fibers affects the diffusion rate in the same way as the value of equilibrium diffusion, but the effect of this treatment is much greater.

The diffusion of phenol through film, i.e., in steady state conditions (see Table 3), is several thousand times more rapid than diffusion in nonsteady conditions into films or fibers. This acceleration of the diffusion of phenol in polyamide films may be explained by the fact that the steady state process takes place in conditions of equilibrium saturation of the polyamide with phenol, i.e., in conditions in which the intermolecular bonds are greatly weakened. When the diffusion process takes place in nonsteady conditions, the phenol molecules encounter an initial stronger structure on penetrating into the polymer, and the diffusion front passes slowly into the fiber or film, because of the stable initial intermolecular structure. As a result of weakening of the intermolecular structure by the action of phenol, not only is diffusion accelerated, but differences in structure are evened out. Therefore, preliminary treatment of the films (treatment with water-phenol mixture, heating in vaseline, etc.) has little effect on the rate of diffusion of phenol through the film in steady state conditions, while the same treatment has a very powerful effect in nonsteady conditions.

The diffusion coefficients calculated with the aid of equation (4) for nonsteady conditions have the same values as those calculated from equation (2). Thus in both cases the rate of diffusion of phenol into the film is determined by its rate of movement through the original polyamide structure, not yet weakened by phenol. Nevertheless, the diffusion coefficient for nonsteady conditions, claculated from equation (4), is somewhat smaller than the same coefficient calculated from equation (2). The explanation for the difference may be that in the second case, the calculation gives a high value of D, the average for the whole thickness of the film.

SUMMARY

1. The isotherms for the sorption of phenol by polyamide fiber are different for different specimens, and depend on the molecular structure of the fiber. The sorption of phenol is less with increase in the number of intermolecular bonds in the fiber.

2. Preliminary treatments which increase the number of intermolecular bonds, such as heating the fiber in mineral oil at 150°, lower the sorption of phenol.

3. The rate of sorption of phenol by polyamide fibers very greatly depends on the molecular structure, and decreases as the latter becomes stronger.

4. Diffusion of phenol in steady state conditions is thousands of times more rapid than in nonsteady conditions. Differences in the molecular structure of polyamide films are evened out if the diffusion of phenol takes place in steady state conditions.

5. The diffusion coefficients of phenol in polyamide fibers calculated for nonsteady conditions from equations (2) and (4) have the same values.

LITERATURE CITED

[1] E. K. Mankash and A. B. Pakshver, J. Appl. Chem., 26, No. 8, 835 (1953).*

[2] A. B. Pakshver and I. V. Bykova, Colloid J., 16, No. 5, 381 (1954).**

[3] R. Barrer, Diffusion in and Through Solids, Moscow (1948).

---

* See Consultants Bureau Translation, page 759.
** "   "   "   "   "   " 365.

ALTERATION OF THE STRUCTURAL-MECHANICAL PROPERTIES OF BREAD DOUGH

BY MECHANICAL TREATMENT

B. A. Nikolaev and L. S. Beganskaya

The raw materials, intermediates, and finished products of many branches of the food industry have the physical properties of dough, paste, puree, etc.. These substances have a definite structure and are solido-fluids. During the manufacturing process, as the result of various physico-chemical actions and processes (heating, cooling, chemical and mechanical processing) . the original structure and the structural-mechanical properties of such substances may be altered considerably.

The structural-mechanical properties of bread dough were studied by measuring the shearing deformation with the aid of a simple apparatus constructed by B. A. Nikolaev. The apparatus is based on the principle of the measurement of the shear of solido-liquid bodies on an inclined plane, put forward by Tolstoi [1]. In this apparatus, the optical method of measurement of small shear deformations (with the aid of a microscope) is replaced by the method of magnifying small deformations with the aid of a light pointer with unequal arms. In this way, instantaneous shear deformation can be measured more exactly, and the apparatus is also more simple. A brief description of the apparatus and its operating technique is given below.

As is seen from Fig. 1, the apparatus has a base 1; on this is fixed symmetrically an iron plate, 2, the face of which is hinged to a support. Its other side rests freely on the wall of the frame, and may be raised to a definite angle (15°) to the horizontal. This angle is measured on a special scale 3, to which the free end of the plate is attached with the aid of a special pin 4 with a spring clip which is released for lifting. To the plate 2 is attached
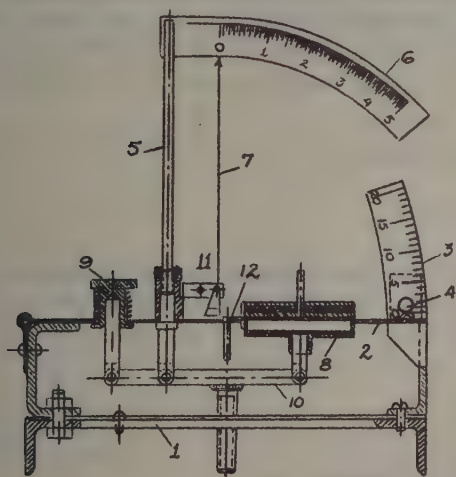
Fig. 1. Scheme of apparatus for the measurement of the structural-mechanical properties of solido-liquid bodies (explanation in text).
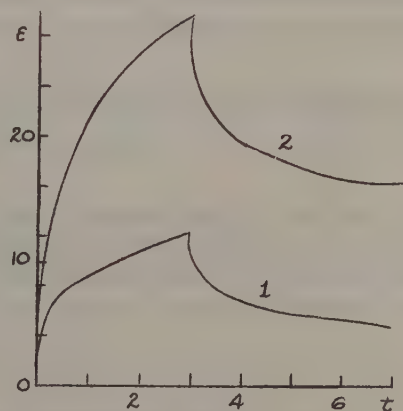
Fig. 2. Curves for the deformation (shear) of grade I wheat dough: 1) after 30 minutes; 2) after 3 hours from mixing.

a stand 5 carrying a measuring scale 6, a lever pointer 7, and the lever mechanism of the lifting plate 8. When at rest, this plate is lowered in an opening 4 X 4 cm on the surface of the inclined plate 2, 5 mm below the level of the latter. The opening has side walls and flanges, on which the plate 8 rests. The plate is raised to the level of 2 by pressing the button 9. The pin on which the head of the button sits then presses down on the end of the hinged lever 10 and its other end raises the plate 8. A turn of the button 9 fixes the plate 8 in the upper position. The pivot of the pointer 7 is attached between the sides of a bracket with an adjustment screw 11. The measuring scale 6 is fixed to the stand and has gradually decreasing divisions (as, during shear, the length of the lower arm of the lever pointer gradually increases).

The apparatus is placed in a thermostat at a constant temperature of 30° and a relative humidity ~90-95% to prevent the sheets of dough from drying on the surface. The average rate of deformation is ~1 mm/min.

The following working procedure was used: the plane of the base 1 is brought into a horizontal position with the aid of leveling screws and a spirit level. The substance tested (dough) is smeared with a spatula on the lowered lifting plate 8, up to the level of the plate 2, and smoothed out. The layer of dough is covered with a thin aluminum cover plate 12, with a corrugated lower surface. The cover plate, 5 g in weight, has a tongue-shaped notch which is brought flush with the lower end of the measuring pointer 7. Excess material which protrudes from under the edges of the cover plate is thoroughly cleaned off. The plate 12 is covered with a loading plate of minimum definite weight (10 g), with a vertical shaft in the center. On this it is then possible to place other loading plates, which have openings in the center with a diameter sufficient to allow the shaft of the first plate to pass through. To prevent the loading plates from slipping off during tilting, the edges of the cover plate have, on the tongue side, vertical rims 5 mm high, against which the loading plates rest.

After the loading plates are put into position, the button 9 is pressed and the loaded layer of dough is raised to the level of the plate 2. A check is made to see whether the pointer on the scale has been displaced from zero, and whether there is any gap between the tongue of the cover plate and the pointer. This is done by means of a light shearing pressure by the cover plate 12 on the pointer 7; in the absence of a gap, the latter should respond at once.

The measurement is carried out as follows: after the dough is held for about 1 minute, the spring pin is released and the end of the plate 2 is raised smoothly but rapidly to the required angle on scale 3. The inclined plane is fixed in position by releasing the spring of the pin 4, a seconds clock is at the same time switched on, and the magnitudes of the deformations are recorded from the movement of the pointer along the scale 6. When the experiment on deformation of the system during loading is completed, deformation during unloading is recorded. For this purpose the loading plates are carefully removed and the instantaneous deformation during unloading noted. Immediately after this the pin 4 is released and the free end of the plane is lowered into a horizontal position rapidly, but smoothly, without impact. The deformation is usually recorded after 0, 15, 30 and 60 seconds, and then after one minute.

The accuracy of the results of the determination depends not only on the construction of the apparatus, but also on the properties of the material on which the measurements are being made. In addition, the results are affected by the frictional resistance of the bearings of the axis of the measuring pointer. It was found that the greatest deviations of the maximum deformations of dough were from 10 to 15% of the smallest value in parallel determinations.

To calculate the shearing modulus E, the following formula was used:

$$E = \frac{P \sin \alpha \cdot 981 \, a\delta}{\epsilon} \quad \text{dynes} \cdot \text{cm}^{-2}, \tag{1}$$

where P is the stress in g/cm^2, found by dividing the total weight of the cover and loading plates by the area (16 cm^2); α is the angle of inclination of the plate; $\underline{a}$ is the magnification of the deformation produced by the pointer of the apparatus, equal to 20; δ is the thickness of the layer of dough (equal to 5 mm); ϵ is the deformation in scale divisions of the apparatus in a given time (seconds). The viscosity is calculated from the formula:

$$\eta = \frac{P \sin \alpha \cdot 981 \, a\delta\tau}{\epsilon' - \epsilon} \quad \text{poise}, \tag{2}$$

where τ is the time in seconds, corresponding to the difference in deformation $\epsilon' - \epsilon$.

The weights of the loading plates in tests of shear and flow were so chosen that in 3-4 minutes the deformation did not exceed the dimensions of the scale of the apparatus (5 mm). For dough from graded wheat flour of normal quality and moisture content (45-48%) the load was 55 g; for dough from rye flour, 100 g; for moist gluten, 35-90 g; and for starch, 100-120 g. The angle of inclination of the plate was 15-10°.

The main visco-elastic properties of dough given in the present paper — viscosity, elasticity modulus, ratio of viscosity to elasticity modulus, and the elasticity — were adopted according to the scheme proposed and developed by Rebinder [2]. Because of the specific properties of bread dough, it was also necessary to introduce such supplementary characteristics as liquefaction on standing and fermentation, increase of strength on deformation, and arbitrary plasticity.

In an earlier publication [3] the results were given of the measurements of the elastic-viscoplastic properties of bread dough, gluten proteins, and starch pastes. It was shown that the elastic properties of dough depend on the

properties of gluten, which is a body with high elasticity. By applying stresses which differed by a factor of 2-3, it was possible to demonstrate instantaneous and gradually developing shear deformations, which were in fairly good agreement with the proportionality law. It was found that immediately after mixing the values of the viscosity and elasticity modulus of dough decrease. The rate of this decrease depends on the properties of the flour, and also on the presence or absence of yeast. As a relative measure of coefficient of liquefaction, the expression $(1 - \eta_t/\eta_0) \cdot 100$ was proposed, where η_t and η_0 are the mean viscosities of the dough after mixing and after it is kept or fermented during a time t. When the dough was heated in the range 25-60°, the maximum deformations reached in 3 minutes increased at first, and at 40° for rye dough and 50° for wheat dough they decreased again as the result of gelatinization of the starch and denaturation of the proteins which then commenced. It was shown that the result of stirring of dough from 1st grade wheat flour was to decrease the viscosity and the shear modulus; the dough became less resilient but more elastic, the volume of the bread became greater and the porous structure of the crumb was improved.

We give below the results of supplementary investigations of changes in the elastic-viscoplastic properties of dough during deformation and mechanical processing.

The shear curves for dough after the development of high-elastic deformation, which usually occurs during the first minute of deformation (Fig. 2) in most cases show a gradually decreasing rate of change. We may, therefore, introduce, as a measure of this strengthening of structure, the expression.

$$\left(1 - \frac{v_3}{v_2}\right) 100,$$

where v_2 and v_3 are the rates for the second and third minutes of deformation of the dough.

With this relative characterization it is possible to classify arbitrarily the shear curves for dough into two types: Type I, curves with a strengthening characteristic above 10%, and, therefore, without a region of constant rate; Type II, curves with a value of 0 to 10% for this characteristic.

Table 1 shows data for the strengthening values of dough from flour of different sorts, quality, moisture content, and time of standing after mixing. For comparison, the values for the strengthening of gluten proteins washed out of this flour are also shown. Fig. 2 shows the shear curves (P = const) for dough with a moisture content of 60% from grade I flour (Table 1, variety with 60% moisture).

TABLE 1

Elastic-Viscous Properties of Dough from Flour of Different Grades and Quality

Flour grade	Moisture content of dough (%)	Keeping time (min)	Strengthening (%)
Grade I	33	0	55
"	33	180	34
"	46	30	40
"	46	180	0
"	60	30	0
"	60	180	40
Gluten grade I	62	0	36
Grade II, weak	48	0	11
" "	48	30	22
" "	48	180	58
Gluten Grade II, weak	60	0	43
Grade II, strong	48	0	0
" "	48	30	44
" "	48	180	27
Gluten grade II, strong	60	0	56

The data of Tables 1 and 2 show that the strengthening power of dough depends on its moisture content, time of keeping, and grade and quality of the flour. The gluten proteins of flour have a high strengthening power.

Repeated deformation of dough, after removal of load and relaxation of the stresses in it, shows the presence of strengthening as the result of the first test. In firm dough of the macaroni type (moisture content 27-28%) a second deformation leads to loss of plastic flow properties, as can be seen from Fig. 3.
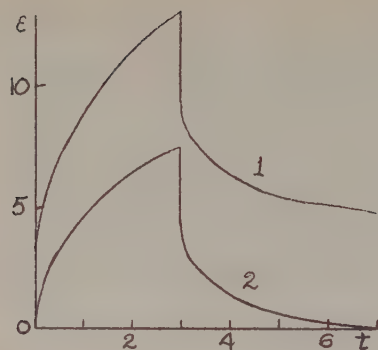
Fig. 3. Curves for the deformation (shear) of macaroni dough. 1) First deformation; 2) second deformation.
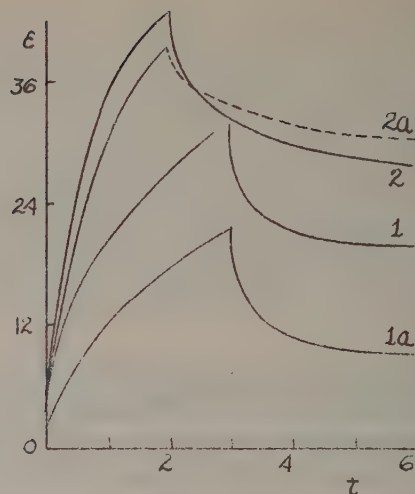
Fig. 4. Curves for the deformation (shear) of gluten. 1) Strong; 1a) the same, after treatment in a mortar for 1 minute; 2) weak; 2a) the same, after treatment in a mortar for 1 minute.

The following attempt can be made to explain the strengthening of dough. The structure of bread dough may be schematically represented as a spatial network of swollen hydrated proteins, filled with fragments of hydrated starch grains, cellulose, and other insoluble and semisoluble high molecular compounds. The mass of such a structure evidently contains a small amount of highly concentrated solutions of sugars and inorganic salts. This structure also contains a considerable quantity of gaseous substances, in non-fermenting (yeastless) dough—air, and in dough with yeast also the carbon dioxide formed by the yeast.

As the result of low velocity shear, the loose structure of the dough loses some of its gaseous content, its specific gravity increases, and the structure becomes more dense. Apparently in the process the macromolecules of high polymeric compounds (mainly proteins) become oriented in the shearing plane. The capacity for strengthening during shear depends on changes in the value of the ratio η/E during deformation. Strengthening increases with increase of this ratio

To determine the degree of change of structure of wheat yeastless dough and its chief components (gluten proteins and starch paste) by mechanical action, the mass of dough was kneaded with a pestle in a porcelain mortar for one minute after keeping; tests before kneading served as controls.

TABLE 2

Viscoelastic Properties of Dough After Keeping and Kneading

Specimen No.	Duration of keeping and treatment of dough	E dynes/cm$_2$ X 10^5	η X 10^6 (poises)	η/E (sec.)	Plasticity (%)	Elasticity (%)
1	After mixing (control)	3.7	7.0	20	70	76
	The same, after kneading	2.8	4.0	14	83	78
	After 30 minutes (control)	2.2	2.5	11	76	75
	The same, after kneading	1.7	1.3	8	82	76
	After 3 hours (control)	1.2	2.5	21	84	70
	The same, after kneading	1.1	1.6	14	86	83
2	After mixing (control)	8.4	43.0	51	48	77
	The same, after kneading	6.4	16.0	25	71	75
	After 30 minutes (control)	2.8	6.0	21	77	73
	The same, after kneading	3.1	5.8	19	83	71
	After 3 hours (control)	2.2	4.0	18	90	73
	The same, after kneading	1.7	4.0	23	90	50

The results of Table 2 show that for dough from grade II flour with a moisture content of 48%, such treatment decreases the average viscosity, shear elasticity modulus, and the ratio η/E (as the result of the great decrease of viscosity); the plasticity, determined by the percentage ratio of the residual deformation after removal of load to the

maximum deformation produced, increased. The elasticity, determined by the percentage ratio of the high-elastic deformation to the total elastic deformation on removal of the load from the system, was almost unchanged by the treatment. The effect of the treatment decreased as the keeping time was greater.

Gluten and starch paste, on the other hand, showed increased values of the main viscoelastic properties after grinding in a mortar for 1 minute. The weaker gluten was changed less by the treatment (Fig. 4).

In order to study the effect of more vigorous mechanical treatment on changes in the viscoelastic properties of dough, it was passed three times through a worm shredder of the meat mincer type immediately after mixing, and also after keeping. Measurements were made after each passage, and the results are shown in Table 3.

TABLE 3

Viscoelastic Properties of Dough After Treatment in Worm Shredder

Flour grade, moisture content of dough	Duration of keeping, nature of treatment	$E_0 \cdot 10^5$ dynes/cm^2	$\eta \cdot 10^6$ (poises)	η/E (sec.)
Grade I, 46%	As mixed (control)............	4.0	14.0	35
	1 passage.................	4.2	9.8	25
	2 "	2.2	8.8	40
	3 "	3.1	9.8	31
	30 minutes after 1st series of treatments			
	1 passage.................	2.4	5.0	20
	2 "	2.8	7.0	25
	3 "	2.6	8.0	30
Grade II, 48%	As mixed (control)............	2.1	7.0	33
	1 passage.................	2.1	4.4	20
	2 "	2.0	4.2	21
	3 "	2.1	4.0	19
	30 minutes after 1st series of treatments	2.1	4.0	19
	1 passage.................	1.7	3.0	17
	2 "	1.9	2.8	14
	3 "	1.7	2.9	17

The results given in Table 3 show that dough from grade I flour in the first series of treatments, has lower viscosity and elasticity modulus as the result of the 1st and 2nd passage through the shredder, but these values increase again after the 3rd passage. The first passage in the second series of treatments of this dough is accompanied again by a decrease of viscosity and of elasticity modulus; this may be attributed not only to the treatment, but also to liquefaction during keeping. However, the second and third passages are accompanied by considerable increase of viscosity and a small increase of the elasticity modulus.

The data for the dough from grade II flour show that both series of treatments result in a gradual decrease of the elasticity modulus and viscosity. It is interesting that after a keeping time of 30 minutes (before the 2nd series of treatments) the viscosity and modulus values for this dough remained unchanged (after the 3rd treatment of the 1st series). Dough from flour for wallpaper paste (wheat and rye), and dough from grade II wheat flour, had decreased values for the viscosity and the elasticity modulus as the result of increasing mechanical treatment.

In order to clarify further the behavior of the structure of dough made from wheat flour without yeast, it was subjected, after mixing to vigorous stirring in a two-blade farinograph kneader for 10 minutes.

The results in Table 4 and Fig. 5 show that, in contrast to untreated (control) dough, which is greatly liquefied after 3-4 hours, dough treated in this manner has practically unchanged viscosity and a much less changed elasticity modulus. This indicates that dough made from this flour has the power, after the primary structure is destroyed, to form a new, restored, fairly viscous and elastic structure; consequently, vigorous mechanical treatment, as it were, retards the liquefaction process of dough.

The gas-forming and gas-retaining capacity*of dough made with yeast is of great significance for the formation

* By gas-forming capacity is understood the amount of carbon dioxide evolved by the fermenting dough during each hour and in 5 hours of fermentation. The gas-retaining capacity is the increase in the height of the dough in the fermentation vessel during fermentation.

of the structure of the bread crumb. To determine the effect of mechanical treatment on these important indexes of dough quality, dough made from grades I and II of wheat flour and from wallpaper paste flour and yeast was allowed to ferment for 1.5 hours, after which it was divided into two portions. Both portions were tested for gas formation and gas retention in a special apparatus, after which the shear deformation was tested.

TABLE 4

Viscoelastic Properties of Dough After Treatment in Farinograph Kneader

Duration of keeping	$E_0 \cdot 10^5$ dynes/cm^2	$\eta \cdot 10^7$ (poises)	η/E (sec.)
After mixing	4.2	2.1	50
After 3.5 hours			
a) treated	2.4	1.9	79
b) untreated (control).	1.7	0.5	30

The results of the shearing tests are shown in Table 5, and those for gas formation and gas retention in Fig. 6.

The results of Fig. 6 show that the gas forming power of treated dough is less than that of the control during the first three hours, but after two more hours they become almost equal. The gas retention of the dough under test is also less than that of the control at first, but after 2-3 hours it is ahead of the control, and the difference at the end of the fifth hour is the greater for the higher grade flour. The explanation for this can be seen from the results of Table 5, which show that the tested dough from grades I and II flour was much more viscous after the gas formation and retention tests than the control.

In the formation of the quality structure of bread crumb, a harmonious combination of the stresses developing in the dough set up by the gaseous fermentation products, with the viscoelastic properties of the dough, its viscosity and elasticity modulus, will be of significance. The value of the ratio of the viscosity to the modulus of elasticity (duration of the relaxation of stresses in the dough) will also be of great importance. In an earlier communication [3] it was already shown that by intensive mechanical treatment of dough it was possible to decrease the viscosity of the dough and to increase the volume, and also to improve the porous structure of the bread. It was shown above that the viscosity of dough made from grade I flour increases with increasing intensity of mechanical treatment.

TABLE 5

Viscoelastic Properties of Dough After Gas Formation

Flour grade, nature of sample	$E_0 \cdot 10^5$ dynes/cm^2	$\eta \cdot 10^6$ (poises)	η/E (sec.)	Plasticity (%)	Elasticity (%)
Grade I, control.	1.4	6.0	48	79	69
" tested.	1.4	8.0	57	62	78
Grade II, control	1.4	1.6	11	63	84
" tested.	0.7	2.0	30	67	78
Wallpaper, control.	1.2	3.0	25	86	76
" tested	1.5	2.2	15	85	79

TABLE 6

Visco-Elastic Properties of Dough after Mechanical Treatment

Treatment	Variation	$E_0 \cdot 10^5$ dynes/cm^2	$\eta \cdot 10^6$ (poises)	η/E (sec)	Density of the bread g/cm^2
Worm shredder	Control	1.4	6.9	49	2.64
	Test	2.1	10.5	50	2.50
Threefold kneading	Control	1.7	7.0	41	2.60
	Test	2.1	8.0	38	2.72

To determine the effect of the intensity of mechanical treatment on the viscoelastic properties of fermenting dough made from grade I flour and on the specific gravity of the bread, the dough under test was passed three times through a worm shredder; in another variation of the experiment the dough was subjected to less intensive treatment,
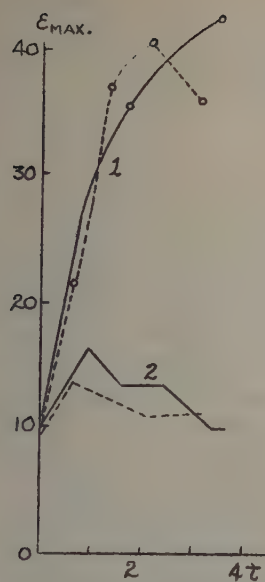
Fig. 5. Curves for the deformation of dough: 1) untreated (two experiments); 2) treated in farinograph kneader (two experiments).
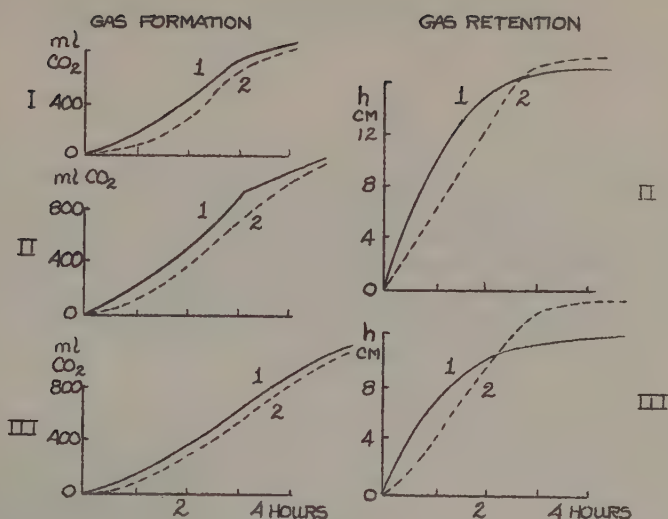
Fig. 6. Effect of mechanical treatment of dough on gas formation and gas retention: 1) control; 2) dough treated in farinograph kneader for 10 minutes; I) dough from wheat flour for wallpaper paste; II) the same, from second grade flour; III) the same, from first grade flour.

and was kneaded three times and then tested together with the control before being put in the oven. The results of these tests are shown in Table 6.

The data of Table 6 show that the result of lowering the intensity of mechanical treatment was to give a lower value of the viscosity, and a greater specific gravity of the bread. In both cases the porous structure of the crumb was improved by mechanical treatment.

SUMMARY

1. The effect of strengthening of bread dough, and also of its basic components (gluten proteins, starch paste) must be considered a valuable characteristic of the structure of these systems, which offers additional possibilities for their study.

2. Mechanical treatments of different intensity alter the viscoelastic properties of dough, its specific powers of gas formation and gas retention, and consequently the bulk and porous structure of the bread. In dough from grade I flour the values of the viscosity and modulus of elasticity at first decrease with greater intensiveness of treatment, and then increase again. By keeping such dough it is possible to "retard" the liquefaction process by restoring the structure. In dough of low grade flour, mechanical treatment continuously decreases the values of the viscosity and the modulus of elasticity.

3. By regulation of the intensity of mechanical treatment of dough according to the grade and quality of the flour, it is possible to improve the quality of bread products.

LITERATURE CITED

[1] D. M. Tolstoi, Trans. All-Union Conf. on Friction and Wear in Machines, 155 (1949).

[2] P. A. Rebinder, Collected Papers, "New Methods of Physico-Chemical Investigation of Surface Phenomena", Academy Sci. USSR Press (1950).

[3] B. A. Nikolaev, Proc. Acad. Sci. USSR, 90, 4 (1953).

ANOMALOUSLY EARLY TURBULENCE OF COLLOIDAL SOLUTIONS

I. I. Rogachev

As is known from hydrodynamics, as the viscosity η increases, there is an increase of the pressure p_c at which the critical value of the Reynolds number Re_c is reached, indicating the beginning of failure of the laminar regime. Therefore, in colloids, which behave, as a first approximation, like normal liquids but have a greater viscosity than water, the beginning of turbulence should be shifted in the direction of greater pressures in comparison with water. However, in a number of sols, as, for example, in concentrated sols of $Fe(OH)_3$ [1], aluminum oleate, and others, turbulent flow begins in the region of lower pressures than for water, and increasingly earlier as the viscosity of the sol is greater. This displacement of the beginning of the turbulent flow of sols toward lower pressures has been termed anomalous turbulence of colloidal solutions.

Explanations of this effect at the present time are based on the views of Wo. Ostwald [2], according to which anomalous turbulence is the consequence of this presence of a structure in the sols. The anisodiametric particles of the disperse phase, becoming oriented in the laminar stream of the dispersion medium, cross layers having different velocities, mix them together, and so favor the formation of vortexes at flow rates which in themselves do not cause them. If such a particle is already oriented with its axis at an angle to the stream, it will, nevertheless, also assist turbulization of the flow, acting as a barrier. In addition to this, early formation of vortexes is also favored by disruption of structure and, finally, by Brownian movement, which displaces particles from one layer into another. We will now show that this viewpoint of Wo. Ostwald on the cause of anomalous turbulence in colloids is in direct contradiction to the modern concept of the nature of turbulence.

The turbulent motion of a liquid at sufficiently high Reynolds numbers is considered [3] as the superposition of two motions: the characteristic of turbulence, randomly changing "pulsation" motion $\vec{v}'$, and the motion with a mean average rate $\vec{u}$. The pulsational motion $\vec{v}'$ is the result of superposition of turbulent pulsations of various scales of magnitude: by the scale of the motion is understood the order of magnitude of the distance, over which the rate of the motion changes significantly. As the Reynolds number increases, the number of turbulent pulsations becomes greater, and their scale decreases. Thus, at high values of Re in turbulent flow there is a whole "spectrum" of pulsations with scales from the greatest to the least; the determining role is played by the large scale pulsations, i.e., pulsations the scale $\underline{l}$ of which is of the order of the characteristic length of the turbulent flow region. Such pulsations have the greatest amplitude and velocity, comparable in magnitude to the change Δu of the average velocity over the characteristic distance $\underline{l}$ of the turbulence region. These pulsations contain the greatest part of the total kinetic energy of the liquid. The small scale pulsations correspond to high frequencies, have considerably lower amplitudes, and therefore contain less kinetic energy. Over distances comparable with $\underline{l}$, the change of the velocity $\vec{v}'$ of the stream is determined by the change in the rate of the large scale pulsations and is, therefore of the order of magnitude of Δu. At distances $\lambda \ll \underline{l}$ change of $\vec{v}'$ is determined by the small scale pulsations. Together with the Reynolds number $Re = \dfrac{vl}{\nu}$, which determines the properties of the flow as a whole, we consider the Reynolds numbers Re_λ, which correspond to turbulent pulsations of different scales:

$$Re_\lambda \sim \frac{v_\lambda \lambda}{\nu},$$

where λ is the order of magnitude of the scale of the given motion, $\underline{v}_\lambda$ is the order of its velocity, and ν is the kinematic viscosity.

Large scale pulsations have the greatest scales of motion, they have large values of the Reynolds number Re_λ, and consequently, the viscosity is low and can be assumed equal to zero. In such pulsations there is no appreciable dissipation of energy; they may be described by the Euler equation. Conversely, for small scale pulsations the value of Re_λ is small and the viscosity of the liquid has a significant value, producing dissipation of kinetic energy as heat. The turbulence properties in regions, the dimensions of which are comparable with the characteristic length $\underline{l}$ (developed turbulence) are completely determined by the density of the liquid ρ, the distance $\underline{l}$, and the velocity Δu.

In contrast to developed turbulence, local turbulence is defined as turbulence of the scale λ, small relative to $\underline{1}$, but much greater than the distances λ_0 at which the viscosity of the liquid begins to play an appreciable part. In this case the determining parameters will be the density ρ, the energy ϵ, and the scale of the motion λ. The order of magnitude of λ_0 is determined from the condition $Re_{\lambda_0} \sim 1$, from which it follows that:

$$\lambda_0 \sim \frac{1}{Re^{3/4}}.\tag{1}$$

The value of λ_0 determines the order of the least scales of turbulence — the lower boundary of the "spectrum" of turbulent pulsations.

Let us now apply the above results to the theory of Wo. Ostwald. According to this, vortex formation in laminar flow is caused either by the colloidal particles themselves, acting as barriers, or by their motion. In both cases, we are dealing with distances of the same order as the size of these particles. Change of the rate of flow of the stream of the medium takes place in distances of this order. On the other hand, as anomalously early turbulence is usually observed in Poiseuille-type flow of sols, the characteristic distance $\underline{1}$ in this case will be the capillary radius R. As the dimensions of the colloidal particles are many times less than R, the turbulence which arises will be local turbulence in its properties, and, in particular, the relationship (1) may be applied to it, which gives the lower boundary of the scales of the smallest turbulent pulsations. Pulsations of smaller scales cannot exist. On the other hand, the order of this boundary will be given by the dimensions of the colloidal particle itself. Let us determine the value of λ_0 from each of these aspects.

The radius of colloidal particles (the equivalent radius) falls within the range from 10^{-5} cm to 10^{-7} cm, so that we may take the mean value $\underline{r}_m = 10^{-6}$ cm. At the same time, if we take for the Reynolds number the deliberately high value $Re_c = 10^4$, and the capillary radius is taken to be of the order of 10^{-1} cm, we then have from the expression (1):

$$\lambda_0 \sim \frac{10^{-1}}{(10^4)^{3/4}} = 10^{-4} \text{ cm},\tag{2}$$

so that

$$\frac{\lambda_0}{r_m} \approx 10^2.\tag{3}$$

Fig. 1.

In reality, the value assumed for the Reynolds number is much too great. For example, the experiments of Rabinerson and Fuks on the anomalous turbulence of $Fe(OH)_3$ sol [1], even for low concentrations, give for this sol $Re_c = 10^3$, and hence

$$\frac{\lambda_0}{r_m} \approx 10^{11/4}.$$

As we see, the dimensions of the colloidal particles are of the order of 10^2–10^3 times less than the lowest possible scales of turbulent pulsations. Hence it follows that the existence of a structure in the sol cannot lead to any significant vortex formation, to disturbance of the laminar flow of the dispersion medium, and hence, cannot lead to earlier turbulization of the colloid.

Therefore, on the basis of the above views it may be asserted that early turbulence observed experimentally in many sols cannot be explained by the existence of a structure in them. Below we give an explanation for this effect, based on purely phenomenological considerations, without the assumption of any structure in the sol.
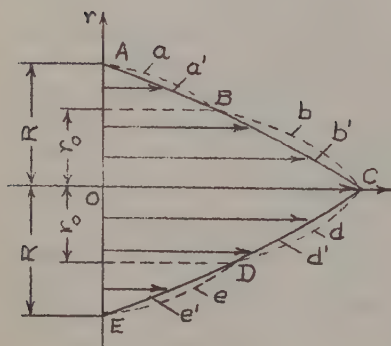
We will limit ourselves to an examination of those colloids, the viscosity of which alters very sharply in a very narrow interval of shear stress σ, and remains almost constant outside the limits of this interval. The motion of such liquids may be described [4] by the methods of hydrodynamics of normal viscous liquids. Let us investigate the stability of the velocity profile AaBbCdDeE (Fig. 1) which is formed when these liquids flow through capillaries. For this it would be necessary to subject to small disturbances $\underline{v}'$ the steady velocity distribution obtained by solution of the equations of motion for a viscous liquid. If these distrubances increase with time, the motion cannot be stable. However, this general method for the investigation of the stability of motion is very complicated in the mathematical sense, and at present has been only achieved for the simplest forms of flow of incompressible Newtonian liquids.

442

For liquids with variable viscosity, which include sols, which have anomalously early turbulence, such investigation can hardly be considered as achieved. To avoid the mathematical difficulties, we replace the sol by an ideal liquid with the velocity profile Aa'Bb'Cd'De'E (Fig. 1). The basis for this approximation is that early turbulence in sols is observed at the fairly large values of Reynolds number Re $\sim 10^3$, and the latter is equivalent to a low viscosity of the liquid. The disturbed motion $\underline{v_z} = \underline{v(r)} + \underline{v'_z}$, $\underline{v_r} = \underline{v'_r}$, $\underline{v'_\theta} = 0$, where

$$v'_z = e^{i(kz-\omega t)} \cdot \varphi(r), \quad v'_r = e^{i(kz-\omega t)} \cdot \psi(r) \tag{4}$$

are the component terms of the distrubance of velocity in a cylindrical system of coordinates, the axis OZ of which coincides with the capillary axis, should satisfy Euler's equation [3]. The function $\psi(\underline{r})$ should be continuous at the boundary between the regions of the velocity profile, while its derivative should, at these points, satisfy the condition:

$$\frac{1}{\psi}\left[\frac{d\psi}{dr}\right] = \frac{k}{vk-\omega}\left[\frac{dv}{dr}\right], \tag{5}$$

where the square brackets indicate the increment of the corresponding value at the boundary of the regions of the profile.

From these properties of the function $\psi(\underline{r})$, we define it as follows:

$$\psi_1 = C_1 e^{-kr} \ (r > R);$$

$$\psi_2 = C_2(\text{ch } kr + a_1 \text{ sh } kr) \ (r_0 < r < R);$$

$$\psi_3 = C_3(\text{ch } kr + a_2 \text{ sh } kr) \ (0 < r < r_0);$$

$$\psi_4 = C_4(\text{ch } kr - a_2 \text{ sh } kr) \ (-r_0 < r < 0),$$

where C_1 and $\underline{a_1}$ are certain constants. If condition (2) is fulfilled at the boundary points of the profile, we obtain the following equation for ω:

$$r_0^2 (R-r_0)^2 \omega^3 + \{\beta r_0^2 (r_0-R) - v_0 k r_0^2 (R-r_0)^2(1 + \text{th } kR) - \beta k r_0^2 (R-r_0)^2(1 + \text{th } kR) - r_0(R-r_0)[\beta R +$$
$$+ (r_0-R)V_\theta] \text{ th } k r_0 \text{ch}^2 k r_0 (1 + \text{th } kR) + r_0(R-r_0)[\beta R + (r_0-R)v_0](1 + \text{th } kR)\text{ch}^2 \ k r_0 + r_0(R-r_0)^2(v_0-\beta)(1 + \text{th } kR)\} \ \omega^2 +$$
$$+ \{\beta r_0[\beta R + (r_0-R)v_0]\text{th } k r_0 \ \text{ch}^2 \ k r_0 - v_0 k r_0(R-r_0)[\beta R + (r_0-R)v_0]\text{ch}^2 \ k r_0(1 + \text{th } kR) + (v_0-\beta)(R-r_0)[\beta R +$$
$$+ (r_0-R)v_0](1 + \text{th } kR) \text{ th } k r_0 \ \text{ch}^2 k r_0 - \beta \ k r_0(R-r_0)^2(v_0-\beta)(1 + \text{th } kR) - \beta r_0[\beta R + (r_0-R)v_0]\text{th } kR \cdot \text{ch}^2 k r_0 -$$
$$- r_0(v_0-\beta)\beta(R-r_0)\text{th } kR + \beta v_0 k^2 r_0^2 (R-r_0)^2(1 + \text{th } kR) + v_0 k r_0(R-r_0)[\beta R + (r_0-R)v_0](1 + \text{th } kR)\text{th } k r_0 \text{ch}^2 k r_0 -$$
$$- (v_0-\beta)(R-r_0)[\beta R + (r_0-R)v_0]\text{th}^2 k r_0(1 + \text{th } kR)\text{ch}^2 \ k r_0 + \beta v_0 k r_0^2 (R-r_0) + \beta^2 k r_0^2 (R-r_0)\} \ \omega + \{v_0 k r_0[\beta R +$$
$$+ (r_0-R)v_0]\beta \cdot \text{th } kR \text{ ch}^2 \ k r_0 - (v_0-\beta)[\beta R + (r_0-R)v_0]\beta \ \text{th } k r_0 \cdot \text{th } kR \cdot \text{ch}^2 \ k r_0 + \beta^2 k r_0(v_0-\beta)(R-r_0)\text{th } kR -$$
$$- \beta^2 v_0 k^2 r_0^2 (R-r_0) - \beta v_0 k r_0[\beta R + (r_0-R)v_0]\text{th } k r_0 \text{ ch}^2 \ k r_0 + \beta(v_0-\beta)[\beta R + (r_0-R)v_0]\text{th}^2 \ k r_0 \cdot$$
$$\cdot \text{ch}^2 \ k r_0\} \ = 0. \tag{6}$$

Here R is the radius of the capillary, β and $\underline{v_0}$ are the values of the velocity of the liquid when $\underline{r} = \underline{r_0}$ and $\underline{r} = 0$.

The nature of the roots of equation (6) determines the result of the investigation. Assume that $\underline{r_0} \neq 0$ and $\underline{r_0} \neq R$. Let us examine two cases:

1. $\underline{kr_0} \gg 1$ (consequently, $kR \gg 1$).
Equation (6) in this case may be reduced to the form:

$$\omega^3 - (v_\theta + \beta)k\omega^2 + \beta v_0 k^2 \omega - \frac{\beta^3 v_0 k^2}{2(R-r_0)} = 0. \tag{7}$$

Here in each of the coefficients of equation (6) remain only the terms of the highest order with respect to the values of $\underline{kr_0}$ and $\underline{kR}$. All the three roots of equation (7) are real. The disturbance $\underline{v^\circ}$ is related to time by the factor $\underline{e^{-i\omega t}}$, and the latter decreases exponentially with time for real values of ω; thus, for $\underline{kr_0} = 1$, the motion of the liquid is stable.

2. $\underline{kR} \ll 1$. If we leave in the coefficients of equation (6) the terms of the least order with respect to the values of $\underline{kr_0}$ and $\underline{kR}$, we have:

443

$$\omega^3 - \beta k\omega^2 + \frac{k^3\left\{[\beta R - (R - r_0)v_0]\left[(R - r_0)\left(\beta R - \frac{1}{3}v_0 r_0 - \frac{2}{3}\beta r_0\right) - \beta r_0\left(R - \frac{2}{3}r_0\right)\right] + \beta v_0(R - r_0)^2 R\right\}}{(R - r_0)^2}\omega +$$

$$+ \frac{\frac{1}{3}\beta k^4\left\{[\beta R - (R - r_0)v_0][vRr_0^3 + 2\beta Rr_0^3 - v_0 r_0^4 - \beta r_0^4] - \beta^2 R^3 r_0^2\right\}}{r_0^2(R - r_0)^2} = 0. \quad (8)$$

Equation (8) has one real root and two conjugate complex roots. The factor $e^{-i\omega t}$ in the expression for v', which corresponds to the value of ω with a positive imaginary part, increases indefinitely with time; the motion of the liquid is absolutely unstable.
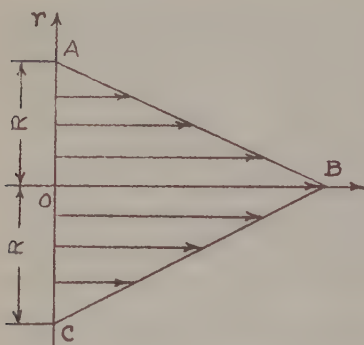
Now let $r_0 = 0$ or $r_0 = R$. The profile becomes the line ABC (Fig. 2). Motion with such a velocity distribution is also unstable (6).

Fig. 2.

Since in the liquid there may exist disturbances with all possible values of kr_0 and kR, among them will be found those for which $kR \ll 1$. These disturbances cause the flow to become turbulent, and as a result, the motion of an ideal liquid with the velocity distribution Aa'Bb'Cd'De'E will be absolutely unstable. This last fact shows the low stability of the velocity profile of a sol flowing through a capillary. However, the less stable is the motion of a liquid, the earlier, with other equal conditions, will turbulence arise in its flow.

We now turn to the cause of the low stability of the motion of sols. It is easily seen that if for a non-Newtonian liquid the viscosity curve $\eta = \eta(\sigma)$ has a relatively sharp jump at a certain "critical" distance r_0, the flow of such a liquid cannot be stable. In this case, the viscosities η_1 and η_2 have sufficiently different values and the condition for uninterrupted velocity when $r = r_0$ is no longer fulfilled; there is a break in the continuity of the tangential component of the velocity. Such tangential interruptions in an incompressible liquid are always absolutely unstable [3]. Therefore, the surface of the tangential break r_0 = const cannot exist for long in the liquid; it becomes "stirred up", and makes the flow turbulent. Thus, the anomalously early turbulence observed in sols is a direct consequence of the tangential breaks of velocity which occur in their flow.

In conclusion, I offer my sincere thanks to Professor V. G. Levich and Professor M. P. Volarovich for their constant attention and assistance in this work.

LITERATURE CITED

[1] A. I. Rabinerson and G. I. Fuks, Proc. Leningrad Dept. Gedroiz Inst. Fert., 22, 50 (1933).

[2] Wo. Ostwald, Koll. Z., 43, 1927.

[3] L. Landau and E. Lifshits, Mechanics of Continuous Media, United State Press (1944).

[4] I. I. Rogachev, Colloid J., 15, No. 5 (1953).•

• See Consultants Bureau Translation, page 393.

INVESTIGATIONS OF THE STRUCTURE OF STARCH

IV. DIELECTRIC PROPERTIES OF NATIVE AND DISPERSED STARCH OF DIFFERENT DEGREES OF HYDRATION

M. S. Shulman and S. M. Lipatov

It was established by studies of the dielectric properties of polymer fractions that the dielectric constant of a polymer solution depends only on the chemical structure of the monomer unit of the given polymer [1, 2, 3]. Our studies of a series of polymer fractions showed that the behavior of the so-called soluble fractions is exactly the same as that of the other fractions, and the curves for the variation of the dielectric constant with concentration coincide for different fractions, although such properties as solubility, high viscosity, power of spontaneous aging, etc., differ greatly. These results are evidence of separate and independent behavior of the polar groups, the nature of which, and not the number in the macromolecule, determines the DC*of a substance. This is shown particularly convincingly by studies of the DC of dextrin, maltose, and starch, which have equal values of dielectric constant in the concentration range studied (Fig. 1).
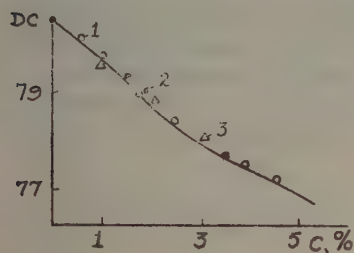
Fig. 1. Dependence of the DC of dextrin, maltose, and starch on the concentration.

We also showed that one can only speak of the dipole moment of the polar groups of a polymer, and not of its macromolecule as a whole. Therefore, the value of the dipole moment for starch calculated by us was taken equal to $1.7 \cdot 10^{-18}$ instead of the value of $56 \cdot 10^{-18}$ according to Dumansky and Kurilenko [4].

Our studies of the variation of the dielectric constant of a fraction with temperature showed that with increased temperature the DC of water and of the solutions of the fractions decreases considerably, and the curves for the variation of the dielectric constant of water and the solutions have a parallel course with a constant difference. From our results, we concluded that the structural changes observed in polymers are mainly due to non-dipole action. These conclusions were confirmed in studies of the dielectric properties of starch at different frequencies (Fig. 2).

The measurements of the dielectric properties of starch were carried out with the aid of a capacity bridge with compensating resistances. The generator permitted a smooth variation of wavelength from 50 to 500 m. The results obtained are also confirmed in studies of the DC by the Drude-Coolidge method, which is as follows. An ultra high frequency generator is inductively coupled to two parallel metallic conductors (Lecher system) terminating in two metallic bridges, one of which is movable. If the Lecher system is in air, then at resonance the distance between the bridges is equal to a whole number of half-waves. The resonance of the system is disturbed if a capacitor with the liquid under test is connected in parallel to the Lecher conductors.
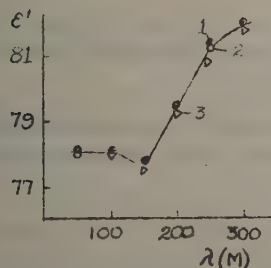
Fig. 2. Dielectric properties of native (1), dispersed (2), and soluble starch (3) at different frequencies.
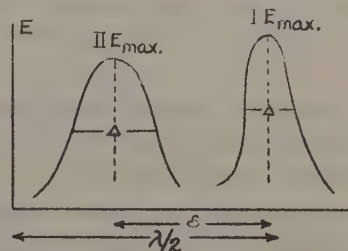
Fig. 3. Resonance curves for starch solutions (explanation in text).

---

* Here and subsequently, DC means the dielectric constant.

Sosinsky and Dmitriev [5] quote formulas for calculating the values of both components of the complex value of the dielectric constant from the displacement of the bridge and the width of the resonance curve.

If the voltage between the conductors of the Lecher system is measured, the position of the movable bridge being varied, then the resonance curves will have the form shown in Fig. 3, where δ is the displacement of the maximum of the resonance curve relative to the maximum for the system in air (I) and when a capacitor with the solution is coupled in (II); Δ is the width of the resonance curve, corresponding to the value of $\frac{1}{2}E_{max}$.

With the aid of the Coolidge equation, modified by Sosinsky and Dmitriev [5], the real and imaginary components of the dielectric constant of starch solutions of different concentrations were calculated for a generator wavelength $\lambda = 6.8$ m. The results obtained are shown in Fig. 4.

Studies of the variation of the dielectric constant of concentrated starch solutions with temperature showed that as the temperature increases the real component of the DC decreases and its imaginary component increases. The changes of the DC of glucose solutions are similar.

Thus, the results obtained in the study of the dielectric constants of highly concentrated solutions of starch and glucose also confirm our views that the dielectric constant of a polymer solution depends only on the chemical structure of the monomer unit of the polymer.

Measurements of the dielectric constant of concentrated starch solutions also showed that DC does not change in the aging process. This confirms yet again that the structural properties associated with changes in the progressive motion of the particles are not related to dipolar interaction, i.e., the rotational motion of the groups is retained.

Studies of the dielectric constants of starches of various degrees of hydration showed that native, gelatinized, and soluble starch give coincident curves. These investigations confirmed the identical nature of starch hydration, and on their basis it is possible to speak of an equal number of OH groups excluded from mutual interaction. The DC method may serve as a method of dielectric titration of the active polar groups of a polymer. Analogous investigations with starch derivatives (mono-, di-, and triacetate) gave results which confirm our views concerning the screening of polar groups and their exclusion by hydration.
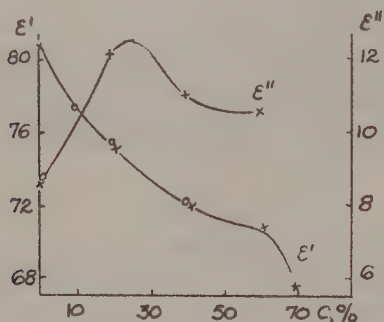
Fig. 4. Real (ϵ') and imaginary (ϵ'') components of the dielectric constant of solutions of: o = potato starch; x = glucose of various concentrations.
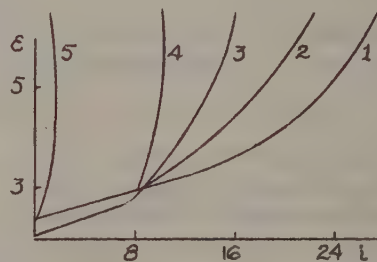
Fig. 5. Dielectric properties: 1) native and gelatinized starch, and its derivatives; 2) monoacetate; 3) diacetate; 4) triacetate; 5) quartz sand.

As the polarities of the substances studied decrease (from mono- to triacetate), the sharp increase of the dielectric constant begins earlier, and corresponds to the amount of chemically bound water determined by the calorimetric method.

Fig. 5 shows the results obtained, and also variation of the dielectric constant of quartz sand with moisture content. It is seen from Fig. 5 that the sharp increase of DC is associated with exclusion of the polar groups and the attainment of sufficient freedom of rotation by them.

In this connection it was also of considerable interest to study the dielectric properties of starches of different moisture contents over a wide range of temperatures. Native and mechanically dispersed potato starch was used for these investigations. Weighed samples of these starches were dried for three days in an electric oven, first at 60-70°, and then at 110°, and were then placed in a desiccator (over calcium chloride) and used in the dry state for the investigations. To obtain starch samples of different degrees of hydration, they were placed in a desiccator over water vapor. The moisture was determined gravimetrically. The dielectric constants were determined by the compensated capacity bridge at a generator wavelength of 100 m.

Description of the capacitor.   All the measurements were carried out in a specially constructed capacitor, which consisted of a copper cylinder 70 mm high and 35 mm diameter, with screwed lid and a threaded nut for the base. The thickness of the cylinder walls was 2 mm. The base of the cylinder was made from a good insulating material, the center of which carried a copper peg 10 mm in diameter and 50 mm high. The base was firmly attached by the threaded nut. On the oustide the copper cylinder was wrapped in asbestos, around which nickel wire was wound for heating the substances studied electrically. The wire was covered by asbestos, which was kept tight by a metal band. The capacitor was inserted in a special panel which was connected to the capacity bridge by two fork connections.

For filling, the copper capacitor (without the panel) was placed under a hand press with a special fitting for pressing powders, consisting of a massive steel rod with a hole in the center, corresponding exactly to the diameter of the copper rod of the capacitor. Consecutive repeated compressions give very reproducible results in determinations of the dielectric constant of powders.

After the material had been pressed, the capacitor was inserted in the panel, which was connected to the DC measurement apparatus. The short ends of the capacitor leads were connected through a rheostat to the electricity supply. The rate of heating was 1-1.5° per minute. The temperature was determined by a calorimetric thermometer which was placed inside the capacitor at a depth of 18-20 mm from the top of the contents.

For determinations of DC the leads of the electric heater were disconnected. The capacity of the empty capacitor was determined with the aid of a standard liquid — benzene — and was found to be 3.24 $\mu\mu$ F (at 20°). To introduce a temperature correction, the capacity of the capacitor was determined over a wide range of temperatures, and it was found that the variation of capacity was 0.02 $\mu\mu$ F per 1° C. Thus, in calculations of the dielectric constants a correction was introduced which allowed for variations of C_0, the capacity of the empty capacitor. For example, at 40° the capacity of the capacitor was 3.24 + 20(0.02) = 3.64.
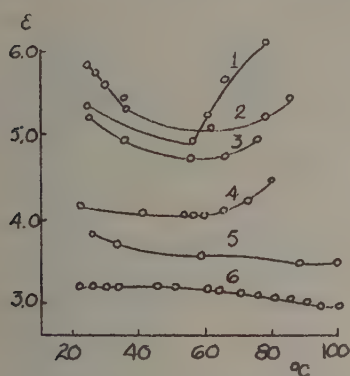
Fig. 6. Dielectric properties of starches with different moisture contents: 1) dispersed, 17.5% H_2O; 2) native, 22.1% H_2O; 3) native, 16% H_2O; 4) dispersed, 12.9% H_2O; 5) native, 4% H_2O; 6 the same, anhydrous.

The results obtained (Fig. 6) show that as the moisture content of the starch increases, an appreciable alteration of structure takes place under the influence of temperature, in all probability characterized by the beginning of fusion of the bonds (gelatinization) which occurs at different temperatures in native and dispersed potato starch. As Lipatov and Meerson [6] showed, for other polar polymers, (gelatin, agar, cellulose ethers, etc.), this effect is general in character, and melting of the polymer can be easily effected if the bonding between the polymer groups is weakened by hydration. The transition from the native to the gelatinized state in the presence of hydration water only in starches may be termed the process of "inner gelatinization", and is characterized by the start of the increase of the dielectric constant, which coincides with the temperature of "inner gelatinization" for a given moisture content of the starch.

A similar state of affairs is found for dispersed starch, and the start of the increase of the dielectric constant is found at lower temperatures and lower moisture content in the starch, for example, for 12% moisture at a temperature of about 60°, and for 17.5% moisture at 55°.

SUMMARY

It is shown that by measurements of the dielectric constants it is possible to show the "melting" of bonds which occurs in starches of different structure depending on the degree of solvation and temperature. In these conditions, it is also possible to establish structural differences in polymers by the DC method.

LITERATURE CITED

[1] S. M. Lipatov and M. S. Shulman, Colloid J., 5, 555 (1939).
[2] M. S. Shulman, Colloid J., 6, 747 (1940).
[3] S. M. Lipatov and M. S. Shulman, Colloid J., 8, 452 (1946).
[4] A. V. Dumansky and O. D. Kurilenko, Proc. Acad. Sci. USSR, 9, 1197 (1948).
[5] S. L. Sosinsky and V. A. Dmitriev, J. Exp. Theoret. Phys., 8, 1384 (1938).
[6] S. M. Lipatov and S. I. Meerson, Colloid J., 12, 122 (1950).

CONFERENCE ON THE STRUCTURAL-MECHANICAL PROPERTIES

OF COLLOIDAL SYSTEMS AND HIGH MOLECULAR COMPOUNDS

A discussion conference on the structural-mechanical properties of colloidal systems and high molecular compounds took place at the Institute of Physical Chemistry, Academy of Sciences, USSR, in December, 1952 and January, 1953. The papers by Academician P. A. Rebinder, Candidate of Chemical Sciences A. A. Trapeznikov, Doctor of Chemical Sciences G. V. Vinogradov, and Candidate of Physico-Mathematical Sciences D. M. Tolstoi contained considerable experimental material and interesting general considerations on the rheological properties of structurized colloidal systems and high molecular compounds.

The discussion conference aroused great interest among scientific and engineering-technological workers of this branch of colloid science. The lively and fruitful discussion of the papers, which was continued during several sessions, clarified the fundamental difficulties which prevent further successful development of this most important branch of rheology, and led to formulation of the basic problems which demand urgent solution.

A number of interesting and important addresses made at the conference should be noted; these include the addresses by G. M. Bartenev, D. S. Velikovsky, Yu. M. Ivanov, N. V. Mikhailov, V. I. Likhtman, K. P. Kashkarev, and others.

The following resolution was adopted as the result of the conference by the organizing committee, consisting of M. P. Volarovich (Chairman), P. A. Rebinder, A. A. Trapeznikov, V. I. Likhtman, D. M. Tolstoi, and N. V. Mikhailov:

"Having heard and discussed the papers and also the numerous contributions to the discussion conference, the participants in the discussion note that:

I. Investigations of the structural-mechanical properties of colloidal systems and high molecular compounds, which constitute the principal content of the physico-chemical mechanics of disperse systems (rheology), form one of the most important branches of colloid chemistry, with a great theoretical and practical importance.

Study of these properties, on the one hand, clearly characterizes the molecular structure and composition of a system, and also the formation in the latter of structures of different kinds, formed as the result of molecular interactions. On the other hand, the structural-mechanical properties, or the elastic-viscoplastic and strength properties of the system, determine the nature of the deformation processes taking place in it under the action of external forces. This determines the outstanding practical significance of the structural-mechanical properties of these systems, as the technological and operational properties of the corresponding materials are in the most general case primarily characterized by their mechanical properties — the capacity for reversible or residual deformations, and also the power of resisting deformation and destruction under the action of external forces.

II. Our national scientists have developed instruments of original design and methods of investigation of different mechanical properties of colloidal systems and high molecular compounds, which assisted the detailed study of these systems and led to new concepts of the role of various factors which determine the practical properties of materials.

Such instruments include the rotational instrument with coaxial cylinders by F. N. Shvedov, the rotational viscosimeter by M. P. Volarovich (State Standard, 1929-1951), the B. P. Veinberg-D. M. Tolstoi apparatus for studying systems in conditions of simple shear between two plates, the S. Ya. Veiler-P. A. Rebinder single plate apparatus, the P. A. Rebinder cone apparatus, the rotational instruments with cones by K. F. Zhigach and D. E. Zlotnik, the capillary type instrument by G. V. Vinogradov and V. P. Pavlov, the rotational instrument by T. Ya. Gorazdovsky with a doubly connected region, the apparatus by A. A. Trapeznikov for complex volume investigations of colloids, incorporating the F. N. Shvedov apparatus, a rotational viscosimeter for a wide range of shearing rates and the vibrational method, M. P. Volarovich's method of X-ray transmission, etc..

A special note must be made of instruments with automatic recording of deformations; the torsional elasto-meter by G. V. Vinogradov and K. I. Klimov with optical photorecording of "instantaneous" deformation, after effects, and strength, the electronic selsyn apparatus by N. V. Mikhailov and coworkers, with automatic oscillographic record-ing of the applied stress, time, and the growth and decrease of deformations, and the capillary type automatic viscosi-meter by A. A. Konstantinov and G. V. Vinogradov.

III. In the development of this branch of colloid chemistry a large part was played by the work of Russian and Soviet scientists; they investigated various colloidal systems, put forward new concepts of the role of different factors, in particular in phenomena of relaxation, thixotropy, viscoplastic flow, etc..

Special mention must be made of the classic work of F. N. Shvedov (1889), who was the first to investigate ex-perimentally the relaxation of shearing stress in structurized solutions of gelatin, discovered anomalous viscosity of colloids, and explained the latter by the existence of shear elasticity in them. B. P. Veinberg and his coworkers studied structurized systems of the bitumen type in conditions of simple shear between two plates; in 1912 they carried out for the first time the integration of Shvedov's equation for the case of coaxial cylinders, with yield stress taken into account.

M. P. Volarovich and coworkers (D. M. Tolstoi, A. A. Leonteva, and others) studied fused glasses, slags, and minerals, and showed that in a number of cases these systems are true viscous liquids, and in some cases they are dis-perse systems with elasticity to shear. Studies were also made on a number of disperse systems, such as clays, lubrica-ting oils, paints, peat suspensions (N. N. Kulakov, A. N. Gutkin, N. V. Lazovskaya) and it was shown that a number of them satisfy Shvedov's equation for viscoplastic flow. Certain cases of thixotropy (V. L. Valdman) and also elastic kinetic effects (R. A. Branopolskaya and T. Ya. Gorazdovsky) were studied. M. P. Volarovich and his coworkers also have the credit for the wide adoption in our country of absolute methods for the measurement of viscosity and the flow limit of high-viscous and viscoplastic bodies.

D. M. Tolstoi determined the laws and mechanism of slip at walls, which is of great significance in the flow processes of structurized systems; he showed that the resistance to shear of the layer adjacent to the wall depends on the mechanism of external friction, and that this concept may be extended to the layers between the particles in the bulk of the liquid. G. V. Vinogradov, V. P. Pavlov, K. I. Klimov, M. M. Gvozdev and others made detailed studies of the origin and development of flow processes in lubricant greases and lubricating oils over a wide range of shear rates and a broad range of temperatures, in relation to peculiarities of their structure. The same field of investigations of the flow of structurized systems includes the work of D. S. Velikovsky, G. I. Fuks, K. S. Ramaiya, S. A. Glikman, and others.

P. A. Rebinder and his coworkers (N. N. Serb-Serbina, E. E. Segalova, L. V. Chumakova, and others) studied the elastic-viscoplastic properties of a series of structurized systems of different types: oleogels, hydrogels, colloidal suspensions of bentonite clays in water, solutions of high polymers over a wide range of concentrations, and structurized systems obtainable from such solutions by the addition of an active filler. These studies included detailed investiga-tions of the elastic-plastic properties of the structures in such systems and of slow flow of the creep type without resi-dual destruction of structure, and effects of elastic relaxation of stress were established together with true relaxation. This work included quantitative studies of thixotropic destruction and restoration of structure in plastic systems, and the effect of restoration of structure was evaluated from the yield stress and the flow limit for the first time.

A. A. Trapeznikov and his coworkers studied the elastic-viscoplastic properties of monolayers (on the surface of water) with different structure and properties: elastic properties, creep, strength, strengthening by deformation. Studies were also made of volume systems of various consistencies, such as fluid highly elastic systems and gels of intermediate consistency, and also lubricant greases. A. A. Trapeznikov and V. A. Fedotova were the first to estab-lish a relationship between the deformational strength and the viscous properties of colloidal structures over a wide range of deformation rates, and also measured the maximum elastic deformation as a function of deformation rate. On the basis of this work they put forward the view that in different ranges of shear stress the same system can behave as a structurized liquid (non-Newtonian, at low shear stresses) and as a plastic body (at high shear stresses), and also that in the region of decreasing viscosity in the system strength properties of the system appear which are quite ana-logous to the strength properties of plastic systems, indicating destruction of the structure. A. A. Trapeznikov and his coworkers established that as the rate of deformation decreases, the maximum on the stress-deformation curve attains a lower value and vanishes at a critical velocity and a critical stress (which corresponds to a transition from variable decreasing viscosity to constant viscosity) and this is regarded as a characteristic of destruction of the struc-ture and as an analog of the flow limit. On this basis, these suthors consider that fluid plastic systems (non-Newtonian liquids) also have thixotropic properties.

V. I. Likhtman and his coworkers developed a phenomenological theory of the creep of metallic monocrystals, and showed that they do not have a final elastic limit, which arises, however, during the process of deformation as

the result of strengthening. Metallic polycrystals, on the other hand, have an elastic limit right from the start (in the non-deformed state) and this is only increased by deformation.

V. V. Stolnikov studied the effect of surface-active additions on the structural-mechanical properties of aqueous cement pastes, and confirmed for these systems the existence of an elastic limit and of a region of creep above this limit.

N. V. Mikhailov and coworkers studied petroleum bitumens and the effects of adding active fillers in the structural-mechanical properties of bitumen mastics, and also the setting and hardening processes of aqueous cement pastes by their structural-mechanical characteristics (E. E. Kalmykova), and in this work they established the existence of systems with a pseudoelastic region and a region of creep, and obtained schemes for the transition of liquid into solid type systems. They demonstrated the characteristic types of deformation kinetics above and below the elastic limit, which distinguish the pseudoelastic region from the true elastic.

The Leningrad school of physicists — A. P. Aleksandrov, P. P. Kobeko, Ya. I. Frenkel, S. E. Bresler, S. N. Zhurkov E. V. Kuvshinsky, G. I. Gurevich and their coworkers, and also V. A. Kargin and G. L. Slonimsky and coworkers, B. A. Dogadkin and coworkers, and G. M. Bartenev developed experimentally and theoretically a wide field of relaxation phenomena in high polymer systems, particularly in elastomers and rubbers.

IV. Rheological investigations in the Soviet Union, both in their content of ideas, and in the methods of investigation, occupy a leading position and are considerably ahead of what is being done in this field by the bourgeois scientists.

The main directions of development of rheological investigations in the Soviet Union are, on the one hand, studies of the mechanism of structure formation processes in colloidal systems, and, on the other hand, utilization of the laws of structure formation and the deformational properties of these systems for practical purposes. Both these directions, being complementary to each other, develop in a close unity.

While the rheological studies of the bourgeois scientists develop often fruitless formalistic model concepts, which hinder an insight into the molecular mechanisms of the phenomena studied (Reiner, Burgers, Alfrey, and others), Soviet rheology, by attracting the foremost modern methods of investigation, develops in the direction of the real nature of the observed effects, and of elucidation of their molecular nature.

The vigorous development of rheological investigations in the Soviet Union in recent years has led to the existence of several viewpoints on certain basic phenomena. Such a situation is quite normal in this relatively young branch of colloid science, and must be considered as an expected result of its intensive and successful development. The different viewpoints in Soviet rheological science should favor its further development.

V. As a result of the discussion, a number of facts, at present mainly of a phenomenological nature, based on modern relaxational concepts, must be considered as established.

Of these, the following deserve special attention:

1. The basic characteristic of structurized systems of the most diverse types is the form of the dependence of the relaxation period in such systems on the acting shear stress, and also the magnitude of this period. According to the nature of this dependence, structurized systems are divided into two groups.

a) Viscoelastic systems, which must be considered as liquids, regardless of their viscosity or relaxation period. In such systems the relaxation period, remaining practically constant or increasing only gradually with decreased stress, does not undergo a sudden increase in the transition to any stress, no matter how small.

Such systems do not have an elastic limit, i.e., an elastic region of stresses which practically do not relax above this limit. The viscosity of these systems decreases fairly smoothly with increase of stress, after they leave the region of practically constant viscosity at low shear stresses. These systems are liquids, as they exhibit steady flow under any stresses, no matter how small, when the time of action of the force is greater than the relaxation period.

b) Solid-like plastic systems, with a limit of flow (elasticity). This limit corresponds to a sudden increase of the relaxation period, i.e., of the viscosity of the system over a sufficiently narrow range of stresses, from quite measurable values of viscosity (relaxation period) above the flow limit to a much greater viscosity below this limit, and even to immeasurably high (practically, infinitely high) viscosity in this region, which must be considered, within the limits of accuracy of the methods of measurement used, the true elastic region.

The yield stress, which characterizes the strength of the structure in solid-like systems, falls with decreasing rate of loading as the result of relaxation down to the elastic (flow) limit, and then practically does not relax further

and is, therefore, a constant for the system. Solid-like systems in which the elastic limit coincides with the limit of structure strength are elastic-brittle systems. In such systems, below this limit, only elastic deformations can develop (sometimes very slowly), while steady flow cannot take place at all.

2. In liquid-like systems, an important part is played by the lower limit of the strength of the structure of the system, in the stress region below which the viscosity remains constant, and above it, the viscosity falls with further increase of stress. This limit of structure strength corresponds to the critical deformation rate for the system. It was established that at constant rates below this critical value steady flow is established without disruption of the structural bonds, which have time to relax completely. At higher rates of deformation, and consequently at stresses greater than the lower limit of structure strength, the establishment of steady flow is preceded by the appearance of a maximum on the stress-deformation curves at a given deformation rate. This maximum increases with growing rate of deformation and characterizes the strength of the structure (yield stress).

3. In the case of solid-like, i.e., plastic systems, with a definite flow limit, above this limit, on considerations of practical calculations, the plastic viscosity should be determined, which is calculated as the ratio of the excess of the acting stress over the flow limit, to the deformation rate. This is of significance both for the lower and the upper flow limit — an arbitrary limit which corresponds to practically complete destruction of the structure in the stream. This plastic viscosity tends to a maximum value as the shear stress decreases to the flow limit, and in a number of cases retains its constant greatest value over a considerable interval of stresses. In such cases, in the calculation of the effective viscosity as the ratio of the total stress to the deformation rate, this viscosity increases sharply with decreasing stress on approaching the flow limit, sometimes becoming practically infinite.

VI. In addition to this, in the course of the discussion a number of still debatable points were examined, which may be clarified as the result of further experimental investigations and development of the molecular-kinetic theory of processes of deformation and flow in structurized systems. Among these debatable points should be included:

1) The question of the mechanism of flow, especially in the case of solid-like bodies at stresses immediately above the flow limit, and also in the region of creep as a whole, in the region where the plastic viscosity is practically constant. It is also necessary to clarify the question of the relationship between the molecular-kinetic meaning of the lower strength limit of the structure in liquid-like systems and the corresponding critical stress in solid-like systems.

2) In this connection it is necessary to clarify the transition from solid-like to liquid-like systems, and also the mechanism of the destruction and formation of bonds in different regions of the flow curve.

3) It is necessary to elucidate the question of the formation and the nature of the destruction of the spatial network (continuous skeleton) which is generally accepted as the cause of the formation of solid-like systems with their thixotropic properties. It is necessary to clarify the question of the possibility and mechanism of flow of such continuous structures without residual destruction.

4) It is also necessary to clarify the mechanism of deformational strengthening in structurized systems of various types.

VII. Workers in this field are recommended to devote particular attention to the development of a molecular mechanism of structure formation, and of the disruption and restoration of structure in flow processes.

Modern methods of microstructure analysis should be more widely applied to investigations of this type. Together with studies of the molecular interaction of structural elements with each other and with the molecules of the medium (solvation), it is necessary to focus attention on the orientation of macromolecules or particles of the disperse phase in flow, and on the role of the entropy factor (flexibility of the macromolecular chains).

VIII. It is necessary to publish the subject matter of the present discussion in the Colloid Journal.

Further discussion, with the addition of new experimental material, should continue in the scientific journals."

Member of the organizing committee A. A. Trapeznikov did not agree with Section V of this resolution. In the opinion of A. A. Trapeznikov, his proposed system of concepts of the rheological properties of structurized colloidal systems is the most strict, which was not stressed in Section V of the resolution. However, the remaining members of the organizing committee, and also most of those who took part in the discussions, did not share A. A. Trapeznikov's view, indicating the incompleteness of his viewpoint and the existence of contradictions in it.

M. P. Volarovich

COLLOID JOURNAL (USSR)

Volume XVI, 1954

Index

IN ENGLISH TRANSLATION

SECTIONS

Pagination of the Consultants Bureau English Translation, by No.

———————————————

Any of the articles listed herein may be purchased separately, exactly as they appear in the published translation, for $ 7.50. Individual issues may be purchased for $ 20.00 each. The price of the translation of the entire volume - $ 80.00.

When ordering articles, please cite title, author, and the English pagination. Direct your orders to:

IN ENGLISH TRANSLATION

Printed in the United States

Annual Subscription $ 80.00
This index   5.00

TABLE OF CONTENTS

TABLE OF CONTENTS

Discussion

Chronicle

TABLE OF CONTENTS

Colloid Journal (U.S.S.R.) in English Translation, July-August, 1954

TABLE OF CONTENTS

TABLE OF CONTENTS

COLLOID JOURNAL OF THE U.S.S.R. in ENGLISH TRANSLATION

November-December, 1954

TABLE OF CONTENTS